

Applications of Crystal Bases to Current Problems in Representation Theory

By

PHILIP MAX STERNBERG
B.A. (University of California, Berkeley) 2002

DISSERTATION

Submitted in partial satisfaction of the requirements for the degree of

DOCTOR OF PHILOSOPHY

in

MATHEMATICS

in the

OFFICE OF GRADUATE STUDIES

of the

UNIVERSITY OF CALIFORNIA

DAVIS

Approved:

Anne Schilling (Chair)

Eric M. Rains

Monica Vazirani

Committee in Charge

© Philip Sternberg, 2006. All rights reserved.

Dedicated to the memory of David Sternberg,
father, scientist, and mentor.

Contents

1	Introduction	1
1.1	Historical Overview and Motivation	1
1.1.1	Representation Theory	1
1.1.2	Crystal Bases	3
1.1.3	Quantum Affine Algebras	4
1.1.4	Local Characterization of Crystals	6
1.2	Summary of Main Results	7
1.2.1	Outline by chapter	9
2	Crystals for Kirillov-Reshetikhin Modules over Quantum Affine Al-	
	gebras of Type $D_n^{(1)}$	11
2.1	Review of Quantum Groups and Crystal Bases	11
2.1.1	Quantum groups	11
2.1.2	Crystal bases	12
2.1.3	Perfect crystals	15
2.1.4	The energy function and one-dimensional sums	16
2.2	Preliminaries on Type D_n crystals	19
2.2.1	Dynkin data	19

2.2.2	Classical crystals	20
2.2.3	Plactic monoid of type D	24
2.2.4	Dual crystals	26
2.2.5	Properties of $B^{r,s}$	28
2.3	A Dynkin Diagram Automorphism and the Branching Component Graph	29
2.3.1	Preliminaries	29
2.3.2	Rectangular partitions	35
2.3.3	Arbitrary partitions	45
2.4	The Crystal Automorphism	47
3	The Family $B^{2,s}$ of Type D Kirillov-Reshetikhin Modules	52
3.1	Specialization of previous work to $r = 2$	52
3.1.1	Classical tableaux	52
3.1.2	Sliding algorithm	53
3.1.3	Technical definitions for operations on tableaux	55
3.1.4	Properties of $B^{r,s}$	56
3.1.5	Specialization of $\check{\sigma}$	56
3.2	Realization of $B^{2,s}$ as a Set of Young-like Tableaux	57
3.2.1	Bijection between affine and classical tableaux	57
3.2.2	Combinatorial construction of σ	64
3.2.3	Properties of f_0 and e_0	69
3.3	Proof of Theorem 1.2.2	70
3.3.1	Overview	70
3.3.2	Connectedness of $\tilde{B}^{2,s}$	71
3.3.3	Preliminary observations	72

3.3.4	Surjectivity	75
3.3.5	Injectivity	77
3.3.6	Uniqueness	86
4	Local Properties of Crystals for Modules over Doubly Laced Algebras	91
4.1	Local Characterization of Simply Laced Crystals	91
4.2	Realization of Crystals for Modules over Type C_2 Algebras	94
4.3	Analysis of Generic C_2 tableaux	98
4.4	Proof of Theorem 1.2.4	107
5	A User's Manual for CrystalView	122
5.1	Overview	122
5.2	Requirements	123
5.3	User input	123
5.4	Limitations	124
5.5	How it works	125
5.6	How to get the software	126
5.7	Examples of output	126
5.8	Legal disclaimer	128
	References	129

Philip Sternberg
June 2006
Mathematics

Abstract

Over the past sixteen years, Kashiwara's construction of crystal bases [18, 19] has been an invaluable tool in addressing questions in representation theory, statistical mechanics, and soliton cellular automata. This dissertation addresses two current questions in the theory of crystal bases: the structure of crystal bases for Kirillov-Reshetikhin modules over algebras of type $D_n^{(1)}$, and the local structure of doubly laced crystals. It also includes a user manual for the CrystalView software package, which was written by the author.

The first of these questions is addressed in Chapters 2 and 3. Specifically, in Chapter 2 we describe a conjecture for the structure of the crystal bases $B^{r,s}$ that correspond to the Kirillov-Reshetikhin modules $W^{r,s}$ of type $D_n^{(1)}$. Specifically, we prove that many aspects of the combinatorial structure of these crystals are determined by representation theoretical concerns, leaving only a small aspect of this structure unspecified. Our conjecture specifies this part of the structure of these crystals uniformly. This result is based on the work and conjectures of the $X = M$ program put forward in [9, 10]. In Chapter 3 we prove that this conjecture is true for the special case of $r = 2$.

The second of these questions is the subject of Chapter 4. Building on the work of [46], we confirm a conjecture of Stembridge that limits the local behavior of crystals for representations of Lie algebras all of whose rank two subalgebras are either $A_1 \times A_1$, A_2 , or C_2 . Specifically, we show that if v is a vertex in such a crystal with both an i -colored and a j -colored edge directed into it, one of four pairs of sequences (E_1, E_2) ,

each composed of the operators e_i and e_j , satisfies $E_1v = E_2v$.

In Chapter 5, we explain the features, usage, and implementation of CrystalView.

Acknowledgments

I first wish to thank Anne Schilling for her excellent supervision of the work contained in this dissertation. The training I received under her guidance both as a creator and communicator of mathematics has been truly exceptional. The results contained here could not have been obtained without Prof. Schilling's help as critic and collaborator.

My thanks are also extended to the other members of my dissertation committee, Eric Rains and Monica Vazirani, who also served on my qualifying examination committee. They have both been a great help to me in many conversations as I have explored many diverse mathematical interests.

I could not have completed my degree without the support of my wife, Mary Orland. The obstacles to completing a Ph.D. are not solely intellectual—Mary helped me to meet many of these other challenges. My gratitude is due to her for keeping me out of the trouble in which I could have very easily found myself without her assistance.

It is unlikely that I would have ever considered pursuing an advanced degree had I not had as a role model my father, David Sternberg. From my earliest memories, my father encouraged me to pursue new knowledge and understanding in every way possible. I am proud to be able to dedicate this dissertation to the honor of his memory. I was also always supported by my mother, Linda Sternberg, throughout

my studies. I am forever grateful to both of my parents for their love and support, and their belief that my capability was limited only by my ambition.

Many thanks are also extended to Isaiah Lankham, who has been a splendid office-mate, travelling companion, and dear friend for the past four years. In particular, Isaiah's editorial improvements on many of my papers and his suggestions pertaining to CrystalView were indispensable.

The result of Chapter 4 could not have been obtained without John Stembridge, to whom I also extend my thanks; not only is he responsible for the seminal paper which it generalizes, but he also provided very helpful insights into the mechanics of this problem. My thanks are also given to Masato Okado, Tomoki Nakanishi, and Mark Shimozone for their very helpful comments regarding the work of Chapters 2 and 3.

I would also like to thank Jesús de Loera and Greg Kuperberg for serving on my qualifying examination committee, and for many helpful and enjoyable conversations over the past years. My thanks are particularly due to Prof. de Loera for his suggestion that I investigate working with Prof. Schilling, and to Prof. Kuperberg for agreeing to serve on my examination committee on very short notice after one of my original committee members found himself suddenly unavailable.

In the course of publishing and presenting the research contained here, several anonymous referees have provided comments and criticisms which have ultimately improved the exposition of these results considerably. I wish to thank these referees for volunteering their time for the betterment of the community.

Parts of this research were carried out while I was a guest at two excellent institutions, the Max-Planck-Institut für Mathematik in Bonn, Germany, and the Research Institute for the Mathematical Sciences in Kyoto, Japan. I extend my thanks to these

organizations for their hospitality.

Chapter 1

Introduction

1.1 Historical Overview and Motivation

1.1.1 Representation Theory

The study of representation theory has as its goal the understanding of algebraic objects in terms of their action on other objects. For instance, we may study groups by their action on a set of elements (a permutation representation) or on a vector space (a linear representation). This notion is formally described by realizing this action as a homomorphism from the object being studied into the the most general set of symmetries of the object being acted upon. In the above examples, these would be a homomorphism from a group into a group of permutations or into the general linear group of a vector space, respectively.

If we wish to study the representation theory of an algebra A over a field \mathbb{K} , we consider morphisms $\rho : A \rightarrow \mathfrak{gl}(V)$, where V is a vector space over \mathbb{K} . If A is a Lie algebra, we take $\mathfrak{gl}(V)$ to be the general linear Lie algebra of transformations of V ;

if A is instead an associative algebra, we take as $\mathfrak{gl}(V)$ the associative general linear algebra of V .

In the following work, we are concerned with representations of Quantum Groups, also known as Quantized Universal Enveloping Algebras. These are associative algebras over the field $\mathbb{C}(q)$ of rational functions with complex coefficients. Denoted by $U_q(\mathfrak{g})$, they can be realized as a quantization deformation of the universal enveloping algebra $U(\mathfrak{g})$ of a Lie algebra \mathfrak{g} . When \mathfrak{g} is a Kac-Moody algebra, there is a straightforward presentation of $U_q(\mathfrak{g})$ by generators and relations.

Specifically, we have the following, after [11].

Definition 1.1.1. Let I be a finite indexing set; let $A = (a_{ij}) : i, j \in I$ be a symmetrizable generalized Cartan matrix with symmetrizing matrix $D = \text{diag}(s_i) : i \in I$, and let Π, Π^\vee, P , and P^\vee be the set of simple roots, simple coroots, weight lattice, and dual weight lattice of the corresponding Kac-Moody Lie algebra \mathfrak{g} . The associated quantum group $U_q(\mathfrak{g})$ is the associative $\mathbb{C}(q)$ -algebra with unit generated by e_i and f_i for $i \in I$ and q^h for $h \in P^\vee$ with the following relations:

- $q^0 = 1, q^h q^{h'} = q^{h+h'}$ for $h, h' \in P^\vee$,
- $q^h e_i q^{-h} = q^{\alpha_i(h)} e_i$ for $h \in P^\vee$,
- $q^h f_i q^{-h} = q^{-\alpha_i(h)} f_i$ for $h \in P^\vee$,
- $e_i f_j - f_j e_i = \delta_{ij} \frac{K_i - K_i^{-1}}{q_i - q_i^{-1}}$ for $i, j \in I$,
- $\sum_{k=0}^{1-a_{ij}} (-1)^k \begin{bmatrix} 1-a_{ij} \\ k \end{bmatrix}_{q_i} e_i^{1-a_{ij}-k} e_j e_i^k = 0$ for $i \neq j$,
- $\sum_{k=0}^{1-a_{ij}} (-1)^k \begin{bmatrix} 1-a_{ij} \\ k \end{bmatrix}_{q_i} f_i^{1-a_{ij}-k} f_j f_i^k = 0$ for $i \neq j$,

where $q_i = s_i$ and $K_i = q^{s_i h_i}$, and the symbol $[n]_q = \frac{q^n - q^{-n}}{q - q^{-1}}$ for $n \in \mathbb{Z}_{\geq 0}$.

The algebra $U_q(\mathfrak{g})$ has a representation theory that refines the representation theory of the associated Lie algebras by means of quantization deformation. More precisely, given a simple highest weight module M over \mathfrak{g} , we can construct a simple module M_q over $U_q(\mathfrak{g})$ whose weight spaces multiplicities are the same as those of M , as proved by Lusztig in [32]. Furthermore, tensor products of such deformed modules decompose into simple modules in the same way as their classical counterparts. Thus, the representation theory of $U_q(\mathfrak{g})$ retains all algebraic information about \mathfrak{g} , in addition to it modules having a natural grading by powers of q .

1.1.2 Crystal Bases

The representation theory of Lie algebras has always had close ties to combinatorics. Using the technique of crystal bases, Kashiwara developed a completely discrete language for describing modules over quantum groups, and thus also modules over Lie algebras [18, 19]. Specifically, given any highest weight integrable $U_q(\mathfrak{g})$ -module V , there is a colored directed graph $B(V)$ called the crystal graph of V that encodes nearly all of the information of the action of $U_q(\mathfrak{g})$ on V . Abstracting this notion, one can define crystals without making an explicit reference to a particular representation. This definition includes all crystals that come from \mathfrak{g} -modules, as well as crystals that cannot be thus realized. Such axiomatic crystals have been used to prove several significant results in the theory of crystal bases.

Precisely, we have the following definition of crystals, after [20].

Definition 1.1.2. Let I be a finite index set, let $A = (a_{ij})$ for $i, j \in I$ be a Cartan matrix, and let $(\Pi, \Pi^\vee, P, P^\vee)$ be the associated Cartan data of a Kac-Moody algebra \mathfrak{g} as in Definition 1.1.1. A \mathfrak{g} -crystal is a set B together with maps $\text{wt} : B \rightarrow P, e_i, f_i :$

$B \rightarrow B \cup \{0\}$, and $\varepsilon_i, \varphi_i : B \rightarrow \mathbb{Z} \cup \{-\infty\}$ for $i \in I$ such that:

- $\varphi_i(b) = \varepsilon_i(b) + \langle h_i, \text{wt}(b) \rangle$ for all $i \in I$,
- $\text{wt}(e_i b) = \text{wt} b + \alpha_i$ if $e_i b \in B$,
- $\text{wt}(f_i b) = \text{wt} b - \alpha_i$ if $f_i b \in B$,
- $\varepsilon_i(e_i b) = \varepsilon_i(b) - 1, \varphi_i(e_i b) = \varphi_i(b) + 1$ if $e_i b \in B$,
- $\varepsilon_i(f_i b) = \varepsilon_i(b) + 1, \varphi_i(f_i b) = \varphi_i(b) - 1$ if $f_i b \in B$,
- $f_i b = b'$ if and only if $b = e_i b$ for $b, b' \in B, i \in I$,
- if $\varphi_i(b) = -\infty$ for $b \in B$, then $e_i b = f_i b = 0$.

The corresponding crystal graph has a vertex for each $b \in B$ and an i -colored edge from b to b' if $f_i b = b'$.

1.1.3 Quantum Affine Algebras

Many current questions involving crystal bases pertain to crystals for modules of quantum affine algebras; i.e., quantum groups $U_q(\mathfrak{g})$ where the underlying algebra \mathfrak{g} is of affine type. Two important classes of representations of these algebras are finite dimensional modules and highest weight modules. Many existing methods for analyzing representations of Lie algebras and quantum groups, both combinatorial and algebraic, only apply to highest weight modules. A great deal of new work was therefore needed to address questions about the finite-dimensional representation theory of quantum affine algebras.

Finite-dimensional modules of quantum affine algebras were classified by Chari and Pressley using Drinfeld polynomials [3], taking a major step toward understanding

these representation theoretical concerns. However, many of the internal aspects of these representations remain poorly understood. One approach to understanding these representations more explicitly is by determining if they have crystal bases, and if so, describing their structure via an explicit discrete construction.

In [25, 26], a relationship was observed between the Bethe ansatz (a method for solving lattice models in statistical mechanics) and the combinatorics of Young tableaux. There it was proposed that a certain family of modules over quantum affine algebras of type $A_n^{(1)}$, which have come to be called Kirillov-Reshetikhin modules, should be combinatorializable (as these papers precede [18], we do not use the term “crystallizable”). This claim is motivated by the fact that another method for solving the same lattice models, the corner transfer matrix, makes use of the combinatorics that govern type A representation theory. The Bethe ansatz gives rise to another set of combinatorial objects, called rigged configurations; since the formulas arising from these two methods are equal, there should be a bijection between rigged configurations and Young tableaux. As this notion was formalized over the next decade, the combinatorial notion of crystals, type-independent tableaux, and type-independent rigged configurations allowed the work of [25, 26] to be generalized.

In [9, 10], the Kyoto school proposed that all Kirillov-Reshetikhin modules of all types have crystal bases, and furthermore that the only finite-dimensional modules of quantum affine algebras with crystal bases are tensor products of Kirillov-Reshetikhin modules. Considerable progress has been made toward understanding these crystals and proving these claims. For a thorough review of the current state of this program, see [41]. Here, we summarize the known results for Kirillov-Reshetikhin crystals [36].

For type $A_n^{(1)}$, the crystals are known to exist [17] and their explicit structure is known [45]. For non-exceptional algebras, [15] gives a realization of $B^{1,s}$ as the set

of lattice points in a convex polytope. The crystal $B^{r,1}$ for all algebras was shown to exist in [22], and a realization using Lakshmibai-Seshadri (L-S) paths has been constructed in [34]. Other cases include those of the spin representations $B^{n,s}$ for $C_n^{(1)}$, $B^{n,s}$ and $B^{n-1,s}$ for $D_n^{(1)}$, and $B^{n,s}$ for $D_{n+1}^{(2)}$, which are shown to exist and given explicitly in [17]. In [1] any case in which the highest classical component of $B^{r,s}$ is the adjoint representation of the classical subalgebra is dealt with. The crystal structures have also been given for $B^{r,1+\delta_{rn}}$ for $B_n^{(1)}$, $B^{r,2}$ with $r \neq n$ for $C_n^{(1)}$, $B^{r,1}$ with $r \neq n$ and $r \neq n-1$ for $D_n^{(1)}$ [28], $B^{r,1}$ for $C_n^{(1)}$, $B^{r,1}$ for $A_{2n}^{(2)}$, $B^{r,1}$ for $A_{2n-1}^{(2)\dagger}$ [13], and $B^{1,s}$ for $G_2^{(1)}$ [48].

The results of [38, 39] reduce the problem to simply laced types using virtual crystals, a technique whereby Dynkin diagram folding is extended to crystals. Therefore, these conjectures need only to be resolved for types $D_n^{(1)}$ ($n \geq 4$) and $E_n^{(1)}$ ($n \in \{6, 7, 8\}$). Furthermore, it has been shown in [7] that given certain assumptions about the crystals $B^{r,s}$, their affine structure is uniquely specified by an isomorphism with Demazure crystals. Thus, defining a crystal structure satisfying these assumptions constitutes a significant step towards understanding their combinatorial structure.

1.1.4 Local Characterization of Crystals

Crystals were originally developed to describe representations of Lie algebras; however, many objects satisfying Definition 1.1.2 do not correspond to any $U_q(\mathfrak{g})$ -module. It is therefore of interest to know when a colored directed graph is the crystal graph of a representation. Such a characterization can be used to show that a graph that does not *a priori* encode representation theoretic information is in fact a crystal graph.

Many explicit combinatorial models have been developed for crystal graphs of representations; two of these are paths in the weight lattice of \mathfrak{g} [30, 31] and generalized Young tableaux [24]. In all of these cases, the combinatorial properties of the crystals are defined globally. In [46], Stembridge introduced a set of graph theoretic axioms, each of which addresses only local properties of a colored directed graph, that characterizes highest weight crystal graphs that come from representations of simply laced algebras.

1.2 Summary of Main Results

The first main result presented here is a conjectural explicit description of crystals for Kirillov-Reshetikhin modules over an algebra of type $D_n^{(1)}$. We investigate the structure of such modules as modules over the embedded algebras of type D_n and D_{n-1} , discovering some very significant symmetries. Based on a refinement of the branching properties of $B^{r,s}$ over these algebras, we formulate a combinatorial conjecture for the structure of these crystals.

Specifically, given $r \in \{1, 2, \dots, n\}$ and $s \in \mathbb{Z}_{\geq 0}$, we construct a crystal $\tilde{B}^{r,s}$.

Conjecture 1.2.1. *Assuming that $B^{r,s}$ exists with the properties conjectured in [9, 10], we have*

$$B^{r,s} \simeq \tilde{B}^{r,s}.$$

The work of [7] shows that if we assume $B^{r,s}$ to have certain properties, its affine structure is specified by the inclusion of a Demazure module in it. Thus, if these hypotheses (which are less demanding than those of [9, 10]) are satisfied, this conjecture is true.

As evidence of this conjecture, we prove in Section 3.3 that in the case of $r = 2$, the affine structure of the Kirillov-Reshetikhin modules respects the observed symmetries. We thus have the following Theorem, as proved in [44].

Theorem 1.2.2. *Assuming that $B^{2,s}$ exists with the properties conjectured in [9, 10], we have*

$$B^{2,s} \simeq \tilde{B}^{2,s}.$$

Further elucidating the structure of $B^{2,s}$ for type $D_n^{(1)}$, we define in Section 2.2 a new generalization of Young tableaux and show that it can be used to index the vertices of $B^{2,s}$. We also give an explicit definition of the affine Kashiwara operators on these tableaux. We encapsulate these results as follows.

Theorem 1.2.3. *The tableaux defined in Definition 3.2.1 are in bijective correspondence with the tableaux used to index the classical components of $B^{2,s}$. Furthermore, Algorithm 3.2.17 explicitly specifies the action of the Kashiwara operators e_0 and f_0 on these tableaux.*

Finally, we confirm a conjecture of Stembridge on the local structure of crystals coming from representations of doubly laced algebras [47].

Theorem 1.2.4. *Let \mathfrak{g} be a doubly laced algebra, i.e., an algebra all of its regular rank 2 subalgebras are of type $A_1 \times A_1$, A_2 , or C_2 . Let B be the crystal graph of an irreducible highest weight module of \mathfrak{g} , and let v be a vertex of B such that $e_i v \neq 0$ and $e_j v \neq 0$, where e_i and e_j denote two different Kashiwara raising operators. Then one of the following is true:*

1. $e_i e_j v = e_j e_i v$,

2. $e_i e_j^2 e_i v = e_j e_i^2 e_j v$ and no other sequences of the operators e_i, e_j with length less than or equal to four satisfy such an equality,
3. $e_i e_j^3 e_i v = e_j e_i e_j e_i e_j v = e_j^2 e_i^2 e_j v$ and no other sequences of the operators e_i, e_j with length less than or equal to five satisfy such an equality,
4. $e_i e_j^3 e_i^2 e_j v = e_i e_j^2 e_i e_j e_i e_j v = e_j e_i^2 e_j^3 e_i v = e_j e_i e_j e_i e_j^2 e_i v$ and no other sequences of the operators e_i, e_j with length less than or equal to seven satisfy such an equality.

The equivalent statement with f_i and f_j in place of e_i and e_j also holds.

1.2.1 Outline by chapter

In Chapter 2, we include in the first section all the necessary prerequisite constructions and well-known theorems on quantum groups and crystal bases, including perfect crystals. In section 2.2 we go into more detail on type D crystals, specifying the combinatorics of representations of even orthogonal algebras and specializing the conjectures on finite-dimensional modules over quantum affine algebras to the type $D_n^{(1)}$ case. Sections 2.3 and 2.4 contain a detailed analysis of the affine crystals that are supposed to exist by these conjectures, and we present our conjecture on the exact structure of these crystals.

In Chapter 3, we begin by specializing the work of the last two sections to the case of $r = 2$ in section 3.1. We extend these results in section 3.2 by constructing an explicit bijection between classical tableaux and what we define to be “affine tableaux”. In section 3.3 we prove Theorem 1.2.2. This chapter is based on [44].

In Chapter 4 we deal with local properties of highest weight crystals coming from

representations of some classes of Lie algebras. In section 4.1, we recall the previously known case of simply laced crystals. Section 4.2 is a review of the combinatorics of type C_2 crystals. Proceeding to section 4.3, we analyze a generic C_2 crystal to see what its neighborhood in the crystal graph may look like. In section 4.4, we prove that only four possible local behaviors may appear in doubly laced crystals. This chapter is based on [47].

Finally, Chapter 5 deals with the software package CrystalView, detailing requirements, user input options, current limitations of the software, and a description of the algorithms used to generate the output of this program.

Chapter 2

Crystals for Kirillov-Reshetikhin

Modules over Quantum Affine

Algebras of Type $D_n^{(1)}$

2.1 Review of Quantum Groups and Crystal Bases

2.1.1 Quantum groups

For $n \in \mathbb{Z}$ and a formal parameter q , we use the notation

$$[n]_q = \frac{q^n - q^{-n}}{q - q^{-1}}, \quad [n]_q! = \prod_{k=1}^n [k]_q, \quad \text{and} \quad \begin{bmatrix} m \\ n \end{bmatrix}_q = \frac{[m]_q!}{[n]_q! [m-n]_q!}.$$

These are all elements of $\mathbb{Q}(q)$, called the q -integers, q -factorials, and q -binomial coefficients, respectively.

Let \mathfrak{g} be an arbitrary Kac-Moody Lie algebra with Cartan datum $(A, \Pi, \Pi^\vee, P, P^\vee)$

and a Dynkin diagram indexed by I . Here $A = (a_{ij})_{i,j \in I}$ is the Cartan matrix, P and P^\vee are the weight lattice and dual weight lattice, respectively, $\Pi = \{\alpha_i \mid i \in I\}$ is the set of simple roots and $\Pi^\vee = \{h_i \mid i \in I\}$ is the set of simple coroots. Furthermore, let $\{s_i \mid i \in I\}$ be the entries of the diagonal symmetrizing matrix of A and define $q_i = q^{s_i}$ and $K_i = q^{s_i h_i}$. Then the quantum enveloping algebra $U_q(\mathfrak{g})$ is the associative $\mathbb{Q}(q)$ -algebra generated by e_i and f_i for $i \in I$, and q^h for $h \in P^\vee$, with the following relations (see e.g. [11, Def. 3.1.1]):

1. $q^0 = 1$, $q^h q^{h'} = q^{h+h'}$ for all $h, h' \in P^\vee$,
2. $q^h e_i q^{-h} = q^{\alpha_i(h)} e_i$ for all $h \in P^\vee$,
3. $q^h f_i q^{-h} = q^{\alpha_i(h)} f_i$ for all $h \in P^\vee$,
4. $e_i f_j - f_j e_i = \delta_{ij} \frac{K_i - K_i^{-1}}{q_i - q_i^{-1}}$
for $i, j \in I$,
5. $\sum_{k=0}^{1-a_{ij}} (-1)^k \begin{bmatrix} 1-a_{ij} \\ k \end{bmatrix}_{q_i} e_i^{1-a_{ij}-k} e_j e_i^k = 0$ for all $i \neq j$,
6. $\sum_{k=0}^{1-a_{ij}} (-1)^k \begin{bmatrix} 1-a_{ij} \\ k \end{bmatrix}_{q_i} f_i^{1-a_{ij}-k} f_j f_i^k = 0$ for all $i \neq j$.

2.1.2 Crystal bases

The quantum algebra $U_q(\mathfrak{g})$ can be viewed as a q -deformation of the universal enveloping algebra $U(\mathfrak{g})$ of \mathfrak{g} . Lusztig [32] showed that the integrable highest weight representations of $U(\mathfrak{g})$ can be deformed to $U_q(\mathfrak{g})$ representations in such a way that the dimension of the weight spaces are invariant under the deformation, provided $q \neq 0$ and $q^k \neq 1$ for all $k \in \mathbb{Z}$ (see also [11]). Let M be a $U_q(\mathfrak{g})$ -module and R the subset of all elements in $\mathbb{Q}(q)$ which are regular at $q = 0$. Kashiwara [18, 19]

introduced Kashiwara operators \tilde{e}_i and \tilde{f}_i as certain linear combinations of powers of e_i and f_i . In the sequel we will use the notation e_i and f_i to refer to the Kashiwara operators, rather than the standard generators of $U_q(\mathfrak{g})$. A crystal lattice \mathcal{L} is a free R -submodule of M that generates M over $\mathbb{Q}(q)$, has the same weight decomposition and has the property that $e_i\mathcal{L} \subset \mathcal{L}$ and $f_i\mathcal{L} \subset \mathcal{L}$ for all $i \in I$. The passage from \mathcal{L} to the quotient $\mathcal{L}/q\mathcal{L}$ is referred to as taking the crystal limit. A crystal basis (also called a crystal base by some authors) is a \mathbb{Q} -basis of $\mathcal{L}/q\mathcal{L}$ with certain properties.

We can think of a $U_q(\mathfrak{g})$ -crystal as a nonempty set B equipped with maps $\text{wt} : B \rightarrow P$ and $e_i, f_i : B \rightarrow B \cup \{\emptyset\}$ for all $i \in I$, satisfying

$$f_i(b) = b' \Leftrightarrow e_i(b') = b \text{ if } b, b' \in B \quad (2.1.2.1)$$

$$\text{wt}(f_i(b)) = \text{wt}(b) - \alpha_i \text{ if } f_i(b) \in B \quad (2.1.2.2)$$

$$\langle h_i, \text{wt}(b) \rangle = \varphi_i(b) - \varepsilon_i(b). \quad (2.1.2.3)$$

In the most general setting, ε_i and φ_i can be integer valued functions on B satisfying further axioms; however, here we consider only normal crystals, in which case we simply define for all $b \in B$

$$\varepsilon_i(b) = \max\{n \geq 0 \mid e_i^n(b) \neq \emptyset\}$$

$$\varphi_i(b) = \max\{n \geq 0 \mid f_i^n(b) \neq \emptyset\}.$$

Here we assume that $\varphi_i(b), \varepsilon_i(b) < \infty$ for all $i \in I$ and $b \in B$, since we restrict our attention to crystals that come from integrable $U_q(\mathfrak{g})$ -modules. A $U_q(\mathfrak{g})$ -crystal B can be viewed as a directed edge-colored graph (the crystal graph) whose vertices are the elements of B , with a directed edge from b to b' labeled $i \in I$ if and only if $f_i(b) = b'$.

Let B_1 and B_2 be $U_q(\mathfrak{g})$ -crystals. The Cartesian product $B_2 \times B_1$ can also be endowed with the structure of a $U_q(\mathfrak{g})$ -crystal. The resulting crystal is denoted by $B_2 \otimes B_1$ and its elements (b_2, b_1) are written $b_2 \otimes b_1$. (The reader is warned that in the interests of compatibility with the combinatorics of Young tableaux, our convention is opposite to that of Kashiwara [21]). For $i \in I$ and $b = b_2 \otimes b_1 \in B_2 \otimes B_1$, we have $\text{wt}(b) = \text{wt}(b_1) + \text{wt}(b_2)$,

$$f_i(b_2 \otimes b_1) = \begin{cases} f_i(b_2) \otimes b_1 & \text{if } \varepsilon_i(b_2) \geq \varphi_i(b_1) \\ b_2 \otimes f_i(b_1) & \text{if } \varepsilon_i(b_2) < \varphi_i(b_1) \end{cases} \quad (2.1.2.4)$$

and

$$e_i(b_2 \otimes b_1) = \begin{cases} e_i(b_2) \otimes b_1 & \text{if } \varepsilon_i(b_2) > \varphi_i(b_1) \\ b_2 \otimes e_i(b_1) & \text{if } \varepsilon_i(b_2) \leq \varphi_i(b_1). \end{cases} \quad (2.1.2.5)$$

Combinatorially, this action of f_i and e_i on tensor products can be described by the signature rule. The i -signature of b is the word consisting of the symbols $+$ and $-$ given by

$$\underbrace{- \cdots -}_{\varphi_i(b_2) \text{ times}} \quad \underbrace{+ \cdots +}_{\varepsilon_i(b_2) \text{ times}} \quad \underbrace{- \cdots -}_{\varphi_i(b_1) \text{ times}} \quad \underbrace{+ \cdots +}_{\varepsilon_i(b_1) \text{ times}} .$$

The reduced i -signature of b is the subword of the i -signature of b , given by the repeated removal of adjacent symbols $+-$ (in that order); it has the form

$$\underbrace{- \cdots -}_{\varphi \text{ times}} \quad \underbrace{+ \cdots +}_{\varepsilon \text{ times}} .$$

If $\varphi = 0$ then $f_i(b) = \emptyset$; otherwise f_i acts on the tensor factor corresponding to the rightmost symbol $-$ in the reduced i -signature of b . Similarly, if $\varepsilon = 0$ then $e_i(b) = \emptyset$; otherwise e_i acts on the leftmost symbol $+$ in the reduced i -signature of b . From this it is clear that

$$\begin{aligned}\varphi_i(b_2 \otimes b_1) &= \varphi_i(b_2) + \max(0, \varphi_i(b_1) - \varepsilon_i(b_2)), \\ \varepsilon_i(b_2 \otimes b_1) &= \varepsilon_i(b_1) + \max(0, -\varphi_i(b_1) + \varepsilon_i(b_2)).\end{aligned}$$

For any dominant weight λ , there is an irreducible highest weight module $V(\lambda)$ with highest weight λ . Provided that $V(\lambda)$ is integrable, it has a crystal basis denoted by $B(\lambda)$.

2.1.3 Perfect crystals

Of particular interest is a class of crystals called perfect crystals, which are crystals for affine algebras satisfying a set of very special properties. These properties ensure that perfect crystals can be used to construct the path realization of crystals for highest weight modules by taking the semi-infinite tensor product of these crystals [17]. To define them, we need a few preliminary definitions.

Recall that P denotes the weight lattice of a Kac-Moody algebra \mathfrak{g} ; for the remainder of this section, \mathfrak{g} is of affine type. The center of \mathfrak{g} is one-dimensional and is generated by the canonical central element $c = \sum_{i \in I} a_i^\vee h_i$, where the a_i^\vee are the numbers on the nodes of the Dynkin diagram of the algebra dual to \mathfrak{g} given in Table Aff of [14, section 4.8]. Moreover, the imaginary roots of \mathfrak{g} are nonzero integer multiples of the null root $\delta = \sum_{i \in I} a_i \alpha_i$, where the a_i are the numbers on the nodes of the Dynkin diagram of \mathfrak{g} given in Table Aff of [14]. Define $P_{\text{cl}} = P/\mathbb{Z}\delta$,

$P_{\text{cl}}^+ = \{\lambda \in P_{\text{cl}} \mid \langle h_i, \lambda \rangle \geq 0 \text{ for all } i \in I\}$, and $U'_q(\mathfrak{g})$ to be the quantum enveloping algebra with the Cartan datum $(A, \Pi, \Pi^\vee, P_{\text{cl}}, P_{\text{cl}}^\vee)$.

Define the set of level ℓ weights to be $(P_{\text{cl}}^+)_\ell = \{\lambda \in P_{\text{cl}}^+ \mid \langle c, \lambda \rangle = \ell\}$. For a crystal basis element $b \in B$, define

$$\varepsilon(b) = \sum_{i \in I} \varepsilon_i(b) \Lambda_i \quad \text{and} \quad \varphi(b) = \sum_{i \in I} \varphi_i(b) \Lambda_i,$$

where Λ_i is the i -th fundamental weight of \mathfrak{g} . Finally, for a crystal basis B , we define B_{min} to be the set of crystal basis elements b such that $\langle c, \varepsilon(b) \rangle$ is minimal over $b \in B$.

Following [16],

Definition 2.1.1. A $U'_q(\mathfrak{g})$ -crystal B is a perfect crystal of level ℓ if:

1. $B \otimes B$ is connected;
2. there exists $\lambda \in P_{\text{cl}}$ such that $\text{wt}(B) \subset \lambda + \sum_{i \neq 0} \mathbb{Z}_{\leq 0} \alpha_i$ and there is a unique $b_\lambda \in B$ such that $\text{wt}(b_\lambda) = \lambda$;
3. there is a finite-dimensional irreducible $U'_q(\mathfrak{g})$ -module V with a crystal base whose crystal graph is isomorphic to B ;
4. for any $b \in B$, we have $\langle c, \varepsilon(b) \rangle \geq \ell$;
5. the maps ε and φ from B_{min} to $(P_{\text{cl}}^+)_\ell$ are bijective.

We use the notation $\text{lev}(B)$ to indicate the level of the perfect crystal B .

2.1.4 The energy function and one-dimensional sums

For an affine crystal B , we can define an integer-valued function on B called an energy function. Let B_1 and B_2 be finite $U'_q(\mathfrak{g})$ -crystals. Then following [17, Section 4]

1. There is a unique isomorphism of $U'_q(\mathfrak{g})$ -crystals $R = R_{B_2, B_1} : B_2 \otimes B_1 \rightarrow B_1 \otimes B_2$.
2. There is a function $H = H_{B_2, B_1} : B_2 \otimes B_1 \rightarrow \mathbb{Z}$, unique up to global additive constant, such that H is constant on classical components and, for all $b_2 \in B_2$ and $b_1 \in B_1$, if $R(b_2 \otimes b_1) = b'_1 \otimes b'_2$, then

$$H(e_0(b_2 \otimes b_1)) = H(b_2 \otimes b_1) + \begin{cases} -1 & \text{if } \varepsilon_0(b_2) > \varphi_0(b_1) \text{ and } \varepsilon_0(b'_1) > \varphi_0(b'_2) \\ 1 & \text{if } \varepsilon_0(b_2) \leq \varphi_0(b_1) \text{ and } \varepsilon_0(b'_1) \leq \varphi_0(b'_2) \\ 0 & \text{otherwise.} \end{cases} \quad (2.1.2.6)$$

The maps R and H are called the local isomorphism and local energy function on $B_2 \otimes B_1$. The pair (R, H) is called the combinatorial R -matrix.

For a finite $U'_q(\mathfrak{g})$ -crystal B , define $u(B)$ to be the unique vector in B such that $\text{wt}(u(B)) = \lambda$, $u(B)$ is the only vector in B with weight λ , and for all $b \in B$, $\text{wt}(b)$ is in the convex hull of the Weyl group action on λ [42]. Then with B_1 and B_2 as above,

$$R(u(B_2) \otimes u(B_1)) = u(B_1) \otimes u(B_2).$$

It is convenient to normalize the local energy function H by requiring that

$$H(u(B_2) \otimes u(B_1)) = 0.$$

With this convention it follows by definition that

$$H_{B_1, B_2} \circ R_{B_2, B_1} = H_{B_2, B_1}$$

as \mathbb{Z} -valued functions on $B_2 \otimes B_1$.

We wish to define an energy function $D_B : B \rightarrow \mathbb{Z}$ for tensor products of perfect crystals of the form $B^{r,s}$ [9, Section 3.3]. Let $B = B^{r,s}$; we for the moment assume that it is perfect. Then there exists a unique element $b^\natural \in B$ such that $\varphi(b^\natural) = \text{lev}(B)\Lambda_0$. Define $D_B : B \rightarrow \mathbb{Z}$ by

$$D_B(b) = H_{B,B}(b \otimes b^\natural) - H_{B,B}(u(B) \otimes b^\natural). \quad (2.1.2.7)$$

The intrinsic energy D_B for the L -fold tensor product $B = B_L \otimes \cdots \otimes B_1$ where $B_j = B^{r_j, s_j}$ is given by

$$D_B = \sum_{1 \leq i < j \leq L} H_i R_{i+1} R_{i+2} \cdots R_{j-1} + \sum_{j=1}^L D_{B_j} R_1 R_2 \cdots R_{j-1},$$

where H_i and R_i are the local energy function and R -matrix on the i^{th} and $i+1^{\text{th}}$ tensor factor, respectively.

Definition 2.1.2. Let B be a tensor product of crystals as above and let λ be a dominant weight. The one-dimensional configuration sum, (referred to in [9, 10] as the X formula) is

$$X(B, \lambda; q) = \sum_{b \in \mathcal{P}(B, \lambda)} q^{D_B(b)},$$

where $\mathcal{P}(B, \lambda)$ is simply the set of vertices in B of weight λ .

One of the motivations for explicitly describing the crystals $B^{r,s}$ is to allow for a combinatorial proof of the equivalence between the above sum and the fermionic formula arising from the Bethe ansatz [9, 10].

2.2 Preliminaries on Type D_n crystals

For the rest of Chapters 2 and 3 we restrict our attention to the finite Lie algebra of type D_n and the affine Kac-Moody algebra of type $D_n^{(1)}$. Denote by $I = \{0, 1, \dots, n\}$ the index set of the Dynkin diagram for $D_n^{(1)}$ (see Figure 2.3.2.1) and by $J = \{1, 2, \dots, n\}$ the Dynkin diagram for type D_n .

2.2.1 Dynkin data

For type D_n , the simple roots are

$$\begin{aligned} \alpha_i &= \epsilon_i - \epsilon_{i+1} & \text{for } 1 \leq i < n \\ \alpha_n &= \epsilon_{n-1} + \epsilon_n \end{aligned} \tag{2.2.2.1}$$

and the fundamental weights are

$$\begin{aligned} \varpi_i &= \epsilon_1 + \dots + \epsilon_i & \text{for } 1 \leq i \leq n-2 \\ \varpi_{n-1} &= (\epsilon_1 + \dots + \epsilon_{n-1} - \epsilon_n)/2 \\ \varpi_n &= (\epsilon_1 + \dots + \epsilon_{n-1} + \epsilon_n)/2 \end{aligned}$$

where $\epsilon_i \in \mathbb{Z}^n$ is the i -th unit standard vector. The central element for $D_n^{(1)}$ is

$$c = h_0 + h_1 + 2h_2 + \dots + 2h_{n-2} + h_{n-1} + h_n.$$

2.2.2 Classical crystals

Kashiwara and Nakashima [24] described the crystal structure of all classical highest weight crystals $B(\Lambda)$ of highest weight Λ explicitly. Kirillov-Reshetikhin crystals corresponding to the last two fundamental weights (the “spin” weights) are treated as a special case in [9, 10]; thus in the sequel, we only need to consider representations of D_n that are quotients of tensor powers of the vector representation, and omit spin representations from our consideration here. Recall that we may interpret such a dominant weight Λ as a partition with $\langle h_i, \Lambda \rangle$ columns of height i . The corresponding crystals can be represented by tableaux on this partition using the partially ordered alphabet

$$1 < 2 < \cdots < n - 1 < \frac{n}{\bar{n}} < \overline{n-1} < \cdots < \bar{2} < \bar{1}$$

where n and \bar{n} are incomparable, such that the following conditions hold [11, page 202]:

Criterion 2.2.1.

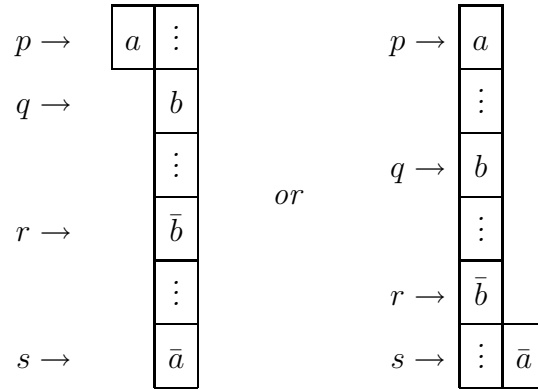
1. If $\begin{array}{|c|c|} \hline a & b \\ \hline \end{array}$ is in the tableau, then $a \leq b$;

2. If $\begin{array}{|c|} \hline a \\ \hline b \\ \hline \end{array}$ is in the tableau, then $b \not\leq a$;

3. If a and \bar{a} appear in a column of length N , with a in row p and \bar{a} in row q , we have

$$(q - p) + a > N;$$

4. If the tableau contains a configuration of the form

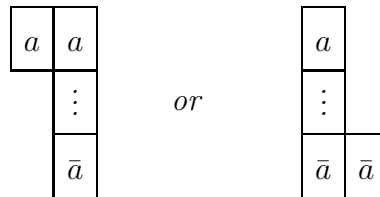


with $1 \leq a < b < n$ then

$$(q - p) + (s - r) < b - a$$

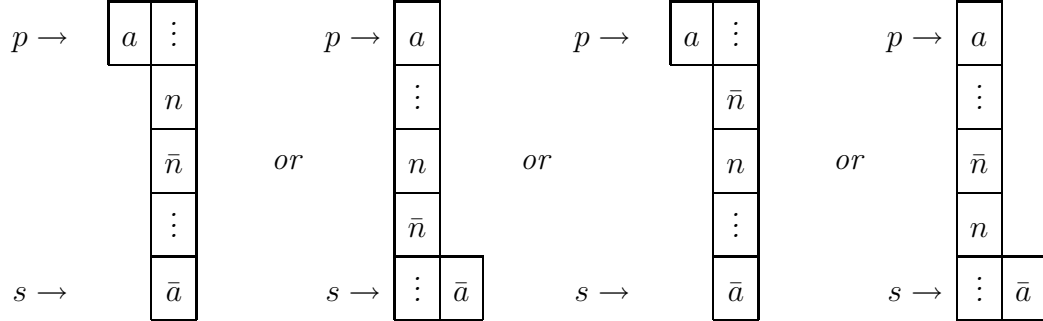
Note that we may have $p = q$ in the first case or $s = r$ in the second case above;

5. No configuration of the form



with $1 \leq a < n$ may appear in the tableau;

6. If the tableau contains a configuration of the form



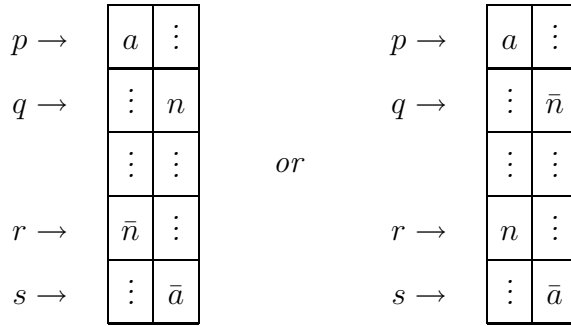
then

$$s - p - 1 < n - a$$

as with condition 4, the number of blocks represented by the \vdots at the elbow of these configurations may be any non-negative integer;

7. if the tableau contains an n or \bar{n} , then neither n nor \bar{n} may appear in the region strictly down and to the right of it;

8. If the tableau has a configuration of the form



with $r - q$ odd or

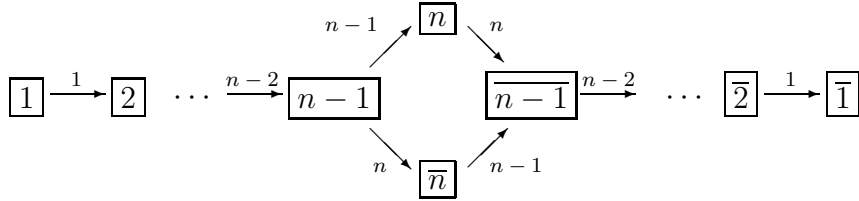
$$\begin{array}{c}
 p \rightarrow \\
 q \rightarrow \\
 \\
 r \rightarrow \\
 s \rightarrow
 \end{array}
 \begin{array}{|c|c|}
 \hline
 a & \vdots \\
 \hline
 \vdots & n \\
 \hline
 \vdots & \vdots \\
 \hline
 n & \vdots \\
 \hline
 \vdots & \bar{a} \\
 \hline
 \end{array}
 \quad \text{or} \quad
 \begin{array}{c}
 p \rightarrow \\
 q \rightarrow \\
 \\
 r \rightarrow \\
 s \rightarrow
 \end{array}
 \begin{array}{|c|c|}
 \hline
 a & \vdots \\
 \hline
 \vdots & \bar{n} \\
 \hline
 \vdots & \vdots \\
 \hline
 \bar{n} & \vdots \\
 \hline
 \vdots & \bar{a} \\
 \hline
 \end{array}$$

with $r - q$ even, we have

$$s - p < n - a.$$

A tableau that satisfies Criterion 2.2.1 is called a type D_n tableau.

The crystal $B(\varpi_1)$, (also called the vector representation) is described pictorially by the crystal graph:



Definition 2.2.2. Let T be a type D_n tableau. The column word of T , denoted by w_T , is the word on the alphabet $\{1, 2, \dots, n, \bar{n}, \dots, \bar{1}\}$ that results from reading

the entries in the tableau beginning with the left-most column and proceeding to the right, reading each column from bottom to top.

If we interpret the column word as a label for a basis vector of a quotient of a tensor power of the vector representation, the action of the Kashiwara operators f_i and e_i on a tableau is determined by the tensor product rule as defined in section 2.1.2.

Example 2.2.3. Let $n = 4$. Then the tableau

$$T = \begin{array}{|c|c|c|c|c|} \hline 1 & 2 & 4 & \bar{3} & \bar{3} \\ \hline 3 & \bar{4} & \bar{4} & \bar{2} & \bar{1} \\ \hline \end{array}$$

has column word $w_T = 31\bar{4}2\bar{4}\bar{4}\bar{2}\bar{3}\bar{1}\bar{3}$. The 2-signature of T is $+ - + - -$, derived from the subword $3\bar{2}\bar{2}\bar{3}\bar{3}$, and the reduced 2-signature is a single $-$. Therefore $e_2(T) = 0$ and

$$f_2(T) = \begin{array}{|c|c|c|c|c|} \hline 1 & 2 & 4 & \bar{3} & \bar{2} \\ \hline 3 & \bar{4} & \bar{4} & \bar{2} & \bar{1} \\ \hline \end{array},$$

since the rightmost $-$ in the reduced 2-signature of T comes from the northeastmost $\bar{3}$. The 4-signature of T is $- + + - ++$, derived from the subword $3\bar{4}\bar{4}\bar{4}\bar{3}\bar{3}$, and the reduced 4-signature is $- + ++$, from the subword $3\bar{4}\bar{3}\bar{3}$. This tells us that

$$f_4(T) = \begin{array}{|c|c|c|c|c|} \hline 1 & 2 & 4 & \bar{3} & \bar{3} \\ \hline \bar{4} & \bar{4} & \bar{4} & \bar{2} & \bar{1} \\ \hline \end{array} \quad \text{and} \quad e_4(T) = \begin{array}{|c|c|c|c|c|} \hline 1 & 2 & 4 & \bar{3} & \bar{3} \\ \hline 3 & \mathbf{3} & \bar{4} & \bar{2} & \bar{1} \\ \hline \end{array}.$$

2.2.3 Plactic monoid of type D

The plactic monoid for type D is the free monoid generated by the letters $\{1, \dots, n, \bar{n}, \dots, \bar{1}\}$, modulo certain relations introduced by Lecouvey [29]. These Lecouvey rela-

tions generalize the Knuth relations governing the RSK correspondence. Note that we write the letters of our words in reverse of the order used in [29]. An admissible column is one whose column word $C = x_L x_{L-1} \cdots x_1$ is such that $x_{i+1} \not\leq x_i$ for $i = 1, \dots, L-1$. Note that the letters n and \bar{n} are the only letters that may appear more than once in C . Let $z \leq n$ be a letter in C . Then $N(z)$ denotes the number of letters x in C such that $x \leq z$ or $x \geq \bar{z}$. A column C is called admissible if $L \leq n$ and for any pair (z, \bar{z}) of letters in C with $z \leq n$ we have $N(z) \leq z$. The Lecouvey D equivalence relations are given by:

1. If $x \neq \bar{z}$, then

$$xzy \equiv zxy \text{ for } x \leq y < z \text{ and } yzx \equiv yxz \text{ for } x < y \leq z.$$

2. If $1 < x < n$ and $x \leq y \leq \bar{x}$, then

$$(x-1)(\overline{x-1})y \equiv \bar{x}xy \text{ and } y\bar{x}x \equiv y(x-1)(\overline{x-1}).$$

3. If $x \leq n-1$, then

$$\left\{ \begin{array}{l} n\bar{x}\bar{n} \equiv n\bar{n}\bar{x} \\ \bar{n}\bar{x}n \equiv \bar{n}n\bar{x} \end{array} \right. \text{ and } \left\{ \begin{array}{l} xn\bar{n} \equiv nx\bar{n} \\ x\bar{n}n \equiv \bar{n}xn \end{array} \right. .$$

- 4.

$$\left\{ \begin{array}{l} \bar{n}\bar{n}n \equiv \bar{n}(n-1)(\overline{n-1}) \\ nn\bar{n} \equiv n(n-1)(\overline{n-1}) \end{array} \right. \text{ and } \left\{ \begin{array}{l} (n-1)(\overline{n-1})\bar{n} \equiv n\bar{n}\bar{n} \\ (n-1)(\overline{n-1})n \equiv \bar{n}nn \end{array} \right. .$$

5. Consider w a non-admissible column word such that every consecutive subword of w with length less than the length of w is admissible. Let z be the lowest unbarred letter such that the pair (z, \bar{z}) occurs in w and $N(z) > z$. Then $w \equiv \tilde{w}$ is the column word obtained by erasing the pair (z, \bar{z}) in w if $z < n$, by erasing a pair (n, \bar{n}) of consecutive letters otherwise.

This monoid gives us a bumping algorithm similar to the Schensted bumping algorithm. It is noted in [29] that a general type D sliding algorithm, if one exists, would be very complicated. However, for tableaux with no more than two rows, we can derive such an algorithm, the details of which are given in Section 3.1.

2.2.4 Dual crystals

Let ω_0 be the longest element in the Weyl group of D_n . The action of ω_0 on the weight lattice P of D_n is given by

$$\omega_0(\varpi_i) = -\varpi_{\tau(i)}$$

$$\omega_0(\alpha_i) = -\alpha_{\tau(i)}$$

where $\tau : J \rightarrow J$ is the identity if n is even and interchanges $n - 1$ and n and fixes all other Dynkin nodes if n is odd.

For any D_n -crystal B there is a unique involution $*$: $B \rightarrow B$, called the dual map, satisfying

$$\text{wt}(b^*) = \omega_0 \text{wt}(b)$$

$$e_i(b)^* = f_{\tau(i)}(b^*)$$

$$f_i(b)^* = e_{\tau(i)}(b^*).$$

The involution $*$ sends the highest weight vector $u \in B(\Lambda)$ to the lowest weight vector (the unique vector in $B(\Lambda)$ of weight $\omega_0(\Lambda)$). We have

$$(B_1 \otimes B_2)^* \cong B_2 \otimes B_1$$

with $(b_1 \otimes b_2)^* \mapsto b_2^* \otimes b_1^*$.

Explicitly, on $B(\varpi_1)$ the involution $*$ is given by

$$i \longleftrightarrow \bar{i}$$

except for $i = n$ with n odd in which case $n \leftrightarrow n$ and $\bar{n} \leftrightarrow \bar{n}$. For $T \in B(\Lambda)$ the dual vertex T^* is obtained by applying the $*$ map defined for $B(\varpi_1)$ to each of the letters of w_T^{rev} (the word with the same letters as T taken in the reverse order), and then rectifying the resulting word by the Lecouvey D equivalence relations.

Example 2.2.4. If

$$T = \begin{array}{|c|c|c|} \hline 1 & 1 & 2 \\ \hline \bar{3} & & \\ \hline \end{array} \in B(2\varpi_1 + \varpi_2)$$

we have

$$T^* = \begin{array}{|c|c|c|} \hline 3 & \bar{1} & \bar{1} \\ \hline \bar{2} & & \\ \hline \end{array}.$$

2.2.5 Properties of $B^{r,s}$

As mentioned in the introduction, it was conjectured in [9, 10] that there are crystal bases $B^{r,s}$ associated with Kirillov–Reshetikhin modules $W^{r,s}$. In addition to the existence, Hatayama et al. [9] conjectured certain properties of $B^{r,s}$ which we state here.

Conjecture 2.2.5 ([9]). *If the crystal $B^{r,s}$ of type $D_n^{(1)}$ exists, it has the following properties:*

1. *As a classical crystal $B^{r,s}$ decomposes as $B^{r,s} \cong \bigoplus_{\Lambda} B(\Lambda)$, where the direct sum is taken over all partitions Λ whose complement in an $r \times s$ rectangle is tiled by vertical dominos.*
2. *$B^{r,s}$ is perfect of level s .*
3. *$B^{r,s}$ is equipped with an energy function $D_{B^{r,s}}$ such that $D_{B^{r,s}}(b) = k - s$ if b is in a D_n component $B(\Lambda)$ for which Λ differs from an $r \times s$ rectangle by k vertical dominos.*

Remark 2.2.6. The decomposition of these Kirillov–Reshetikhin modules as modules over the embedded classical algebra of type D_n specified by Item 1 of Conjecture 2.2.5 was confirmed for the case of untwisted algebras in [2] and for twisted algebras in [35]; therefore if the crystals exist, this is known to be true.

Remark 2.2.7. In [7], it is proved that given the following assumptions, the affine structure of $B^{r,s}$ is specified by the embedding of certain Demazure crystals in $B^{r,s}$. We specialize their statement to the type D case.

1. $B^{r,s}$ is a regular crystal (i.e., eliminating all edges of color $\{i_1, \dots, i_m\} \subset I$ results in a crystal over $\mathfrak{g}_{I \setminus \{i_1, \dots, i_m\}}$),
2. There is a unique element $u \in B^{r,s}$ such that

$$\varepsilon(u) = s\Lambda_0 \quad \text{and} \quad \varphi(u) = s\Lambda_{r(\bmod 2)},$$

3. $B^{r,s}$ admits the automorphism corresponding to σ , the Dynkin diagram automorphism interchanging 0 and 1, leaving all other nodes fixed.

2.3 A Dynkin Diagram Automorphism and the Branching Component Graph

2.3.1 Preliminaries

We know that there is a map $\sigma : B^{r,s} \rightarrow B^{r,s}$ such that $e_0 = \sigma e_1 \sigma$ and $f_0 = \sigma f_1 \sigma$, arising from the automorphism of $U'_q(\widehat{\mathfrak{so}}_{2n})$ which interchanges nodes 0 and 1 of its Dynkin diagram (Figure 2.3.2.1). Let $J \subset I$, and denote by B_J the graph that results from removing all j -colored edges from $B^{r,s}$ for $j \in J$. Then as directed graphs, $B_{\{0\}}$ (which has the structure of a D_n crystal) is isomorphic to $B_{\{1\}}$. This motivates the introduction of the “branching component graph” of $B^{r,s}$ in Definition 2.3.1 below, which records all the relevant information about $B_{\{0,1\}}$.

It is easy to see that the connected components of $B_{\{0,1\}}$ will be D_{n-1} -crystals whose highest weights correspond to partitions as characterized by the propositions below. The branching component graph for $B^{r,s}$, which we denote $\mathcal{BC}(B^{r,s})$, is determined by this decomposition. We will describe the decomposition into irreducible

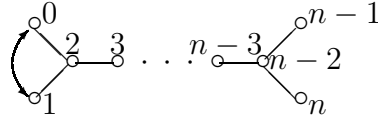


Figure 2.3.2.1: Dynkin diagram automorphism

D_{n-1} -crystals of a D_n -crystal indexed by a partition λ whose complement in an $r \times s$ rectangle is tiled by vertical dominos, calling the resulting graph $\mathcal{BC}(\lambda)$. Given the result of Chari specifying the decomposition of $B^{r,s}$ as a module over the classical algebra, $\mathcal{BC}(B^{r,s})$ is simply the union of these graphs.

Definition 2.3.1. Let λ be a partition labeling a D_n highest weight. The branching component graph $\mathcal{BC}(\lambda)$ has one vertex for each connected D_{n-1} -crystal that results from removing the 1 arrows from $B(\lambda)$. We associate to each vertex the partition corresponding to the D_{n-1} highest weight of that crystal. For a vertex $v \in \mathcal{BC}(\lambda)$, let $B(v)$ denote the set of crystal vertices in $B(\lambda)$ contained in the D_{n-1} -crystal indexed by v . Then $\mathcal{BC}(\lambda)$ has an edge from v to w if there is a crystal vertex $b \in B(v)$ such that $f_1(b) \in B(w)$.

This definition is essentially a refinement of the classically known D_n to D_{n-1} branching rule, which is as follows: let Λ be a D_n dominant weight with no spin part (i.e., such that $\langle h_n, \Lambda \rangle = \langle h_{n-1}, \Lambda \rangle = 0$) and let V_Λ denote the irreducible D_n module with highest weight Λ . Recall that we may interpret Λ as a partition with $\langle h_i, \Lambda \rangle$ columns of height i . A horizontal strip is a subset H of a partition λ such that distinct elements of H are in distinct columns of λ and $\lambda \setminus H$ is a partition. Then as a D_{n-1} module, V_Λ is the direct sum of D_{n-1} modules V_μ with D_{n-1} highest weight μ for each μ that can be obtained by successively removing two horizontal strips from Λ . As an illustration, see Example 2.3.3. This rule can be obtained by combining the

D_n to B_{n-1} branching rule with the B_{n-1} to D_{n-1} branching rule [8].

This motivates the following definition, formulated by Schilling and Shimozono [43].

Definition 2.3.2. Consider a sequence of partitions $\lambda \subset \mu \subset \Lambda$ such that μ/λ and Λ/μ are horizontal strips. A \pm diagram D of shape Λ/λ is the partition Λ with a +’s in each box of μ/λ and -’s in each box of Λ/μ . We call $\Lambda = \text{outer}(D)$ and $\lambda = \text{inner}(D)$ the outer and inner shape of D , respectively.

The set of \pm diagrams with outer shape Λ is in natural bijection with the D_{n-1} highest weights of the D_{n-1} to D_n branching components of the D_n module $V(\Lambda)$; i.e., as D_{n-1} modules we have the following isomorphism:

$$V_{D_n}(\Lambda) \cong \bigoplus_{\substack{\pm \text{ diagrams } D \\ \text{outer}(D)=\Lambda}} V_{D_{n-1}}(\text{inner}(D)),$$

where the subscript on V indicates the algebra that defines the representation.

Example 2.3.3. Consider the D_n module with highest weight $\Lambda_2 + \Lambda_4$, which corresponds to the partition $(2, 2, 1, 1)$. As a B_{n-1} module, this is the multiplicity-free sum of the modules labeled by $(2, 2, 1, 1)$, $(2, 2, 1, 0)$, $(2, 1, 1, 1)$, and $(2, 1, 1, 0)$. As a D_{n-1} module, it is the sum of the modules associated with the following partitions with the given multiplicities.

Partition	Multiplicity
(2, 2, 1, 1)	1
(2, 2, 1)	2
(2, 1, 1, 1)	2
(2, 1, 1)	4
(2, 2)	1
(2, 1)	2
(1, 1, 1, 1)	1
(1, 1, 1)	2
(1, 1)	1

This correspondence is made explicit by the following algorithm.

Algorithm 2.3.4. Let d be the difference between the number of $+$'s and the number of $-$'s in the \pm diagram.

1. Place the maximal number of 1 's and $\bar{1}$'s in the diagram such that:
 - the difference between the number of 1 's and the number of $\bar{1}$'s is d ,
 - the $\bar{1}$'s are placed in boxes containing $-$'s, starting from the right, and
 - the result is a legal tableau;
2. given that all letters $1, \bar{1}, 2, \bar{2}, \dots, i-1, \overline{i-1}$ have been placed, fill the empty boxes of row $i-1$ with i 's;
3. place the maximal number of i 's in row i and \bar{i} 's in the unfilled boxes with $-$'s, respectively, such that

- the resulting i -weight of the tableau agrees with the inner shape of the \pm diagram,
- the \bar{i} 's are placed in boxes containing $-$'s, starting from the right, and
- the result is a legal tableau.

Proposition 2.3.5. *Algorithm 2.3.4 bijectively maps the set of \pm diagrams of shape Λ to the set of D_{n-1} highest weight tableaux of shape Λ .*

Proof. The output of the algorithm is easily verified to be a D_{n-1} highest weight tableaux. The classical branching rule tells us that there are precisely as many such tableaux as \pm diagrams. By the pigeonhole principle, this correspondence must be bijective. \square

The notion of “ α_1 -height” of a D_{n-1} irreducible component $B(\lambda)$ as a subset of a D_n crystal $B(\Lambda)$ will play a crucial role in our understanding of branching component graphs. There are three equivalent ways to understand this statistic, each of which is useful in certain contexts.

Let T be an arbitrary element of $B(\lambda) \subset B(\Lambda)$. The definition of the α_1 -height of $B(\lambda)$ is simply the value of $\langle h_1, \mu \rangle$ where μ is the D_n weight of T . This is equal to the difference between the number of columns of Λ and the number of 1-arrows in a minimal path in the crystal graph between the highest weight tableau and T . Finally, we can also take this to be the number of 1's minus the number of $\bar{1}$'s in T , which is also the difference between $+$'s and $-$'s in the \pm diagram corresponding to $B(\lambda)$. In Algorithm 2.3.4, this is the statistic d .

Because the edges of the branching component graph indicate the action of f_1 , which decreases the α_1 -height by 1, this graph is the Hasse diagram of a ranked poset.

To avoid confusion with algebra rank, we use the term “stratum” to describe the poset ranks. Uniformly labeling the strata by their α_1 -height, we have that the stratum that is equidistant from the “highest weight” and “lowest weight” branching component vertices is designated “stratum 0”; the strata in the direction of the highest weight vertex are labeled by consecutive positive integers, those in the opposite direction by negative integers.

Proposition 2.3.6. *If $\lambda = (\lambda_1, \lambda_2, \dots, \lambda_\ell)$, then $\mathcal{BC}(\lambda)$ has $2\lambda_1 + 1$ strata. Furthermore, the partitions labeling stratum j also label stratum $-j$ for $0 \leq j \leq \lambda_1$, including multiplicities.*

Proof. The first of these follows from the observation that the α_1 -height ranges from λ_1 to $-\lambda_1$ in increments of 1. The second claim is a consequence of the symmetry of the weight lattice of any classical finite dimensional representation. \square

It therefore suffices to describe strata 0 through λ_1 for any $\mathcal{BC}(\lambda)$, appealing to symmetry for the negative strata.

Proposition 2.3.7. *Let v and w be vertices of a branching component graph with an edge between them. Then the partitions associated to v and w are adjacent in Young’s lattice; i.e., they differ by a single box.*

Proof. Observe that the Kashiwara operator f_1 only changes a single box of a tableau, either changing a 1 to a 2 or a $\bar{2}$ to a $\bar{1}$. It follows that the edges of the branching component graph only connect partitions that differ by a single box. In the case of changing a 1 to a 2, the partition associated with the new branching component vertex has one more box than the old one if the $-$ in the 2-signature from the new 2 is unbracketed; otherwise it has one less box. Conversely, when changing a $\bar{2}$ to a $\bar{1}$,

the partition associated with the new branching component vertex has one less box than the old one if the $+$ in the 2 signature from the disappearing $\bar{2}$ is unbracketed; otherwise it has one more box. \square

When characterizing branching component graphs, it therefore suffices to show that all edges described in the statements of Proposition 2.3.8 and Conjecture 2.3.11 are in fact present. We do not need to show that pairs of vertices whose partitions differ by more than one box are non-adjacent.

2.3.2 Rectangular partitions

Proposition 2.3.8. *Let $\lambda = (s, s, \dots, s)$ be a $k \times s$ rectangle. Then $\mathcal{BC}(\lambda)$ is as follows: stratum s of $\mathcal{BC}(\lambda)$ has a single vertex, which is labeled by a $(k - 1) \times s$ rectangle. The vertices of stratum $j - 1$ for $j \geq 1$ are labeled by one of each partition contained in λ that differs from some partition in stratum j by a single box and whose first $k - 2$ parts are s . Two vertices in strata j and $j - 1$ labeled by partitions μ_1 and μ_2 have an edge between them if μ_1 and μ_2 are adjacent in Young's lattice.*

Before proving this statement we examine the top two strata of $\mathcal{BC}(s\varpi_2)$ in detail. The highest weight branching component vertex (i.e., the branching component vertex containing the highest weight vertex) is indexed by the one-part partition (s) . To see that this is true, simply observe that the highest weight tableau of $B(s\varpi_2)$ is $\underbrace{\begin{matrix} 1 & \cdots & 1 \\ 2 & \cdots & 2 \end{matrix}}_s$, and acting by f_2, \dots, f_n in the most general possible way will affect only the bottom row. When we map these bottom row subtableaux componentwise by $a \mapsto a - 1$ and $\bar{a} \mapsto \overline{a - 1}$ to tableaux of shape (s) , and apply the same map to the colors of the arrows, this is clearly isomorphic to the D_{n-1} -crystal with highest weight $s\varpi_1$.

According to Algorithm 2.3.4 and the D_n to D_{n-1} branching rule, the two D_{n-1} highest weight tableaux in stratum $s - 1$ are

$$\begin{array}{ccccc} 1 & 1 & \cdots & 1 & 2 \\ 2 & 2 & \cdots & 2 & 3 \end{array} \quad \text{and} \quad \begin{array}{ccccc} 1 & 1 & \cdots & 1 & 2 \\ 2 & 2 & \cdots & 2 & \bar{2} \end{array}.$$

In the former case, the operators f_2, \dots, f_n act freely on the bottom row and the rightmost box in the top row; in the latter case, they act on all boxes in the bottom row except the rightmost, since f_i, e_i for $i = 2, \dots, n$ do not act on the last column. It follows that the corresponding partitions are $(s, 1)$ and $(s - 1)$, with respective \pm diagrams

$$\begin{array}{|c|c|c|c|c|} \hline & & \cdots & & \\ \hline & + & \cdots & + & + \\ \hline \end{array} \quad \text{and} \quad \begin{array}{|c|c|c|c|c|} \hline & & \cdots & & + \\ \hline + & + & \cdots & + & - \\ \hline \end{array}.$$

Now, observe what can result from acting on a tableau $T = \begin{smallmatrix} a_1 & \cdots & a_s \\ b_1 & \cdots & b_s \end{smallmatrix}$ in the highest weight branching component vertex by f_1 . Since $a_1 = \cdots = a_s = 1$, a_s will turn into a 2. There are two cases to consider: if $b_s = \bar{2}$, this results in a tableau with a configuration $\bar{2}$ at the right end; otherwise, it is a tableau with $a_1 = \cdots = a_{s-1} = 1$ where some element of D_{n-1} can act on the rightmost column. It follows that there are edges from the vertex in stratum s to both of the vertices in stratum $s - 1$.

Proof of Proposition 2.3.8. The number of each partition and their strata follow from Algorithm 2.3.4 and the D_n to D_{n-1} branching rule. Explicitly, consider the content of stratum j , which is determined by the set of \pm diagrams such that the difference between the number of +’s and the number of -’s is j . Thanks to Proposition 2.3.6, we may assume $j \geq 0$. Because we currently only consider rectangular partitions, the possible configurations of +’s and -’s can be explicitly characterized. First, we have

ℓ columns with only a $+$ in the last row with $j \leq \ell \leq s$. We furthermore have $\ell - j$ columns with only a $-$ in the last row, located immediately to the right of the columns with only a $+$. Finally, we may have between 0 and $s - 2\ell + j$ columns with a \pm pair in the last two rows, located immediately to the right of the columns with only a $-$ and extending to the right edge of the rectangle. The choices of the number of $+$'s and \pm columns are independent of each other up to the bounds described above. In other words, stratum j has one vertex for each partition contained in a $k \times s$ rectangle such that the first $k - 2$ parts are s , the last part is no greater than $s - j$, and the difference between the size of the partition and $k \times s$ is congruent mod 2 to j . This is equivalent to the characterization of vertices prescribed by Proposition 2.3.8; i.e., those partitions contained in a $k \times s$ rectangle such that the first $k - 2$ parts are s and which differ from a $(k - 1) \times s$ rectangle by $s - j$ additions or removals of boxes in the last two rows.

To show that the edges of this graph are as prescribed by Proposition 2.3.8, we explicitly construct tableaux with the following properties. Each of these tableaux is in a D_{n-1} crystal whose highest weight corresponds to a partition that can have a box added in at least one of the last two rows. We will then show that acting by the Kashiwara operator f_1 produces a tableau in a D_{n-1} crystal whose highest weight corresponds to the partition with one of the last two rows augmented thusly.

The claims that f_1 may also have the effect of removing a box from one of the last two rows of the partition labeling its D_{n-1} crystal's highest weight follows by the $*$ -duality of the crystal. To see this, let v be a branching component vertex labeled by a partition μ such that $\mu_k \geq 1$ (and consequently j , the stratum of v , is at least $-s+1$); we wish to show that there is an edge from v to w , where w is in stratum $j-1$ and its partition differs from μ only by diminishing the last part by one. We know

that there is a vertex v' also labeled by μ in stratum $-j$ called the complementary vertex of v ; the vertices in $B(v')$ are precisely the image under the $*$ map of the vertices in $B(v)$. We know from the above paragraph that v' has an incoming edge from w' , the complementary vertex of w . This means that for some crystal vertex $b \in B(w')$, we know that $f_1 b \in B(v')$. It follows that $e_1(b^*) \in B(v)$ and $b^* \in B(w)$, and we thus conclude that there is an edge from v to w . An identical argument shows that a branching component vertex v in stratum $j \geq -s + 1$ labeled by a partition μ such that $\mu_{k-1} \geq \mu_k + 1$ has an edge to the vertex w in stratum $j - 1$ whose partition differs from μ only by diminishing the penultimate part by one.

We now construct tableaux such that the action of the Kashiwara operator f_1 has the described effect on the branching component vertices. We begin by constructing an arbitrary D_{n-1} highest weight tableau, as given by Algorithm 2.3.4. We have two cases to consider. One is

$$\begin{array}{cccccccccccc}
 1 & \cdots & 1 & 1 & \cdots & 1 & 2 & \cdots & 2 & 2 & \cdots & 2 \\
 2 & \cdots & 2 & 2 & \cdots & 2 & 3 & \cdots & 3 & 3 & \cdots & 3 \\
 \vdots & \cdots & \vdots & \vdots & \cdots & \vdots & \vdots & \cdots & \vdots & \vdots & \cdots & \vdots \\
 k-1 & \cdots & k-1 & k-1 & \cdots & k-1 & k & \cdots & k & k & \cdots & k \\
 k & \cdots & k & k+1 & \cdots & k+1 & k+1 & \cdots & k+1 & \bar{1} & \cdots & \bar{1} \\
 \underbrace{\hspace{10em}}_{s_1} & \underbrace{\hspace{10em}}_{s_2} & \underbrace{\hspace{10em}}_{s_3} & \underbrace{\hspace{10em}}_{s_4}
 \end{array}$$

with D_{n-1} weight $s_2\varpi_{k-2} + (s_1 + s_4 - s_2)\varpi_{k-1} + (s_2 + s_3)\varpi_k$. This tableau corresponds by Algorithm 2.3.4 to the \pm diagram with s_1 columns with a $+$, $s_4 - s_2$ columns with

a $-$, and s_2 columns with a \pm pair. Note that this implies $s_2 \leq s_4$. The other case is

$$\begin{array}{cccccccccccc}
 1 & \cdots & 1 & 1 & \cdots & 1 & 1 & \cdots & 1 & 2 & 2 & \cdots & 2 \\
 2 & \cdots & 2 & 2 & \cdots & 2 & 2 & \cdots & 2 & 3 & 3 & \cdots & 3 \\
 \vdots & \cdots & \vdots & \vdots & \cdots & \vdots & \vdots & \vdots & \cdots & \vdots & \vdots & \cdots & \vdots \\
 k-1 & \cdots & k-1 & k-1 & \cdots & k-1 & k-1 & \cdots & k-1 & k & k & \cdots & k \\
 k & \cdots & k & k+1 & \cdots & k+1 & \bar{k} & \cdots & \bar{k} & \bar{k} & \bar{1} & \cdots & \bar{1}
 \end{array}$$

$$\underbrace{\hspace{10em}}_{s_1} \quad \underbrace{\hspace{10em}}_{s_2} \quad \underbrace{\hspace{10em}}_{s_3} \quad \delta \quad \underbrace{\hspace{10em}}_{s_4}$$

where δ may be 0 or 1. This tableau has D_{n-1} weight $(s_2 + 2s_3 + \delta)\varpi_{k-2} + (s_1 + s_4 - s_2 - s_3)\varpi_{k-1} + s_2\varpi_k$, corresponding by Algorithm 2.3.4 to the \pm diagram with s_1 columns with a $+$, $s_4 - s_2 - s_3$ columns with a $-$, and s_2 columns with a \pm pair. In this case we must have $s_2 + s_3 \leq s_4$. To make the second case exclusive of the first, we add the requirement that $\delta + s_3 > 0$.

Consider the action on these tableaux of the sequence $f_1 f_2 \cdots f_{k-1}$. In the first case, we assume $s_2 \neq 0$, otherwise the $k - 1^{\text{st}}$ part of the associated partition has size s . We therefore know that this sequence acts entirely on the $(s_1 + s_2)^{\text{th}}$ column, counting from the left. It has the effect of increasing by 1 each entry in this column except the bottom entry, resulting in the D_{n-1} highest weight tableau with D_{n-1} weight $(s_2 - 1)\varpi_{k-2} + (s_1 + s_4 - s_2 + 1)\varpi_{k-1} + (s_2 + s_3)\varpi_k$.

In the second case, we consider the subcases of $\delta = 0$ and $\delta = 1$. If $\delta = 0$, we have $s_3 \neq 0$, and the sequence $f_1 f_2 \cdots f_{k-1}$ acts entirely on the $(s_1 + s_2 + s_3)^{\text{th}}$ column, counting from the left, resulting in the D_{n-1} highest weight tableau with D_{n-1} weight $(s_2 + 2s_3 - 1)\varpi_{k-2} + (s_1 + s_4 - s_2 - s_3 + 1)\varpi_{k-1} + s_2\varpi_k$. On the other hand, if $\delta = 1$, this sequence acts entirely on the letter in the bottom row

of the “ δ ” column, giving us the D_{n-1} highest weight tableau with D_{n-1} weight $(s_2 + 2s_3)\varpi_{k-2} + (s_1 + s_4 - s_2 - s_3 + 1)\varpi_{k-1} + s_2\varpi_k$.

In any case, we have constructed a tableau (namely, $f_2 f_3 \cdots f_{k-1}$ applied to a D_{n-1} highest weight tableau) such that acting by f_1 adds a box to the penultimate row of the partition associated to its branching component vertex, according to Algorithm 2.3.4.

Moving our attention to adding a box in the last row, consider the tableau that results from applying the sequence of operators

$$f_2^{s_1+s_4-s_2} f_3^{s_1+s_4-s_2} \cdots f_k^{s_1+s_4-s_2}$$

to our first case of highest weight tableau. This produces

$$\begin{array}{cccccccccccccccc}
 1 & \cdots & 1 & 1 & \cdots & 1 & 2 & \cdots & 2 & 2 & \cdots & 2 & 3 & \cdots & 3 \\
 2 & \cdots & 2 & 3 & \cdots & 3 & 3 & \cdots & 3 & 3 & \cdots & 3 & 4 & \cdots & 4 \\
 \vdots & \cdots & \vdots & \vdots & \cdots & \vdots & \vdots & \cdots & \vdots & \vdots & \cdots & \vdots & \vdots & \cdots & \vdots \\
 k-1 & \cdots & k-1 & k & \cdots & k & k & \cdots & k & k & \cdots & k & k+1 & \cdots & k+1 \\
 k+1 & \cdots & k+1 & k+1 & \cdots & k+1 & k+1 & \cdots & k+1 & \bar{1} & \cdots & \bar{1} & \bar{1} & \cdots & \bar{1}
 \end{array}$$

$$\underbrace{\hspace{10em}}_{s_2} \quad \underbrace{\hspace{10em}}_{s_1} \quad \underbrace{\hspace{10em}}_{s_3} \quad \underbrace{\hspace{10em}}_{s_2} \quad \underbrace{\hspace{10em}}_{s_4-s_2}$$

Applying f_1 to this tableau gives us

1	...	1	1	...	1	2	...	2	2	...	2	3	...	3	
2	...	2	3	...	3	3	...	3	3	...	3	4	...	4	
⋮	...	⋮	⋮	...	⋮	⋮	...	⋮	⋮	...	⋮	⋮	...	⋮	
$k-1$...	$k-1$	k	...	k	k	...	k	k	...	k	$k+1$...	$k+1$	
$k+1$...	$k+1$	$k+1$...	$k+1$	$k+1$...	$k+1$	$\bar{1}$...	$\bar{1}$	$\bar{1}$...	$\bar{1}$	
⏟		⏟		⏟		⏟		⏟		⏟		⏟		⏟	
s_2		s_1-1		s_3+1		s_2		s_4-s_2		s_2		s_4-s_2		s_4-s_2	

and on this tableau the sequence

$$e_k^{s_1+s_4-s_2-1} e_{k-1}^{s_1+s_4-s_2-1} \dots e_2^{s_1+s_4-s_2-1}$$

produces a D_{n-1} highest weight tableau with D_{n-1} weight $s_2\varpi_{k-2} + (s_1 + s_4 - s_2 - 1)\varpi_{k-1} + (s_2 + s_3 + 1)\varpi_k$, corresponding to adding a box to the last row of the associated partition.

We now consider the sequence

$$F = f_2^{s_1+s_4-s_2-s_3} f_3^{s_1+s_4-s_2-s_3} \dots f_k^{s_1+s_4-s_2-s_3}$$

applied to our second case of highest weight tableau. We consider separately the cases of whether s_1 is greater than or less than $2s_3 + \delta$.

If $s_1 \leq 2s_3 + \delta$, the sequence F applied to our highest weight tableau produces

$$\begin{array}{cccccccccccccccc}
 1 & \cdots & 1 & 1 & \cdots & 1 & & 1 & 1 & \cdots & 1 & 2 & 2 & \cdots & 2 & 3 & \cdots & 3 \\
 2 & \cdots & 2 & 2 & \cdots & 2 & & 3 & 3 & \cdots & 3 & 3 & 3 & \cdots & 3 & 4 & \cdots & 4 \\
 \vdots & \cdots & \vdots & \vdots & \cdots & \vdots & & \vdots & \vdots & \cdots & \vdots & \vdots & \vdots & \cdots & \vdots & \vdots & \cdots & \vdots \\
 k-1 & \cdots & k-1 & k-1 & \cdots & k-1 & & k & k & \cdots & k & k & k & \cdots & k & k+1 & \cdots & k+1 \\
 k+1 & \cdots & k+1 & \bar{k} & \cdots & \bar{k} & & \bar{k} & \bar{2} & \cdots & \bar{2} & \bar{2} & \bar{1} & \cdots & \bar{1} & \bar{1} & \cdots & \bar{1}
 \end{array}$$

$$\underbrace{\hspace{10em}}_{s_1+s_2} \quad \underbrace{\hspace{10em}}_{s_3 - \lfloor \frac{s_1-\delta}{2} \rfloor} \quad (s_1 - \delta)_{\text{mod}2} \quad \underbrace{\hspace{10em}}_{\lfloor \frac{s_1-\delta}{2} \rfloor} \quad \delta \quad \underbrace{\hspace{10em}}_{s_2+s_3} \quad \underbrace{\hspace{10em}}_{s_4-s_2-s_3}$$

and if $s_1 > 2s_3 + \delta$, we have

$$\begin{array}{cccccccccccccccc}
 1 & \cdots & 1 & 1 & \cdots & 1 & 1 & \cdots & 1 & 2 & 2 & \cdots & 2 & 3 & \cdots & 3 \\
 2 & \cdots & 2 & 3 & \cdots & 3 & 3 & \cdots & 3 & 3 & 3 & \cdots & 3 & 4 & \cdots & 4 \\
 \vdots & \cdots & \vdots & \vdots & \cdots & \vdots & \vdots & \cdots & \vdots & \vdots & \vdots & \cdots & \vdots & \vdots & \cdots & \vdots \\
 k-1 & \cdots & k-1 & k & \cdots & k & k & \cdots & k & k & k & \cdots & k & k+1 & \cdots & k+1 \\
 k+1 & \cdots & k+1 & k+1 & \cdots & k+1 & \bar{2} & \cdots & \bar{2} & \bar{2} & \bar{1} & \cdots & \bar{1} & \bar{1} & \cdots & \bar{1}
 \end{array}$$

$$\underbrace{\hspace{10em}}_{s_2+2s_3+\delta} \quad \underbrace{\hspace{10em}}_{s_1-(2s_3-\delta)} \quad \underbrace{\hspace{10em}}_{s_3} \quad \delta \quad \underbrace{\hspace{10em}}_{s_2+s_3} \quad \underbrace{\hspace{10em}}_{s_4-s_2-s_3}$$

We treat the subcases of $\delta = 0$ and $\delta = 1$ separately. In both of the above tableaux, if $\delta = 1$, the Kashiwara operator f_1 acts on the $\bar{2}$ at the bottom of the δ column, and if $\delta = 0$, it acts on the 1 at the top of the column immediately to the left of where the δ column would be.

If $s_1 \leq 2s_3 + \delta$ and $\delta = 0$ we get

$$\begin{array}{cccccccccccccccc}
 1 & \cdots & 1 & 1 & \cdots & 1 & 1 & 1 & \cdots & 1 & 2 & 2 & \cdots & 2 & 3 & \cdots & 3 \\
 2 & \cdots & 2 & 2 & \cdots & 2 & 3 & 3 & \cdots & 3 & 3 & 3 & \cdots & 3 & 4 & \cdots & 4 \\
 \vdots & \cdots & \vdots & \vdots & \cdots & \vdots & \vdots & \vdots & \cdots & \vdots & \vdots & \vdots & \cdots & \vdots & \vdots & \cdots & \vdots \\
 k-1 & \cdots & k-1 & k-1 & \cdots & k-1 & k & k & \cdots & k & k & k & \cdots & k & k+1 & \cdots & k+1 \\
 k+1 & \cdots & k+1 & \bar{k} & \cdots & \bar{k} & \bar{k} & \bar{2} & \cdots & \bar{2} & \bar{2} & \bar{1} & \cdots & \bar{1} & \bar{1} & \cdots & \bar{1}
 \end{array}$$

$$\underbrace{\hspace{10em}}_{s_1+s_2} \quad \underbrace{\hspace{10em}}_{s_3 - \lfloor \frac{s_1-\delta}{2} \rfloor} \quad (s_1 - \delta)_{\text{mod}2} \quad \underbrace{\hspace{10em}}_{\lfloor \frac{s_1-\delta}{2} \rfloor - 1} \quad 1 \quad \underbrace{\hspace{10em}}_{s_2+s_3} \quad \underbrace{\hspace{10em}}_{s_4-s_2-s_3}$$

If $s_1 \leq 2s_3 + \delta$ and $\delta = 1$ we get

$$\begin{array}{cccccccccccccccc}
 1 & \cdots & 1 & 1 & \cdots & 1 & 1 & 1 & \cdots & 1 & 2 & \cdots & 2 & 3 & \cdots & 3 \\
 2 & \cdots & 2 & 2 & \cdots & 2 & 3 & 3 & \cdots & 3 & 3 & \cdots & 3 & 4 & \cdots & 4 \\
 \vdots & \cdots & \vdots & \vdots & \cdots & \vdots & \vdots & \vdots & \cdots & \vdots & \vdots & \cdots & \vdots & \vdots & \cdots & \vdots \\
 k-1 & \cdots & k-1 & k-1 & \cdots & k-1 & k & k & \cdots & k & k & \cdots & k & k+1 & \cdots & k+1 \\
 k+1 & \cdots & k+1 & \bar{k} & \cdots & \bar{k} & \bar{k} & \bar{2} & \cdots & \bar{2} & \bar{1} & \cdots & \bar{1} & \bar{1} & \cdots & \bar{1}
 \end{array}$$

$$\underbrace{\hspace{10em}}_{s_1+s_2} \quad \underbrace{\hspace{10em}}_{s_3 - \lfloor \frac{s_1-\delta}{2} \rfloor} \quad (s_1 - \delta)_{\text{mod}2} \quad \underbrace{\hspace{10em}}_{\lfloor \frac{s_1-\delta}{2} \rfloor} \quad \underbrace{\hspace{10em}}_{s_2+s_3+1} \quad \underbrace{\hspace{10em}}_{s_4-s_2-s_3}$$

On the other hand, if $s_1 > 2s_3 + \delta$ and $\delta = 0$, we have

$$\begin{array}{cccccccccccccccc}
 1 & \cdots & 1 & 1 & \cdots & 1 & 1 & \cdots & 1 & 2 & 2 & \cdots & 2 & 3 & \cdots & 3 \\
 2 & \cdots & 2 & 3 & \cdots & 3 & 3 & \cdots & 3 & 3 & 3 & \cdots & 3 & 4 & \cdots & 4 \\
 \vdots & \cdots & \vdots & \vdots & \cdots & \vdots & \vdots & \cdots & \vdots & \vdots & \vdots & \cdots & \vdots & \vdots & \cdots & \vdots \\
 k-1 & \cdots & k-1 & k & \cdots & k & k & \cdots & k & k & k & \cdots & k & k+1 & \cdots & k+1 \\
 k+1 & \cdots & k+1 & k+1 & \cdots & k+1 & \bar{2} & \cdots & \bar{2} & \bar{2} & \bar{1} & \cdots & \bar{1} & \bar{1} & \cdots & \bar{1}
 \end{array}$$

$$\underbrace{\hspace{10em}}_{s_2+2s_3+\delta} \quad \underbrace{\hspace{10em}}_{s_1-(2s_3-\delta)} \quad \underbrace{\hspace{10em}}_{s_3-1} \quad 1 \quad \underbrace{\hspace{10em}}_{s_2+s_3} \quad \underbrace{\hspace{10em}}_{s_4-s_2-s_3}$$

and if $s_1 > 2s_3 + \delta$ and $\delta = 1$, we have

$$\begin{array}{ccccccccccccccc}
 1 & \cdots & 1 & 1 & \cdots & 1 & 1 & \cdots & 1 & 2 & \cdots & 2 & 3 & \cdots & 3 \\
 2 & \cdots & 2 & 3 & \cdots & 3 & 3 & \cdots & 3 & 3 & \cdots & 3 & 4 & \cdots & 4 \\
 \vdots & \cdots & \vdots & \vdots & \cdots & \vdots & \vdots & \cdots & \vdots & \vdots & \cdots & \vdots & \vdots & \cdots & \vdots \\
 k-1 & \cdots & k-1 & k & \cdots & k & k & \cdots & k & k & \cdots & k & k+1 & \cdots & k+1 \\
 k+1 & \cdots & k+1 & k+1 & \cdots & k+1 & \bar{2} & \cdots & \bar{2} & \bar{1} & \cdots & \bar{1} & \bar{1} & \cdots & \bar{1}
 \end{array}$$

$$\underbrace{\hspace{10em}}_{s_2+2s_3+\delta} \quad \underbrace{\hspace{10em}}_{s_1-(2s_3-\delta)} \quad \underbrace{\hspace{3em}}_{s_3} \quad \underbrace{\hspace{3em}}_{s_2+s_3+1} \quad \underbrace{\hspace{10em}}_{s_4-s_2-s_3}$$

In all of these cases, we find that applying the sequence

$$E = e_k^{(s_1+s_4-s_2-s_3-1)} e_3^{(s_1+s_4-s_2-s_3-1)} \dots e_2^{(s_1+s_4-s_2-s_3-1)}$$

has the effect of producing the tableau

$$\begin{array}{ccccccccccccccc}
 1 & \cdots & 1 & 1 & \cdots & 1 & 1 & \cdots & 1 & 2 & 2 & \cdots & 2 \\
 2 & \cdots & 2 & 2 & \cdots & 2 & 2 & \cdots & 2 & 3 & 3 & \cdots & 3 \\
 \vdots & \cdots & \vdots & \vdots & \cdots & \vdots & \vdots & \vdots & \cdots & \vdots & \vdots & \cdots & \vdots \\
 k-1 & \cdots & k-1 & k-1 & \cdots & k-1 & k-1 & \cdots & k-1 & k & k & \cdots & k \\
 k & \cdots & k & k+1 & \cdots & k+1 & \bar{k} & \cdots & \bar{k} & \bar{k} & \bar{1} & \cdots & \bar{1}
 \end{array}$$

$$\underbrace{\hspace{10em}}_{s_1-1} \quad \underbrace{\hspace{10em}}_{s_2+1} \quad \underbrace{\hspace{10em}}_{s_3-\bar{\delta}} \quad 1-\delta \quad \underbrace{\hspace{10em}}_{s_4+\delta}$$

This tableau is a D_{n-1} highest weight tableau with D_{n-1} weight $(s_2 + 2s_3 + \delta)\varpi_{k-2} + (s_1 + s_4 - s_2 - s_3 - 1)\varpi_{k-1} + (s_2 + 1)\varpi_k$, which precisely corresponds to adding a box to the last row of the partition we started with. □

Example 2.3.9. Figure 2.3.2.2 depicts the non-negative strata of $\mathcal{BC}((3))$.

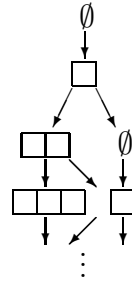


Figure 2.3.2.2: Strata 3 through 0 of the branching component graph $\mathcal{BC}((3))$

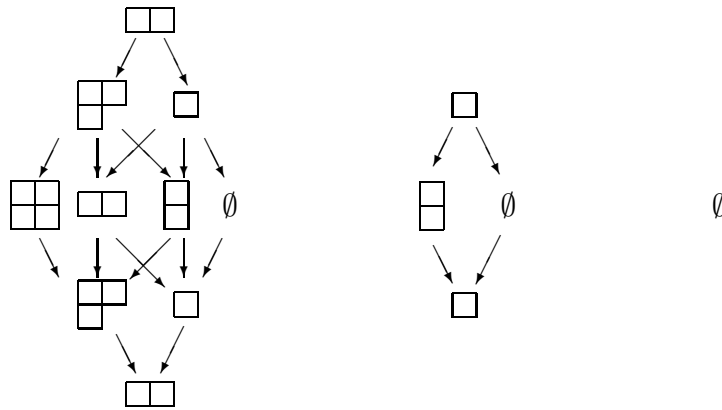


Figure 2.3.2.3: Branching component graph $\mathcal{BC}(B^{2,2})$

Example 2.3.10. Figure 2.3.2.3 depicts $\mathcal{BC}(B^{2,2})$, which is the union of $\mathcal{BC}(\emptyset)$, $\mathcal{BC}((1, 1))$, and $\mathcal{BC}((2, 2))$.

2.3.3 Arbitrary partitions

All partitions can be constructed by vertically juxtaposing some number of rectangles all with different heights. Just as we can build up these partitions, we can also build up the branching component graphs by combining the graphs for those constituent rectangles.

Note that while the structure of branching component graphs for non-rectangular

partitions is presented as a conjecture, the main result of this chapter (Conjecture 1.2.1) does not depend on its validity. It is included here simply to present as much information as possible about branching component graphs. Also note that the statements regarding the vertices and their associated D_{n-1} weights is proved; only the properties of edges are conjectural.

Conjecture 2.3.11. *Let $\lambda^{(1)}, \lambda^{(2)}$ be partitions, let $\ell(\lambda^{(2)})$ denote the number of parts of $\lambda^{(2)}$, and let $m_1^{(1)}$ denote the multiplicity of $\lambda_1^{(1)}$ in $\lambda^{(1)}$. Suppose that $\ell(\lambda^{(2)}) \leq m_1^{(1)} - 2$. Let $\lambda^{(1)}\lambda^{(2)}$ denote the horizontal concatenation of $\lambda^{(1)}$ and $\lambda^{(2)}$; i.e. $(\lambda^{(1)}\lambda^{(2)})_i = \lambda_i^{(1)} + \lambda_i^{(2)}$. Then*

$$\mathcal{BC}(\lambda^{(1)}\lambda^{(2)}) = \mathcal{BC}(\lambda^{(1)}) \times \mathcal{BC}(\lambda^{(2)}),$$

where \times denotes the directed graph product of the two smaller graphs, and the vertex $(\mu^{(1)}, \mu^{(2)})$ is labeled by $\mu^{(1)}\mu^{(2)}$.

Proof. The construction of \pm diagrams treats each maximal rectangle in such a partition independently, and the difference between the number of $+$'s and $-$'s is additive, so the partitions, their multiplicities, and their strata are given precisely by the above proposition.

Now, as in the proof of 2.3.8, we give sequences of operators that have the effect of adding a box to a row of a partition indexing a branching component vertex. Suppose that $\mu = \mu^{(1)}\mu^{(2)}$ is a partition such that in $\mathcal{BC}(\lambda^{(1)})$ and $\mathcal{BC}(\lambda^{(2)})$, at least one of $\mu^{(1)}$ or $\mu^{(2)}$ has an edge to the partition differing from it by the addition of a box in the k^{th} row. Denote the partition differing from μ by the addition of a box in the k^{th} row by μ_{+k} . Our conjecture breaks into two cases. If k is not congruent modulo 2 to the

number of parts of λ , we claim that the sequence

$$f_1 f_2 \cdots f_k$$

applied to the D_{n-1} highest weight tableau of $B(\mu)$ produces the D_{n-1} highest weight tableau of $B(\mu_{+k})$. Otherwise, k is congruent modulo 2 to the number of parts of λ . Let r be the number of columns of height k in μ . Then the sequence

$$e_k^{r-1} e_{k-1}^{r-1} \cdots e_2^{r-1} f_1 f_2 f_3 \cdots f_k^r$$

applied to the D_{n-1} highest weight tableau of $B(\mu)$ produces the D_{n-1} highest weight tableau of $B(\mu_{+k})$. Compare these statements to those of Proposition 2.3.8.

The heuristic for these to be separate cases is that the first corresponds to removing the $+$ from a \pm pair in a single column, whereas the second case corresponds to removing a $+$ from a column where it was alone.

□

Proposition 2.3.8 and Conjecture 2.3.11 characterize all branching component graphs in our current scope of interest, since for a classical component $B(\mu)$ to be in $B^{r,s}$, the complement of μ in an $r \times s$ rectangle must be tileable by vertical dominos.

2.4 The Crystal Automorphism

Recall that the automorphism $\sigma : B^{r,s} \rightarrow B^{r,s}$, where $B^{r,s}$ is taken as a D_{n-1} -crystal, corresponds to the $D_n^{(1)}$ Dynkin diagram automorphism interchanging nodes 0 and 1. As a result, we know that σ must be a crystal isomorphism when restricted to any

D_{n-1} -crystal corresponding to a vertex in $\mathcal{BC}(B^{r,s})$. We may therefore describe σ by first specifying a shape-preserving automorphism $\check{\sigma}$ of $\mathcal{BC}(B^{r,s})$, then defining σ to be the union of the corresponding crystal isomorphisms.

To explicitly determine $\sigma(b)$ from $\check{\sigma}$ for any $b \in B^{r,s}$, let v be the branching component vertex such that $b \in B(v)$, and let T_v denote the D_{n-1} -highest weight vertex of $B(v)$. We know that for some finite sequence i_1, \dots, i_k of integers in $\{2, \dots, n\}$, we have $f_{i_1} \cdots f_{i_k} T_v = b$. Let $T_{\check{\sigma}(v)}$ be the highest weight vector of $B(\check{\sigma}(v))$. For any such sequence of integers, we may define $\sigma(b) = f_{i_1} \cdots f_{i_k} T_{\check{\sigma}(v)}$.

Proposition 2.4.1. *Let $b \in B^{r,s}$, and suppose $f_0(b) \neq 0$. Then the stratum of $f_0(b)$ must be one greater than the stratum of b , and therefore the map $\check{\sigma}$ must send a vertex from stratum j to a vertex in stratum $-j$.*

Proof. Recall from the weight structure of type D algebras that $\alpha_0 = 2\Lambda_0 - \varpi_2$ and $\text{wt}(f_0(b)) = \text{wt}(b) - \alpha_0$. Define $\text{cw}(b) = \text{wt}(b) - (\varphi_0(b) - \varepsilon_0(b))\Lambda_0$. The above implies that $\text{cw}(f_0(b)) = \text{cw}(b) + \varpi_2 = \text{cw}(b) + (e_1 + e_2)$, where e_1, e_2 are the first and second elementary basis vectors in the weight space. Similarly, $\text{cw}(f_i(b)) = \text{cw}(b) - \alpha_i$ for $i = 1, \dots, n$, so that among f_1, \dots, f_n , only f_1 changes the e_1 component of a weight by -1 . Since f_1 decreases the stratum by one and f_0 changes the e_1 component of a weight by $+1$, it follows that f_0 increases the stratum by one. \square

Recall that \pm diagrams can be used to label vertices of $\mathcal{BC}(B^{r,s})$. We state a conjectural construction of $\check{\sigma}$ due to Schilling and Shimozono [43] defined in terms of \pm diagrams that satisfies the condition of Proposition 2.4.1.

Conjecture 2.4.2. *Let D be a \pm diagram of shape Λ/λ such that the complement of Λ in an $r \times s$ rectangle can be tiled by vertical dominos. Let m_i^o, m_i^+, m_i^- and m_i^\pm*

denote the number of columns of height i in D with no symbol, a $+$, a $-$, and a \pm pair, respectively. If r is even, set $m_0^\circ = s - \Lambda_1$. Note that if $i \equiv r + 1 \pmod{2}$ then $m_i^* = 0$ for $* \in \{\circ, +, -, \pm\}$. Then $\check{\sigma}(D)$ is the \pm diagram with m_{i+2}^\pm empty columns of height i , m_i^- columns of height i with a $+$, m_i^+ columns of height i with a $-$, and m_i° columns of height $i + 2$ with a \pm pair for all $0 \leq i \leq r$.

This conjectural $\check{\sigma}$ also respects a symmetry that appears in the poset of D_n components of $B^{r,s}$. To state this precisely, we need to know which D_n components of $B^{r,s}$ have μ as a D_{n-1} highest weight. In other words, we want to know for which outer shapes Λ there is a \pm diagram with inner shape μ . The smallest such partition, which we denote by $\mu_{\check{0}}$, is the outer shape of the \pm diagram with inner shape μ none of whose columns have a \pm pair. Complementarily, the largest such partition, which we denote by $\mu_{\check{1}}$, is the outer shape of the \pm diagram of which μ is the inner shape and such that every column of height less than r has at least one $+$ or one $-$ in it. It is also the result of adding a vertical domino with a \pm pair to those columns of $\mu_{\check{0}}$ that have fewer than r boxes and do not have a $+$ or $-$ in them.

Remark 2.4.3. In the above, $\mu_{\check{0}}$ and $\mu_{\check{1}}$ depend on the parity of r .

Example 2.4.4. Consider those classical components $B(\lambda)$ of $B^{4,4}$ for which $\mu = (2, 1)$ is associated with a vertex of $\mathcal{BC}(\lambda)$. The smallest such λ is $\mu_{\check{0}} = (2, 2)$; the largest is $\mu_{\check{1}} = (4, 4, 1, 1)$. The intermediate partitions are $(2, 2, 1, 1)$, $(3, 3)$, $(3, 3, 1, 1)$, and $(4, 4)$.

Given a partition λ whose complement is tiled by vertical dominos, let $\bar{\lambda}$ be the partition whose columns have length equal to the floor of half the length of the columns of λ . In words, $\bar{\lambda}$ is the result of including only every other part of λ ,

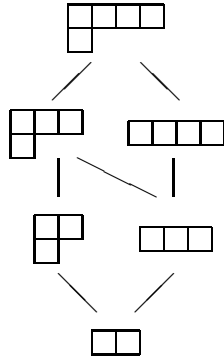


Figure 2.4.2.1: Interval in Young's lattice between (2) and $(4, 1)$

omitting the first part if λ has an odd number of parts. It is easy to see that $\overline{\mu_0}$ and $\overline{\mu_1}$ differ by a horizontal strip, and that the partitions containing μ as described above form the poset interval between them in Young's lattice. Consider the multiset of rows with boxes in $\overline{\mu_1}/\overline{\mu_0}$. Taking the complement in this multiset provides a canonical symmetry of this interval. Explicitly, define the map t from this interval to itself by saying that both $\lambda/\overline{\mu_0}$ and $\overline{\mu_1}/t(\lambda)$ must have m_i boxes in row i .

Conjecture 2.4.2 implies that $\check{\sigma}$ respects this symmetry. Observe that the outer shape of $\check{\sigma}(D)$ differs from $\text{outer}(D)$ by replacing m_i^\pm columns with \pm pairs by $c_{i-2} - m_i^\pm$ many such columns when $i \equiv r \pmod{2}$. This is precisely the same involution of the interval as t in the above paragraph.

Example 2.4.5. Consider $\mu = (2, 1)$ in $B^{4,4}$ as in Example 2.4.4 above. The interval between $\overline{\mu_0}$ and $\overline{\mu_1}$ is shown in figure 2.4.2.1.

In the case of $r = 2$ these intervals are simply linear orderings, and Conjecture 2.4.2 has been proved in this special case (Theorem 1.2.2; see Section 3.3). This symmetry appears to be the only generally consistent procedure for determining what

the classical component of $\check{\sigma}(v)$ should be, and it is the most natural generalization of the behavior of $\check{\sigma}$ in the case of $B^{2,s}$.

We have now defined $\check{\sigma}$ on $\mathcal{BC}(B^{r,s})$, which in turn defines σ on $B^{r,s}$.

Conjecture 2.4.6 (Restatement of Conjecture 1.2.1). *Define a $D_n^{(1)}$ -crystal $\tilde{B}^{r,s}$ by adding 0 arrows to the classical crystals according to the rule*

$$f_0 = \sigma f_1 \sigma.$$

Then if $B^{r,s}$ exists, $\tilde{B}^{r,s} \simeq B^{r,s}$.

Chapter 3

The Family $B^{2,s}$ of Type D

Kirillov-Reshetikhin Modules

3.1 Specialization of previous work to $r = 2$

In this chapter we restrict our attention to $B^{2,s}$, proving Theorems 1.2.2 and 1.2.3. We begin by specializing the statements and constructions of Chapter 2 to the case of $r = 2$.

3.1.1 Classical tableaux

First, we note that given the assumption that our tableaux are height 2 rectangles, the following simpler Criterion replaces Criterion 2.2.1.

Criterion 3.1.1.

1. If ab is in the filling, then $a \leq b$;
2. If $\begin{smallmatrix} a \\ b \end{smallmatrix}$ is in the filling, then $b \not\leq a$;

- 3. No configuration of the form $\begin{smallmatrix} a & a \\ \bar{a} & \bar{a} \end{smallmatrix}$ or $\begin{smallmatrix} a & \\ \bar{a} & \bar{a} \end{smallmatrix}$ appears;
- 4. No configuration of the form $\begin{smallmatrix} n-1 & & n \\ n & \dots & n-1 \end{smallmatrix}$ or $\begin{smallmatrix} n-1 & & \bar{n} \\ \bar{n} & \dots & n-1 \end{smallmatrix}$ appears;
- 5. No configuration of the form $\begin{smallmatrix} 1 \\ \bar{1} \end{smallmatrix}$ appears.

Note that for $k \geq 2$, condition 5 follows from conditions 1 and 3. Also, observe that Criterion 3.1.1 is unchanged by replacing condition 4 with the following:

- (4a) No configuration of the form $\begin{smallmatrix} n-1 & n \\ n & n-1 \end{smallmatrix}$ or $\begin{smallmatrix} n-1 & \bar{n} \\ \bar{n} & n-1 \end{smallmatrix}$ appears.

To see this equivalence, observe that by conditions 1 and 2 the only columns that can appear between $\begin{smallmatrix} n-1 \\ n \end{smallmatrix}$ and $\begin{smallmatrix} n \\ n-1 \end{smallmatrix}$ are $\begin{smallmatrix} n-1 \\ n \end{smallmatrix}$, $\begin{smallmatrix} n-1 \\ n-1 \end{smallmatrix}$, and $\begin{smallmatrix} n \\ n-1 \end{smallmatrix}$, and if present, they must appear in that order from left to right. If a column of the form $\begin{smallmatrix} n-1 \\ n-1 \end{smallmatrix}$ appears, we have a configuration of the form $\begin{smallmatrix} n-1 & n-1 \\ n-1 & n-1 \end{smallmatrix}$, which is forbidden by condition 3. On the other hand, if no column of the form $\begin{smallmatrix} n-1 \\ n-1 \end{smallmatrix}$ appears, the columns $\begin{smallmatrix} n-1 \\ n \end{smallmatrix}$ and $\begin{smallmatrix} n \\ n-1 \end{smallmatrix}$ are adjacent, which is disallowed by condition 4a.

3.1.2 Sliding algorithm

In section 2.2, we saw the Lecouvey relations of the Type D plactic monoid. Here we have the derived sliding algorithm for the case of height 2 rectangles.

- 1. If $x \neq \bar{z}$, then

$$\begin{array}{c}
 \begin{array}{|c|c|} \hline & y \\ \hline x & z \\ \hline \end{array} \equiv \begin{array}{|c|c|} \hline x & y \\ \hline & z \\ \hline \end{array} \equiv \begin{array}{|c|c|} \hline x & y \\ \hline & z \\ \hline \end{array} \text{ for } x \leq y < z, \\
 \text{and} \\
 \begin{array}{|c|c|} \hline & x \\ \hline y & z \\ \hline \end{array} \equiv \begin{array}{|c|c|} \hline x & \\ \hline y & z \\ \hline \end{array} \equiv \begin{array}{|c|c|} \hline x & z \\ \hline y & \\ \hline \end{array} \text{ for } x < y \leq z.
 \end{array}$$

2. If $1 < x < n$ and $x \leq y \leq \bar{x}$, then

$$\begin{array}{c}
 \begin{array}{|c|c|} \hline & y \\ \hline x-1 & \overline{x-1} \\ \hline \end{array} \equiv \begin{array}{|c|c|} \hline x-1 & y \\ \hline & \overline{x-1} \\ \hline \end{array} \equiv \begin{array}{|c|c|} \hline x & y \\ \hline & \bar{x} \\ \hline \end{array} \\
 \\
 \text{and} \\
 \begin{array}{|c|c|} \hline & x \\ \hline y & \bar{x} \\ \hline \end{array} \equiv \begin{array}{|c|c|} \hline x-1 & \\ \hline y & \overline{x-1} \\ \hline \end{array} \equiv \begin{array}{|c|c|} \hline x-1 & \overline{x-1} \\ \hline y & \\ \hline \end{array} .
 \end{array}$$

3. If $x \leq n - 1$, then

$$\begin{array}{c}
 \left\{ \begin{array}{l}
 \begin{array}{|c|c|} \hline & \bar{n} \\ \hline n & \bar{x} \\ \hline \end{array} \equiv \begin{array}{|c|c|} \hline \bar{n} & \\ \hline n & \bar{x} \\ \hline \end{array} \equiv \begin{array}{|c|c|} \hline \bar{n} & \bar{x} \\ \hline n & \\ \hline \end{array} \\
 \\
 \begin{array}{|c|c|} \hline & n \\ \hline \bar{n} & \bar{x} \\ \hline \end{array} \equiv \begin{array}{|c|c|} \hline n & \\ \hline \bar{n} & \bar{x} \\ \hline \end{array} \equiv \begin{array}{|c|c|} \hline n & \bar{x} \\ \hline \bar{n} & \\ \hline \end{array} \\
 \\
 \begin{array}{|c|c|} \hline & \bar{n} \\ \hline x & n \\ \hline \end{array} \equiv \begin{array}{|c|c|} \hline x & \bar{n} \\ \hline & n \\ \hline \end{array} \equiv \begin{array}{|c|c|} \hline x & \bar{n} \\ \hline & n \\ \hline \end{array} \\
 \\
 \begin{array}{|c|c|} \hline & n \\ \hline x & \bar{n} \\ \hline \end{array} \equiv \begin{array}{|c|c|} \hline x & n \\ \hline & \bar{n} \\ \hline \end{array} \equiv \begin{array}{|c|c|} \hline x & n \\ \hline & \bar{n} \\ \hline \end{array} .
 \end{array}
 \right.
 \end{array}$$

4.

$$\text{and } \left\{ \begin{array}{l} \left\{ \begin{array}{l} \begin{array}{|c|c|} \hline n \\ \hline \bar{n} \quad \bar{n} \\ \hline \end{array} \equiv \begin{array}{|c|c|} \hline n-1 \\ \hline \bar{n} \quad \overline{n-1} \\ \hline \end{array} \equiv \begin{array}{|c|c|} \hline n-1 \quad \overline{n-1} \\ \hline \bar{n} \\ \hline \end{array} \\ \\ \begin{array}{l} \begin{array}{|c|c|} \hline \bar{n} \\ \hline n \quad n \\ \hline \end{array} \equiv \begin{array}{|c|c|} \hline n-1 \\ \hline n \quad \overline{n-1} \\ \hline \end{array} \equiv \begin{array}{|c|c|} \hline n-1 \quad \overline{n-1} \\ \hline n \\ \hline \end{array} \end{array} \right. \\ \\ \left. \begin{array}{l} \begin{array}{|c|c|} \hline \bar{n} \\ \hline n-1 \quad \overline{n-1} \\ \hline \end{array} \equiv \begin{array}{|c|c|} \hline n-1 \quad \bar{n} \\ \hline \overline{n-1} \\ \hline \end{array} \equiv \begin{array}{|c|c|} \hline \bar{n} \quad \bar{n} \\ \hline n \\ \hline \end{array} \\ \\ \begin{array}{l} \begin{array}{|c|c|} \hline n \\ \hline n-1 \quad \overline{n-1} \\ \hline \end{array} \equiv \begin{array}{|c|c|} \hline n-1 \quad n \\ \hline \overline{n-1} \\ \hline \end{array} \equiv \begin{array}{|c|c|} \hline n \quad n \\ \hline \bar{n} \\ \hline \end{array} \end{array} \right. \end{array} \right\} .$$

If a word is composed entirely of barred letters or entirely of unbarred letters, only relation (1) (the Knuth relation) applies, and the type A jeu de taquin may be used.

3.1.3 Technical definitions for operations on tableaux

Definition 3.1.2. A null-configuration of size k is

$$\boxed{\emptyset}_k = \begin{cases} \underbrace{\begin{array}{cccc} 1 & \cdots & 1 & 2 & \cdots & 2 \\ \bar{2} & \cdots & \bar{2} & \bar{1} & \cdots & \bar{1} \end{array}}_{\frac{k}{2}} & \text{if } k \text{ is even} \\ \underbrace{\begin{array}{ccccccc} 1 & & 1 & 2 & 2 & \cdots & 2 \\ \bar{2} & \cdots & \bar{2} & \bar{2} & \bar{1} & \cdots & \bar{1} \end{array}}_{\frac{k+1}{2}} & \text{if } k \text{ is odd.} \end{cases}$$

Null-configurations are named thus because e_i and f_i for $i = 2, \dots, n$ send b to 0, where b is the $2 \times s$ tableau which is a null-configuration of size s . Therefore, b is

the basis vector for the trivial representation of D_{n-1} in the D_n crystal $B(s\varpi_2)$. Put another way, inserting a null-configuration into a tableau T has no effect on $\varepsilon_i(T)$ or $\varphi_i(T)$ for $i = 2, \dots, n$.

Definition 3.1.3. Let $T \in B(s\varpi_2)$. The reduced form of T , denoted by $T^\#$, is the skew tableau that results from removing all 1's, $\bar{1}$'s, and any null-configuration from T . The rectification of $T^\#$ by the sliding algorithm in section 3.1.2 is called the completely reduced form of T .

Since the type D plactic operations cannot increase the length of a column of a skew tableau, we know that the completely reduced form of T must have no more than two rows.

3.1.4 Properties of $B^{r,s}$

The properties of $B^{r,s}$ in Conjecture 2.2.5 can be described more simply in the case of $r = 2$. We may restate the classical direct sum decomposition (item 1) as

$$B^{2,s} \simeq \bigoplus_{i=0}^s i\varpi_2 \quad (3.1.3.1)$$

and restate the description of the energy function as $D_{B^{2,s}}(b) = k$ if b is in a D_n component with highest weight $k\varpi_2$.

3.1.5 Specialization of $\check{\sigma}$.

In the special case of $r = 2$ the definition of $\check{\sigma}$ on the set of branching component vertices has a very easy combinatorial description, since there is only one pair of rows in which +’s and -’s can appear in its \pm diagrams.

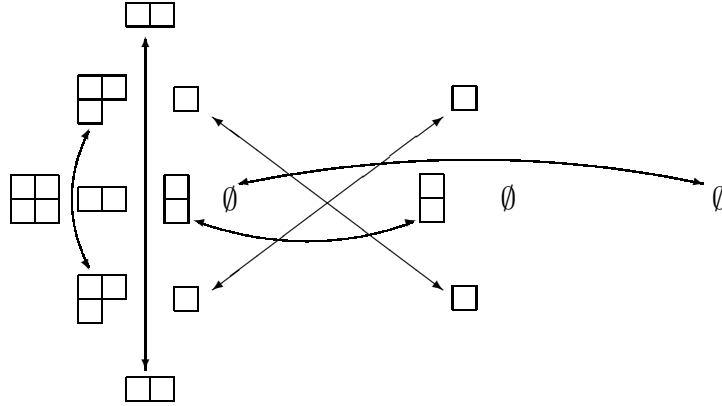


Figure 3.1.3.1: Definition of $\check{\sigma}$ on $\mathcal{BC}(\tilde{B}^{2,2})$

Suppose $v \in \mathcal{BC}(k\varpi_2)$ is labeled by the partition (λ_1, λ_2) . The corresponding \pm diagram must have $k - \lambda_1$ columns with a \pm pair, so $\check{\sigma}(v) \in \mathcal{BC}(s - (k - \lambda_1))$. By Proposition 2.3.8, we know that the strata of $\mathcal{BC}(k\varpi_2)$ are multiplicity free for all $k \geq 0$, so Proposition 2.4.1 specifies $\check{\sigma}(v)$ by telling us that it is in the opposite stratum of v .

Example 3.1.4. The action of $\check{\sigma}$ on $\mathcal{BC}(\tilde{B}^{2,2})$ is given in Figure 3.1.3.1.

3.2 Realization of $B^{2,s}$ as a Set of Young-like Tableaux

3.2.1 Bijection between affine and classical tableaux

We now define a D_n -crystal with vertices labeled by the set $\mathcal{T}(s)$ of tableaux of shape (s, s) satisfying conditions 1, 2, and 4 of Criterion 3.1.1, but not condition 3. We will construct a bijection between $\mathcal{T}(s)$ and the vertices of $\bigoplus_{i=0}^s B(i\varpi_2)$, so that $\mathcal{T}(s)$ may be viewed as a D_n -crystal with the classical decomposition (3.1.3.1). In

section 3.2 we will consider f_0 and e_0 on $\mathcal{T}(s)$ as given by $\check{\sigma}$ to give it the structure of a perfect $D_n^{(1)}$ -crystal, which we call $\tilde{B}^{2,s}$; we will then prove that $\tilde{B}^{2,s}$ is the only crystal satisfying Conjecture 2.2.5 for the case of $r = 2$.

Definition 3.2.1. The set $\mathcal{T}(s)$ of affine tableaux of width s is the set of tableaux satisfying conditions 1, 2, and 4 of Criterion 3.1.1.

Proposition 3.2.2. *Let $T \in \mathcal{T}(s) \setminus B(s\varpi_2)$ with $T \neq \frac{1}{1} \cdots \frac{1}{1}$, and define $\bar{i} = i$ for $1 \leq i \leq n$. Then there is a unique $a \in \{1, \dots, n, \bar{n}\}$ and $m \in \mathbb{Z}_{>0}$ such that T contains one of the following configurations (called an a -configuration) in consecutive columns:*

$$\begin{array}{l} \begin{array}{c} a \ a \ \cdots \ a \ c_1 \\ b_1 \ \underbrace{\bar{a} \ \cdots \ \bar{a}}_m \ d_1 \end{array}, \quad \text{where } b_1 \neq \bar{a}, \text{ and } (c_1 \neq a \text{ or } d_1 \neq \bar{a}); \\ \\ \begin{array}{c} b_2 \ a \ \cdots \ a \ d_2 \\ c_2 \ \underbrace{\bar{a} \ \cdots \ \bar{a}}_m \ \bar{a} \end{array}, \quad \text{where } d_2 \neq a, \text{ and } (b_2 \neq a \text{ or } c_2 \neq \bar{a}); \\ \\ \begin{array}{c} b_3 \ a \ \cdots \ a \ d_3 \\ c_3 \ \underbrace{\bar{a} \ \cdots \ \bar{a}}_{m+1} \ e_3 \end{array}, \quad \text{where } b_3 \neq a \text{ and } e_3 \neq \bar{a}. \end{array}$$

Proof. If $s = 1$, the set $\mathcal{T}(s) \setminus B(s\varpi_2)$ contains only $\frac{1}{1}$, so the statement of the proposition is empty. Assume that $s \geq 2$. The existence of an a -configuration for some $a \in \{1, \dots, n, \bar{n}\}$ follows from the fact that T violates condition 3 of Criterion 3.1.1. The conditions on b_i, c_i, d_i for $i = 1, 2, 3$ and e_3 mean that m is chosen to maximize the size of the a -configuration. Condition 1 of Criterion 3.1.1 and the conditions on the parameters b_i, c_i, d_i, e_3 imply that there can be no other a -configurations in T . \square

The map $D_{2,s} : \mathcal{T}(s) \rightarrow \bigoplus_{k=0}^s B(k\varpi_2)$, called the height-two drop map, is defined as follows for $T \in \mathcal{T}(s)$. If $T = \frac{1}{1} \cdots \frac{1}{1}$, then $D_{2,s}(T) = \emptyset \in B(0)$. If $T \in B(s\varpi_2)$,

$D_{2,s}(T) = T$. Otherwise T contains a unique a -configuration by Proposition 3.2.2, and $D_{2,s}(T)$ is obtained from T by removing $\underbrace{\bar{a} \cdots \bar{a}}_m$ from it.

Theorem 3.2.3. *Let $T \in \mathcal{T}(s)$. Then $D_{2,s}(T)$ satisfies Criterion 3.1.1, and is therefore a tableau in $\bigoplus_{k=0}^s B(k\varpi_2)$.*

Proof. Condition 1 is satisfied since the relation \leq on our alphabet is transitive. Conditions 2 and 5 are automatically satisfied, since the columns that remain are not changed. Condition 3 is satisfied since by Proposition 3.2.2, there can be no more than one a -configuration in T . Condition 4 is satisfied since $D_{2,s}$ does not remove any columns of the form $\begin{smallmatrix} n-1 \\ n \end{smallmatrix}$, $\begin{smallmatrix} n-1 \\ \bar{n} \end{smallmatrix}$, $\begin{smallmatrix} n \\ n-1 \end{smallmatrix}$, or $\begin{smallmatrix} \bar{n} \\ n-1 \end{smallmatrix}$. \square

Proposition 3.2.6 shows that $D_{2,s}$ is a bijection by constructing its inverse.

Example 3.2.4. We have

$$T = \begin{array}{|c|c|c|c|} \hline 1 & 2 & 3 & 3 \\ \hline \bar{4} & \bar{2} & \bar{2} & \bar{1} \\ \hline \end{array}, \quad D_{2,4}(T) = \begin{array}{|c|c|c|} \hline 1 & 3 & 3 \\ \hline \bar{4} & \bar{2} & \bar{1} \\ \hline \end{array}.$$

The inverse of $D_{2,s}$ is the height-two fill map $F_{2,s} : \bigoplus_{k=0}^s B(k\varpi_2) \rightarrow \mathcal{T}(s)$. Let $t = \begin{smallmatrix} a_1 & \cdots & a_k \\ b_1 & \cdots & b_k \end{smallmatrix} \in B(k\varpi_2)$. If $k = s$, $F_{2,s}(t) = t$. If $k < s$, then $F_{2,s}(t)$ is obtained by finding a subtableau $\begin{smallmatrix} a_i & a_{i+1} \\ b_i & b_{i+1} \end{smallmatrix}$ in t such that

Criterion 3.2.5.

$$b_i \leq \bar{a}_i \leq b_{i+1} \quad \text{or} \quad a_i \leq \bar{b}_{i+1} \leq a_{i+1}.$$

(Recall that $\bar{\bar{i}} = i$ for $i \in \{1, \dots, n\}$.) Note that the first pair of inequalities imply that a_i is unbarred, and the second pair of inequalities imply that b_{i+1} is barred. We

may therefore insert between columns i and $i+1$ of t either the configuration $\underbrace{a_i \dots a_i}_{\bar{a}_i \dots \bar{a}_i}$ or $\underbrace{\bar{b}_{i+1} \dots \bar{b}_{i+1}}_{b_{i+1} \dots b_{i+1}}$, depending on which part of Criterion 3.2.5 is satisfied. We say that i is the filling location of t . If no such subtableau exists, then $F_{2,s}$ will either prepend $\underbrace{\bar{b}_1 \dots \bar{b}_1}_{b_1 \dots b_1}$ to t or append $\underbrace{a_k \dots a_k}_{\bar{a}_k \dots \bar{a}_k}$ to the end of t . In these cases the filling locations are k and 0 , respectively.

Proposition 3.2.6. *The map $F_{2,s}$ is well-defined on $\bigoplus_{i=0}^s B(i\varpi_2)$.*

The proof of this proposition follows from the next three lemmas.

Lemma 3.2.7. *Suppose that $t \in \bigoplus_{k=0}^{s-1} B(k\varpi_2)$ has no subtableaux $\begin{smallmatrix} a_i & a_{i+1} \\ b_i & b_{i+1} \end{smallmatrix}$ satisfying Criterion 3.2.5. Then either appending $\underbrace{a_k \dots a_k}_{\bar{a}_k \dots \bar{a}_k}$ or prepending $\underbrace{\bar{b}_1 \dots \bar{b}_1}_{b_1 \dots b_1}$ to t will produce a tableau in $\mathcal{T}(s) \setminus B(s\varpi_2)$.*

Proof. Suppose $t = \begin{smallmatrix} a_1 & \dots & a_k \\ b_1 & \dots & b_k \end{smallmatrix} \in B(k\varpi_2)$ is as above for $k < s$. We will show that if prepending $\bar{b}_1 \dots \bar{b}_1$ to t does not produce a tableau in $\mathcal{T}(s) \setminus B(s\varpi_2)$, then appending $\begin{smallmatrix} a_k & \dots & a_k \\ \bar{a}_k & \dots & \bar{a}_k \end{smallmatrix}$ to t will produce a tableau in $\mathcal{T}(s) \setminus B(s\varpi_2)$. There are two reasons we might not be able to prepend $\bar{b}_1 \dots \bar{b}_1$; b_1 may be unbarred, or we may have $a_1 < \bar{b}_1$.

First, suppose b_1 is unbarred. If b_k is also unbarred, then b_k is certainly less than \bar{a}_k , so we may append $\begin{smallmatrix} a_k & \dots & a_k \\ \bar{a}_k & \dots & \bar{a}_k \end{smallmatrix}$ to t . Hence, suppose that b_k is barred. We will show that a_k is unbarred and $\bar{a}_k > b_k$.

We know that t has a subtableau of the form $\begin{smallmatrix} a_i & a_{i+1} \\ b_i & b_{i+1} \end{smallmatrix}$ such that b_i is unbarred and b_{i+1} is barred. It follows that a_i is unbarred, and therefore $\bar{a}_i > b_i$. Since our hypothesis states that $\begin{smallmatrix} a_i & a_{i+1} \\ b_i & b_{i+1} \end{smallmatrix}$ must not satisfy Criterion 3.2.5, this means that $\bar{a}_i > b_{i+1}$, which is equivalent to $\bar{b}_{i+1} > a_i$. Once again observing that $\begin{smallmatrix} a_i & a_{i+1} \\ b_i & b_{i+1} \end{smallmatrix}$ does

not satisfy Criterion 3.2.5, this implies that $\bar{b}_{i+1} > a_{i+1}$; i.e., a_{i+1} is unbarred, and $\bar{a}_{i+1} > b_{i+1}$.

We proceed with an inductive argument on $i < j < k$. Suppose that $\begin{smallmatrix} a_j & a_{j+1} \\ b_j & b_{j+1} \end{smallmatrix}$ is a subtableau of t such that b_j and b_{j+1} are barred, a_j is unbarred, and $\bar{a}_j > b_j$. By reasoning identical to the above, we conclude that

$$\bar{a}_j > b_{j+1} \Rightarrow \bar{b}_{j+1} > a_j \Rightarrow \bar{b}_{j+1} > a_{j+1} \Rightarrow \bar{a}_{j+1} > b_{j+1}, \quad (3.2.3.1)$$

which once again means that a_{j+1} is unbarred.

This inductively shows that a_k is unbarred and $\bar{a}_k > b_k$, so we may append $\begin{smallmatrix} a_k & \cdots & a_k \\ \bar{a}_k & \cdots & \bar{a}_k \end{smallmatrix}$ to t to get a tableau in $\mathcal{T}(s) \setminus B(s\varpi_2)$. By a symmetrical argument, we conclude that if a_k is barred, then we may prepend $\begin{smallmatrix} \bar{b}_1 & \cdots & \bar{b}_1 \\ b_1 & \cdots & b_1 \end{smallmatrix}$ to t .

Now, suppose that b_1 is barred and $\bar{b}_1 > a_1$. This means that a_1 is unbarred and $\bar{a}_1 > b_1$, so the induction carried out in equation 3.2.3.1 applies. It follows that a_k is unbarred and $\bar{a}_k > b_k$, so once again we may append $\begin{smallmatrix} a_k & \cdots & a_k \\ \bar{a}_k & \cdots & \bar{a}_k \end{smallmatrix}$ to t . Also, by a symmetrical argument, when a_k is unbarred and $b_k > \bar{a}_k$, we may prepend $\begin{smallmatrix} \bar{b}_1 & \cdots & \bar{b}_1 \\ b_1 & \cdots & b_1 \end{smallmatrix}$ to t . Thus, when no subtableau of t satisfy Criterion 3.2.5, either appending $\begin{smallmatrix} a_k & \cdots & a_k \\ \bar{a}_k & \cdots & \bar{a}_k \end{smallmatrix}$ or prepending $\begin{smallmatrix} \bar{b}_1 & \cdots & \bar{b}_1 \\ b_1 & \cdots & b_1 \end{smallmatrix}$ to t will produce a tableau in $\mathcal{T}(s) \setminus B(s\varpi_2)$. \square

Lemma 3.2.8. *Any tableau $t = \begin{smallmatrix} a_1 & \cdots & a_k \\ b_1 & \cdots & b_k \end{smallmatrix} \in \bigoplus_{k=0}^{s-1} B(k\varpi_2)$ has no more than two filling locations. If it has two, they are consecutive integers, and $F_{2,s}(t)$ doesn't depend on this choice.*

Proof. Let $0 \leq i_* \leq k$ be minimal such that i_* is a filling location of t . First assume that $0 < i_* < k$. This implies the existence of a subtableau $\begin{smallmatrix} a_{i_*} & a_{i_*+1} \\ b_{i_*} & b_{i_*+1} \end{smallmatrix}$ which satisfies Criterion 3.2.5.

Suppose that the first condition $b_{i_*} \leq \bar{a}_{i_*} \leq b_{i_*+1}$ of Criterion 3.2.5 is satisfied, and consider whether $i_* + 1$ can be a filling location. If $b_{i_*+1} \leq \bar{a}_{i_*+1} \leq b_{i_*+2}$, we have

$$b_{i_*+1} \leq \bar{a}_{i_*+1} \leq \bar{a}_{i_*} \leq b_{i_*+1},$$

which implies that $\bar{a}_{i_*} = \bar{a}_{i_*+1} = b_{i_*+1}$, so that t violates part 3 of Criterion 3.1.1. Similarly, if $a_{i_*+1} \leq \bar{b}_{i_*+2} \leq a_{i_*+2}$, then we have

$$\bar{a}_{i_*+1} \leq \bar{a}_{i_*} \leq b_{i_*+1} \leq b_{i_*+2} \leq \bar{a}_{i_*+1},$$

which also implies that $\bar{a}_{i_*} = \bar{a}_{i_*+1} = b_{i_*+1}$, once again violating part 3 of Criterion 3.1.1. We conclude that if i_* is a filling location for which Criterion 3.2.5 is satisfied by $b_{i_*} \leq \bar{a}_{i_*} \leq b_{i_*+1}$, then $i_* + 1$ is not a filling location. Furthermore, this argument shows that $a_{i_*+1} > a_{i_*}$ or $b_{i_*+1} > \bar{a}_{i_*}$. By the partial ordering on our alphabet, it follows that t has no other filling locations.

Now, suppose for the filling location i_* , Criterion 3.2.5 is satisfied by $a_{i_*} \leq \bar{b}_{i_*+1} \leq a_{i_*+1}$. The condition $a_{i_*+1} \leq \bar{b}_{i_*+2} \leq a_{i_*+2}$ for $i_* + 1$ to be a filling location implies that

$$\bar{b}_{i_*+2} \leq \bar{b}_{i_*+1} \leq a_{i_*+1} \leq \bar{b}_{i_*+2},$$

which as above leads to a violation of part 3 of Criterion 3.1.1. However, $i_* + 1$ may be a filling location if Criterion 3.2.5 is satisfied by $b_{i_*+1} \leq \bar{a}_{i_*+1} \leq b_{i_*+2}$. Note that this inequality implies that $a_{i_*+1} \leq \bar{b}_{i_*+1}$, which tells us that $a_{i_*+1} = \bar{b}_{i_*+1}$. Thus, choosing to insert $\frac{\bar{b}_{i_*+1}}{b_{i_*+1}} \cdots \frac{\bar{b}_{i_*+1}}{b_{i_*+1}}$ between columns i_* and $i_* + 1$ or to insert $\frac{a_{i_*+1}}{\bar{a}_{i_*+1}} \cdots \frac{a_{i_*+1}}{\bar{a}_{i_*+1}}$ between columns $i_* + 1$ and $i_* + 2$ does not change $F_{2,s}(t)$. Since $i_* + 1$ is a filling location with Criterion 3.2.5 satisfied by $b_{i_*} \leq \bar{a}_{i_*} \leq b_{i_*+1}$, the preceding paragraph

implies that there are no other filling locations in t .

Finally, suppose that $i_* = 0$ is a filling location for t ; i.e., b_1 is barred, a_1 is unbarred, and $\bar{b}_1 \leq a_1$. If 1 is a filling location, Criterion 3.2.5 is satisfied by $b_1 \leq \bar{a}_1 \leq b_2$; otherwise, part 3 of Criterion 3.1.1 is violated. Put together, this means that $\bar{a}_1 = b_1$, so prepending $\bar{b}_1 \cdots \bar{b}_1$ to t and inserting $\bar{a}_1 \cdots \bar{a}_1$ between columns 1 and 2 results in the same tableau. As in the above cases, part 3 of Criterion 3.1.1 and the partial order on the alphabet prohibit any other filling locations. \square

Example 3.2.9. Let $s = 4$. Then

$$t = \begin{array}{|c|c|c|} \hline 1 & 2 & 3 \\ \hline \bar{4} & \bar{2} & \bar{1} \\ \hline \end{array}, \quad F_{2,4}(t) = \begin{array}{|c|c|c|c|} \hline 1 & 2 & 2 & 3 \\ \hline \bar{4} & \bar{2} & \bar{2} & \bar{1} \\ \hline \end{array}.$$

While we could choose either column two or column three as the filling location, either choice results in the same tableau.

Lemma 3.2.10. *If a filling location of $t = \begin{smallmatrix} a_1 & \cdots & a_k \\ b_1 & \cdots & b_k \end{smallmatrix} \in \bigoplus_{i=0}^{s-1} B(i\varpi_2)$ satisfies Criterion 3.2.5 with both inequalities, then $F_{2,s}(t)$ is independent of this choice.*

Proof. Suppose that $i_* \neq 0, k$ is a filling location for t where both parts of Criterion 3.2.5 are satisfied. This means that the subtableau $\begin{smallmatrix} a_{i_*} & a_{i_*+1} \\ b_{i_*} & b_{i_*+1} \end{smallmatrix}$ satisfies both $\bar{a}_{i_*} \leq b_{i_*+1}$ and $a_{i_*} \leq \bar{b}_{i_*+1}$. The latter of these implies that $b_{i_*+1} \leq \bar{a}_{i_*}$, so we have $\bar{a}_{i_*} = b_{i_*+1}$ and $\bar{b}_{i_*+1} = a_{i_*}$. Thus, filling with either $\begin{smallmatrix} a_{i_*} & \cdots & a_{i_*} \\ \bar{a}_{i_*} & \cdots & \bar{a}_{i_*} \end{smallmatrix}$ or $\begin{smallmatrix} \bar{b}_{i_*+1} & \cdots & \bar{b}_{i_*+1} \\ b_{i_*+1} & \cdots & b_{i_*+1} \end{smallmatrix}$ between columns i_* and $i_* + 1$ results in the same tableau $F_{2,s}(t)$. \square

Example 3.2.11. To illustrate, for

$$t = \begin{array}{|c|c|c|} \hline 2 & 3 & 3 \\ \hline \bar{4} & \bar{2} & \bar{1} \\ \hline \end{array} \quad \text{we have} \quad F_{2,s}(t) = \begin{array}{|c|c|c|c|} \hline 2 & 2 & 3 & 3 \\ \hline \bar{4} & \bar{2} & \bar{2} & \bar{1} \\ \hline \end{array}.$$

By identifying $\mathcal{T}(s)$ with $\bigoplus_{i=0}^s B(i\varpi_2)$ via the maps $D_{2,s}$ and $F_{2,s}$, we have defined a $U_q(D_n)$ -crystal with the decomposition (3.1.3.1), with vertices labeled by the $2 \times s$ tableaux of $\mathcal{T}(s)$. The action of the Kashiwara operators e_i, f_i for $i \in \{1, \dots, n\}$ on this crystal is defined in terms of the above bijection, explicitly

$$\begin{aligned} e_i(T) &= F_{2,s}(e_i(D_{2,s}(T))) \\ f_i(T) &= F_{2,s}(f_i(D_{2,s}(T))), \end{aligned} \tag{3.2.3.2}$$

for $T \in \mathcal{T}(s)$, where the e_i and f_i on the right are the standard Kashiwara operators on $U_q(D_n)$ -crystals [24]. In section 3.2 we will discuss the action of e_0 and f_0 on $\mathcal{T}(s)$, which makes $\mathcal{T}(s)$ into an affine crystal called $\tilde{B}^{2,s}$.

Remark 3.2.12. Using the filling and dropping map we obtain a natural inclusion of $\mathcal{T}(s')$ into $\mathcal{T}(s)$ for $s' < s$.

Definition 3.2.13. For $s' < s$, the map $\Upsilon_{s'}^s : \mathcal{T}(s') \hookrightarrow \mathcal{T}(s)$ is defined by $\Upsilon_{s'}^s = F_{2,s} \circ D_{2,s'}$.

3.2.2 Combinatorial construction of σ .

Conjecture 2.4.2 defines $\check{\sigma}$ in terms of \pm diagrams, which gives a definition of σ via D_{n-1} highest weight tableaux. In the case of $B^{2,s}$, we can also give a direct combinatorial description of $\sigma(T)$ for any crystal vertex T . As an auxilliary con-

struction which will be useful in its own right later on, we combinatorially describe $\iota_{i_1}^{i_2} : B(i_1\varpi_2) \hookrightarrow B(i_2\varpi_2)$, the unique crystal embedding that agrees with $\iota_{i_1}^{i_2} : \mathcal{BC}(i_1\varpi_2) \hookrightarrow \mathcal{BC}(i_2\varpi_2)$.

Remark 3.2.14. It will often be useful to identify $B(k\varpi_2)$ with its image in $\tilde{B}^{2,s}$. We will use the notation $T \in B(k\varpi_2) \subset \tilde{B}^{2,s}$ to indicate this identification.

Let $i_1, i_2 \in \{0, \dots, s\}$, and $i_1 < i_2$, so $\iota_{i_1}^{i_2}$ denotes the embedding of $B(i_1\varpi_2)$ in $B(i_2\varpi_2)$. Let $T \in B(i_1\varpi_2) \subset \tilde{B}^{2,s}$. This embedding can be combinatorially understood through the following observations:

Remark 3.2.15.

- $\varphi_k(T) = \varphi_k(\iota_{i_1}^{i_2}(T))$ and $\varepsilon_k(T) = \varepsilon_k(\iota_{i_1}^{i_2}(T))$ for $k = 2, \dots, n$;
- $D_{2,s}(\iota_{i_1}^{i_2}(T))$ has $(i_2 - i_1)$ more columns than $D_{2,s}(T)$ (section 3.2.1);
- $v(T)$ and $v(\iota_{i_1}^{i_2}(T))$ are in the same stratum, where $v(T)$ is the branching component vertex containing T .

In other words, we know that T has a maximal a -configuration of size $s - i_1$ (section 3.2.1), and has completely reduced form $T^\#$ (Definition 3.1.3). Furthermore, let r_{1T} be the number of 1's in the first row of $D_{2,s}(T)$ to the left of a null-configuration, let r_{2T} be the size of the null-configuration therein, (possibly $r_{2T} = 0$), and let r_{3T} be the number of $\bar{1}$'s to the right of the null-configuration. We then have $t_{1T} = r_{1T} + r_{2T}$ and $t_{2T} = r_{2T} + r_{3T}$, and the stratum of $v(T)$ and $v(\iota_{i_1}^{i_2}(T))$ is $t_{1T} - t_{2T}$.

Remark 3.2.16. Observe that t_{1T} and t_{2T} are the number of +’s and –’s, respectively, in the \pm diagram associated with the D_{n-1} highest weight tableaux of $v(T)$, but these numbers can be extracted directly from any tableau, not just one that is D_{n-1} highest weight.

We wish to construct a tableau S with an a -configuration of size $s - i_2$ such that $S^\# = T^\#$ and $t_{1S} - t_{2S} = t_{1T} - t_{2T}$. Based on properties of the height 2 type D sliding algorithm of section 3.1.2, these conditions can only be satisfied when $t_{jS} = t_{jT} + (i_2 - i_1)$ for $j = 1, 2$.

We can calculate $\iota_{i_1}^{i_2}(T)$ by the following algorithm:

Algorithm 3.2.17.

1. Remove the a -configuration of size $s - i_1$ from T and slide it to get a $2 \times i_1$ tableau.
2. Remove the 1's, $\bar{1}$'s and the null-configuration from the result to get a skew tableau of shape $(i_1, i_1 - t_{2T}) / (t_{1T})$.
3. Using the type D sliding algorithm, produce a skew tableau of shape

$$((i_2), (i_2) - (t_{2T} + (i_2 - i_1))) / (t_{1T} + (i_2 - i_1))$$

4. Fill this tableau with 1's, $\bar{1}$'s, and a null-configuration so that the result is a $2 \times i_2$ tableau.
5. Use the height 2 fill map $F_{2,s}$ (section 3.2.1) to insert $s - i_2$ columns into the tableau.

This produces the unique tableau satisfying the three properties of Remark 3.2.15.

Example 3.2.18. Let

$$T = \begin{array}{|c|c|c|c|c|c|c|} \hline 1 & 1 & 2 & 2 & 2 & \bar{3} & \bar{2} \\ \hline 2 & 2 & 3 & \bar{2} & \bar{2} & \bar{2} & \bar{1} \\ \hline \end{array} \in B(5\varpi_2) \subset \tilde{B}^{2,7}.$$

Running through the steps of our algorithm (using relation (2) of section 2.2.3 for step (3)) gives us

$$1. \quad \begin{array}{|c|c|c|c|c|} \hline 1 & 1 & 2 & \bar{3} & \bar{2} \\ \hline 2 & 2 & 3 & \bar{2} & \bar{1} \\ \hline \end{array}$$

$$2. \quad \begin{array}{|c|c|c|c|} \hline & & 2 & \bar{3} & \bar{2} \\ \hline 2 & 2 & 3 & \bar{2} & \\ \hline \end{array}$$

$$3. \quad \begin{array}{|c|c|c|c|c|} \hline & & & 3 & \bar{3} & \bar{2} \\ \hline 2 & 2 & 3 & \bar{3} & & \\ \hline \end{array}$$

$$4. \quad \begin{array}{|c|c|c|c|c|c|} \hline 1 & 1 & 1 & 3 & \bar{3} & \bar{2} \\ \hline 2 & 2 & 3 & \bar{3} & \bar{1} & \bar{1} \\ \hline \end{array}$$

$$5. \quad \iota_5^6(T) = \begin{array}{|c|c|c|c|c|c|c|} \hline 1 & 1 & 1 & 3 & 3 & \bar{3} & \bar{2} \\ \hline 2 & 2 & 3 & \bar{3} & \bar{3} & \bar{1} & \bar{1} \\ \hline \end{array} \in B(6\varpi_2) \subset \tilde{B}^{2,7}.$$

We can also define a map $\iota_{i_1}^{i_2} : B(i_1\varpi_2) \rightarrow B(i_2\varpi_2) \cup \{0\}$ for $i_2 < i_1$ by

$$\iota_{i_1}^{i_2}(T) = \begin{cases} (\iota_{i_2}^{i_1})^{-1}(T) & \text{if } T \in \iota_{i_2}^{i_1}(B(j\varpi_2)), \\ 0 & \text{otherwise .} \end{cases}$$

Reversing Algorithm 3.2.17 makes this map explicit. Lastly, we define ι_i^i to be the identity map on $B(i\varpi_2)$, so $\iota_{i_1}^{i_2}$ is defined for all $i_1, i_2 \in \{0, \dots, s\}$.

Definition 3.2.19. Let $T \in B(k\varpi_2) \subset \tilde{B}^{2,s}$ be a tableau whose branching component vertex is in stratum j . Then T^{*BC} is the tableau in $B(k\varpi_2)$ with the same completely reduced form as T whose branching component vertex is in stratum $-j$.

Alternatively, we can interpret this involution as follows. Let $T \in B(v)$, where v is a branching component vertex with D_{n-1} highest weight tableau u , and whose complementary vertex is v' . (Recall from section 2.3 that the complementary vertex of v is defined to be the vertex in the opposite stratum from v that is associated with the same partition as v .) Let i_1, \dots, i_m be a sequence such that $T = f_{i_1} \cdots f_{i_m} u$. Then $T^{*BC} = f_{i_1} \cdots f_{i_m} u'$, where u' is the D_{n-1} -highest weight tableau of $B(v')$. Alternatively, this map is the composition of $*$ with the “local $*$ ” map, which applies only to the tableaux in $B(v)$ viewed as a D_{n-1} -crystal.

We now define $\sigma(T)$ in terms of the above combinatorial operations.

Definition 3.2.20. Suppose $T \in B(k\varpi_2) \subset \tilde{B}^{2,s}$, and ℓ be minimal such that $\iota_k^s(T) \in \iota_\ell^s(B(\ell\varpi_2))$ (i.e., ℓ is the first part of the partition corresponding to the highest weight of the D_{n-1} -crystal containing T). Then

$$\sigma(T) = \iota_k^{s+\ell-k}(T^{*BC}). \quad (3.2.3.3)$$

Remark 3.2.21. Since $\iota_{i_1}^{i_2}$ commutes with $*_{BC}$, we also have

$$\sigma(T) = (\iota_k^{s+\ell-k}(T))^{*BC}.$$

3.2.3 Properties of f_0 and e_0 .

This explicit combinatorial construction immediately gives us useful information about this crystal, such as the following lemma.

Lemma 3.2.22. *For $k = 0, 1, \dots, s$, let u_k denote the D_n highest weight vector of the classical component $B(k\varpi_2) \subset \tilde{B}^{2,s}$. Then*

$$f_0(u_k) = \begin{cases} u_{k+1} & \text{if } k < s, \\ 0 & \text{if } k = s. \end{cases}$$

Proof. Observe that

$$u_k = \underbrace{\begin{matrix} 1 & \cdots & 1 & 1 & \cdots & 1 \\ 2 & & 2 & \bar{1} & & \bar{1} \end{matrix}}_k \underbrace{\quad}_{s-k};$$

We wish to calculate $f_0(u_k) = \sigma f_1 \sigma(u_k)$.

Note that $u_k \notin \iota_{k-1}^k(B((k-1)\varpi_2))$, so $\ell = k$ in the combinatorial definition of σ above. It follows that $\sigma(u_k) = \iota_k^s(u_k^{*BC})$, which is

$$\iota_k^s(u_k^{*BC}) = \iota_k^s \left(\underbrace{\begin{matrix} 1 & \cdots & 1 & 2 & \cdots & 2 \\ \bar{1} & & \bar{1} & \bar{1} & & \bar{1} \end{matrix}}_{s-k} \underbrace{\quad}_k \right) = \boxed{\emptyset}_{s-k} \underbrace{\begin{matrix} 2 & \cdots & 2 \\ \bar{1} & & \bar{1} \end{matrix}}_k,$$

where $\boxed{\emptyset}_i$ denotes a null-configuration of size i (see Definition 3.1.2). If $k = s$, f_1 kills this tableau, as claimed in the second case of the Lemma. Otherwise, acting by f_1 will decrease the size of the null-configuration by 1 and add another $\frac{2}{\bar{1}}$ to the columns on the right. It follows that ι_s^k kills this tableau, but ι_s^{k+1} does not, so now $\ell = k + 1$

in the combinatorial definition of σ . Thus,

$$\sigma f_1 \sigma(u_k) = t_s^{k+1} \left(\underbrace{\begin{array}{c} 1 \cdots 1 \\ 2 \cdots 2 \end{array}}_{k+1} \boxed{\emptyset_{s-k-1}} \right) = \underbrace{\begin{array}{c} 1 \cdots 1 \\ 2 \cdots 2 \end{array}}_{k+1} \underbrace{\begin{array}{c} 1 \cdots 1 \\ \bar{1} \cdots \bar{1} \end{array}}_{s-k-1} = u_{k+1}.$$

□

Corollary 3.2.23. *Let u_k be as above for $k > 0$. Then*

$$e_0(u_k) = u_{k-1}.$$

A similar combinatorial analysis can be carried out on lowest weight tableaux to show that $f_0(u_k^*) = u_{k-1}^*$ and $e_0(u_k^*) = u_{k+1}^*$ for appropriate values of k . Since $u_0 = u_0^*$, this gives us the following Corollary:

Corollary 3.2.24. *For D_n highest weight vectors u_k and D_n lowest weight vectors u_k^* , we have*

$$\varphi_0(u_k) = \varepsilon_0(u_k^*) = s - k \quad \text{and} \quad \varphi_0(u_k^*) = \varepsilon_0(u_k) = s + k$$

3.3 Proof of Theorem 1.2.2

3.3.1 Overview

To show that $\tilde{B}^{2,s}$ is perfect, it must be shown that all criteria of Definition 2.1.1 are satisfied with $\ell = s$. We have taken part 3 of Definition 2.1.1 as part of our hypothesis for Theorem 1.2.2, so we do not attempt to prove this here.

Part 2 of Definition 2.1.1 is satisfied by simply noting that $\lambda = \varpi_2 = s\Lambda_2 - 2s\Lambda_0$ is a weight in P_{cl} such that $B_\lambda = \{u_s\}$ contains only one crystal vertex and all other vertices in $\tilde{B}^{2,s}$ have “lower” weights, in the ordering designated by part 2 of Definition 2.1.1.

In section 3.3.2, we show that $\tilde{B}^{2,s} \otimes \tilde{B}^{2,s}$ is connected, proving that part 1 of Definition 2.1.1 is satisfied. Parts 4 and 5 of Definition 2.1.1 will be dealt with simultaneously in sections 3.3.4 and 3.3.5 by examining the levels of tableaux combinatorially. We will see that the level of a generic tableau is at least s and the tableaux of level s are in bijection with the level s weights. In section 3.3.6 we show that $\tilde{B}^{2,s}$ is the unique affine crystal satisfying the properties of Conjecture 2.2.5 thereby proving Theorem 1.2.2.

3.3.2 Connectedness of $\tilde{B}^{2,s}$

Lemma 3.3.1 (Part 1 of Definition 2.1.1). *The crystal $\tilde{B}^{2,s} \otimes \tilde{B}^{2,s}$ is connected as a $D_n^{(1)}$ -crystal.*

Proof. (This proof is very similar to that of [28, Proposition 5.1].) For $k = 0, 1, \dots, s$, let u_k denote the highest weight vector of the classical component $B(k\varpi_2) \subset \tilde{B}^{2,s}$, as in Lemma 3.2.22. We will show that an arbitrary vertex $b \otimes b' \in \tilde{B}^{2,s} \otimes \tilde{B}^{2,s}$ is connected to $u_0 \otimes u_0$.

We know that for some $j \in \{0, \dots, s\}$, we have $b' \in B(j\varpi_2)$. Then for some pair of sequences i_1, i_2, \dots, i_p (with entries in $\{1, \dots, n\}$) and m_1, m_2, \dots, m_p (with entries in $\mathbb{Z}_{>0}$) and some $b^1 \in \tilde{B}^{2,s}$, we have $e_{i_1}^{m_1} e_{i_2}^{m_2} \dots e_{i_p}^{m_p}(b \otimes b') = b^1 \otimes u_j$.

By Corollary 3.2.24, $\varphi_0(u_j) = s - j$, so if $\varepsilon_0(b^1) \leq s - j$, Lemma 3.2.22 tells us that $e_0^j(b^1 \otimes u_j) = b^1 \otimes u_0$. If $\varepsilon_0(b^1) = r > s - j$, then $e_0^{r-s+j}(b^1 \otimes u_j) = b^2 \otimes u_j$, where

$\varepsilon_0(b^2) = r - (r - s + j) = s - j$, so $e_0^j(b^2 \otimes u_j) = b^2 \otimes u_0$. In either case, our arbitrary $b \otimes b'$ is connected to an element of the form $b'' \otimes u_0$.

Let j' be such that $b'' \in B(j'\varpi_2)$. Since u_0 is the unique element of $B(0)$, the crystal for the trivial representation of $U_q(D_n)$, we know that $B(j'\varpi_2) \otimes B(0) \simeq B(j'\varpi_2)$. Therefore, $b'' \otimes u_0$ is connected to $u_{j'} \otimes u_0$. Finally, we note that $\varphi_0(u_0) = s < s + j' = \varepsilon_0(u_{j'})$ for $j' \neq 0$, so $e_0^{j'}(u_{j'} \otimes u_0) = e_0^{j'}(u_{j'}) \otimes u_0 = u_0 \otimes u_0$, completing the proof. \square

3.3.3 Preliminary observations

We first make a few observations.

Proposition 3.3.2. *Let $T \in B(k\varpi_2) \subset \tilde{B}^{2,s}$, and set $T^{(m)} = \iota_k^m(T)$ for $m \in \{\ell, \ell + 1, \dots, s\}$, where ℓ is minimal such that $\iota_k^\ell(T) \neq 0$. If $\ell \neq s$, we have for $\ell \leq m < s$*

$$\begin{aligned} \varepsilon_1(T^{(m+1)}) &= \varepsilon_1(T^{(m)}) + 1 \text{ and } \varepsilon_0(T^{(m+1)}) = \varepsilon_0(T^{(m)}) - 1, \\ \varphi_1(T^{(m+1)}) &= \varphi_1(T^{(m)}) + 1 \text{ and } \varphi_0(T^{(m+1)}) = \varphi_0(T^{(m)}) - 1. \end{aligned}$$

Proof. Let $\ell \leq m \leq s - 1$, so ι_m^{m+1} is defined. We first consider the difference between the reduced 1-signatures of $D_{2,s}(T^{(m)})$ and $D_{2,s}(T^{(m+1)}) = D_{2,s}(\iota_m^{m+1}(T^{(m)}))$, since the action of e_1 on these tableaux is defined by the action of the classical e_1 on their image under $D_{2,s}$. Let $-M+P$ be the reduced 1-signature of $D_{2,s}(T^{(m)})$. Let r_1 denote the number of 1's in $D_{2,s}(T^{(m)})$, r_3 the number of $\bar{1}$'s, r_2 the size of the null-configuration, and $t_1 = r_1 + r_2$, $t_2 = r_2 + r_3$. Then there is a contribution $-r_2+r_2$ to the 1-signature from the null-configuration, and the remaining $-$'s and $+$'s come from 1's with a letter greater than 2 below them and $\bar{1}$'s with a letter less than $\bar{2}$ above them, respectively.

We now have two cases. If $t_1 + t_2 \geq s$, ι_m^{m+1} simply increases the size of the null-configuration in $D_{2,s}(T^{(m)})$ by 1. It follows that the reduced 1-signature of $D_{2,s}(T^{(m+1)})$ is $-M+1+P+1$, as we wished to show. On the other hand, if $t_1 + t_2 < s$, after step (2) of Algorithm 3.2.17 for ι_m^{m+1} we have a tableau of shape $(m, m-r_3)/(r_1)$. In step (3), we slide this into shape $(m+1, m+1-(r_3+1))/(r_1+1)$. We claim that the rightmost “uncovered” letter in the second row of this tableau is greater than 2 and the leftmost “unsupported” letter in the first row is less than $\bar{2}$. As observed in the preceding paragraph, this implies that after refilling the empty spaces as in step (4) of Algorithm 3.2.17 the reduced 1-signature of our tableau is $-M+1+P+1$ in this case as well.

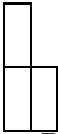
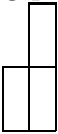
Let us first consider the leftmost “unsupported” letter. After step (2), our tableau is of the form

			a_{r_1+1}	\cdots	a_{m-r_3}	a_{m-r_3+1}	\cdots	a_s
b_1	\cdots	b_{r_1}	b_{r_1+1}	\cdots	b_{m-r_3}			

and its column word is unchanged by the slide

			a_{r_1+1}	\cdots			a_{m-r_3}	a_{m-r_3+1}	\cdots	a_s
b_1	\cdots	b_{r_1}	b_{r_1+1}	\cdots	b_{m-r_3}					

so we have $a_{m-r_3} < b_{m-r_3} \leq \bar{2}$.

The second row of this tableau has $m-r_3$ boxes just as it did before sliding, so the boxes in the bottom row will never be moved. It follows that this sliding procedure only changes L-shaped subtableaux into J-shapes (i.e.,  into ) and never involves any Γ - or Υ -shapes. According to the Lecouvey D -equivalence relations

from section 2.2.3, such moves can only be made when the letters in the bottom row are strictly greater than 2. Specifically, in relations (3) and (4), the letter which is “uncovered” is either n or \bar{n} , while in relations (1) and (2) only the second case of each relation applies. This proves our claim, and thus the first half of the proposition.

Since $e_0 = \sigma \circ e_1 \circ \sigma$, we can derive the statements about ε_0 and φ_0 from the corresponding statements about ε_1 and φ_1 . More precisely, $\varepsilon_0(T) = \varepsilon_1(\sigma(T))$ and $\varphi_0(T) = \varphi_1(\sigma(T))$ and by (3.2.3.3) we have

$$\sigma(T^{(m)}) = (\iota_m^{s+\ell-m} \circ \iota_k^m(T))^{*BC} = \iota_k^{s+\ell-m}(T^{*BC}).$$

Hence

$$\begin{aligned} \varepsilon_0(T^{(m+1)}) &= \varepsilon_1(\sigma(T^{(m+1)})) = \varepsilon_1(\iota_k^{s+\ell-m-1}(T^{*BC})) \\ &= \varepsilon_1(\iota_k^{s+\ell-m}(T^{*BC})) - 1 = \varepsilon_1(\sigma(T^{(m)})) - 1 = \varepsilon_0(T^{(m)}) - 1. \end{aligned}$$

A similar computation can be carried out for φ_0 . □

Corollary 3.3.3. *Given the above hypotheses, we have*

$$\langle h_0 + h_1, \varepsilon(T^{(s)}) \rangle = \langle h_0 + h_1, \varepsilon(T^{(s-1)}) \rangle = \cdots = \langle h_0 + h_1, \varepsilon(T^{(\ell)}) \rangle \neq 0.$$

The following observation is an immediate consequence of Remark 3.2.15:

Corollary 3.3.4. *For $i = 2, \dots, n$,*

$$\langle h_i, \varepsilon(T^{(s)}) \rangle = \langle h_i, \varepsilon(T^{(s-1)}) \rangle = \cdots = \langle h_i, \varepsilon(T^{(\ell)}) \rangle.$$

Lemma 3.3.5. *The map $\Upsilon_{s-1}^s : \mathcal{T}(s-1) \leftrightarrow \mathcal{T}(s)$ sending each summand $B(k\varpi_2) \subset \tilde{B}^{2,s-1}$ to $B(k\varpi_2) \subset \tilde{B}^{2,s}$ for $k = 0, \dots, s-1$ increases the level of all tableaux by exactly 1.*

Proof. Let $T \in \tilde{B}^{2,s-1}$. We have $\varphi_i(\Upsilon_{s-1}^s(T)) = \varphi_i(T)$ for $i = 1, \dots, n$. To calculate the change in $\varphi_0(T)$, we must consider the difference between $\varphi_1(\sigma_{s-1}(T))$ and $\varphi_1(\sigma_s(\Upsilon_{s-1}^s(T)))$. By our descriptions of maps on crystals, we have $\sigma_s(\Upsilon_{s-1}^s(T)) = \Upsilon_{s-1}^s(\iota_j^{j+1}(\sigma_{s-1}(T)))$, where j is determined by $\sigma_{s-1}(T) \in B(j\varpi_2) \subset \tilde{B}^{2,s-1}$. By Proposition 3.3.2, $\varphi_1(\iota_j^{j+1}(\sigma_{s-1}(T))) = \varphi_1(\sigma_{s-1}(T)) + 1$. \square

3.3.4 Surjectivity

Given a weight $\lambda \in (P_{\text{cl}}^+)_s$, we construct a tableau $T_\lambda \in \tilde{B}^{2,s}$ such that $\varepsilon(T_\lambda) = \varphi(T_\lambda) = \lambda$. This amounts to constructing T_λ so that its reduced i -signature is $-\varepsilon_i(T_\lambda) + \varepsilon_i(T_\lambda)$. Note that such a tableau is invariant under the $*$ -involution, so its symmetry allows us to define it beginning with the middle columns, proceeding outwards.

For $i = 0, \dots, n$, let $k_i = \langle h_i, \lambda \rangle$. We first construct a tableau $T_{\lambda'}$ corresponding to the weight $\lambda' = \sum_{i=2}^n k_i \Lambda_i$. We begin with the middle $k_{n-1} + k_n$ columns of $T_{\lambda'}$. If $k_{n-1} + k_n$ is even and $k_n \geq k_{n-1}$, these columns of $T_{\lambda'}$ are

$$\underbrace{\begin{array}{cccc} n-2 & \cdots & n-2 & n-1 \\ n-1 & & n-1 & n \end{array}}_{k_{n-1}} \underbrace{\begin{array}{cccc} n-1 & \cdots & n-1 & n \end{array}}_{(k_n - k_{n-1})/2} \underbrace{\begin{array}{cccc} \bar{n} & \cdots & \bar{n} & \overline{n-1} \\ \overline{n-1} & \cdots & \overline{n-1} & \overline{n-2} \end{array}}_{(k_n - k_{n-1})/2} \underbrace{\begin{array}{cccc} \overline{n-1} & \cdots & \overline{n-1} & \overline{n-2} \\ \overline{n-2} & \cdots & \overline{n-2} & \overline{n-2} \end{array}}_{k_{n-1}}$$

If $k_{n-1} + k_n$ is odd and $k_n \geq k_{n-1}$, we have

$$\underbrace{\begin{array}{cccc} n-2 & \cdots & n-2 & n-1 \\ n-1 & \cdots & n-1 & n \end{array}}_{k_{n-1}} \underbrace{\begin{array}{cccc} n-1 & \cdots & n-1 & \bar{n} \end{array}}_{(k_n - k_{n-1} - 1)/2} \underbrace{\begin{array}{cccc} \bar{n} & \cdots & \bar{n} & \overline{n-1} \\ \overline{n-1} & \cdots & \overline{n-1} & \overline{n-2} \end{array}}_{(k_n - k_{n-1} - 1)/2} \underbrace{\begin{array}{cccc} \overline{n-1} & \cdots & \overline{n-1} & \overline{n-2} \\ \overline{n-2} & \cdots & \overline{n-2} & \overline{n-2} \end{array}}_{k_{n-1}}$$

In either case, if $k_n < k_{n-1}$, interchange n with \bar{n} and k_n with k_{n-1} in the above configurations.

Next we put a configuration of the form

$$\underbrace{\begin{array}{ccc} 1 & 1 & 2 \\ 2 & \cdots & 2 \end{array}}_{k_2} \underbrace{\begin{array}{ccc} 2 & 3 & \cdots \\ 3 & \cdots & 3 \end{array}}_{k_3} \cdots \underbrace{\begin{array}{ccc} n-3 & \cdots & n-3 \\ n-2 & \cdots & n-2 \end{array}}_{k_{n-2}}$$

on the left, and a configuration of the form

$$\underbrace{\begin{array}{ccc} \overline{n-2} & \cdots & \overline{n-2} \\ \overline{n-3} & \cdots & \overline{n-3} \end{array}}_{k_{n-2}} \underbrace{\begin{array}{ccc} \overline{n-2} & \overline{n-3} & \cdots \\ \overline{n-3} & \overline{n-4} & \cdots \end{array}}_{k_{n-3}} \cdots \underbrace{\begin{array}{ccc} \bar{2} & \cdots & \bar{2} \\ \bar{1} & \cdots & \bar{1} \end{array}}_{k_2}$$

on the right, completing $T_{\lambda'}$. Denote the set of tableaux constructed by the procedure up to this point by $\mathcal{M}(s')$, where s' denotes the level of λ' .

Observe that the reduced 1-signature of $T_{\lambda'}$ is empty, so $\langle h_1, \varphi(T_{\lambda'}) \rangle = 0$. Furthermore, since λ' has the same number of 1's as $\bar{1}$'s, it is fixed by σ , so $\langle h_0, \varphi(T_{\lambda'}) \rangle = 0$ as well. Thus Proposition 3.3.2 implies that $T_{\lambda'} \in \tilde{B}_{\min}^{2,s} \cap B(s'\varpi_2) \setminus \iota_{s'-1}^{s'}(B((s'-1)\varpi_2))$ as a subset of $\tilde{B}^{2,s'}$. Recall the embedding $\Upsilon_{s'}^{s'} : \tilde{B}^{2,s'} \hookrightarrow \tilde{B}^{2,s}$ from Definition 3.2.13. Since s' is the minimal m for which $\iota_{s'}^m(T_{\lambda'}) \neq 0$, Lemma 3.3.5 and its proof tell us that $\varepsilon_0(F_{2,s}(T_{\lambda'})) = s - s'$, where the fill map $F_{2,s}$ inserts an a -configuration to increase the width of $T_{\lambda'}$ to s . By the same proposition the desired tableau is $T_{\lambda} = \iota_{s'}^{s'+k_1} \circ F_{2,s}(T_{\lambda'})$. We denote by $\mathcal{M}_{\min}(s)$ the set of tableaux constructed by this procedure.

3.3.5 Injectivity

In this subsection we show that the tableaux in $\mathcal{M}_{\min}(s)$ are all the minimal tableaux in $\tilde{B}^{2,s}$.

We first introduce some useful notation. Observe that any tableau T can be written as $T = T_1T_2T_3T_4T_5$, where the block T_i has width w_i , and all letters in T_1 (resp. T_5) are unbarred or \bar{n} in the second row (resp. barred or n in the first row), all columns in T_2 (resp. T_4) are of the form $\begin{smallmatrix} a \\ b \end{smallmatrix}$ where $a < b \leq n-1$ (resp. $b < a \leq n-1$), and all columns in T_3 are of the form $\begin{smallmatrix} a \\ a \end{smallmatrix}$ for some a . Note that for a tableau in $B(s\varpi_2) \subset \tilde{B}^{2,s}$ we have $0 \leq w_3 \leq 1$. Also note that T_2 and T_4 do not contain any n 's or \bar{n} 's.

Theorem 3.3.6. *We have $\mathcal{M}_{\min}(s) = \tilde{B}_{\min}^{2,s}$.*

Proof. Our proof is by induction on s . For the base case, we have explicitly verified by exhaustion that the statement of the theorem is true for $s = 0, 1, 2$.

By our induction hypothesis, $\mathcal{M}_{\min}(s-1) = \tilde{B}_{\min}^{2,s-1}$. By Lemma 3.3.5, Υ_{s-1}^s increases the level of a tableau by 1, and therefore $\Upsilon_{s-1}^s(\tilde{B}_{\min}^{2,s-1}) = (\tilde{B}^{2,s} \setminus B(s\varpi_2))_{\min}$. By Corollaries 3.3.3 and 3.3.4, ι_{s-1}^s does not change the level of a tableau, so it suffices to show that

$$\mathcal{M}(s) = \tilde{B}_{\min}^{2,s} \cap (B(s\varpi_2) \setminus \iota_{s-1}^s(B((s-1)\varpi_2))). \quad (3.3.3.1)$$

By Lemmas 3.3.8 and 3.3.9 below, if T is a minimal tableau not in the image of ι_{s-1}^s , it has $w_2 = w_4 = 0$, and if $w_3 = 1$, then $T_3 = \begin{smallmatrix} n \\ \bar{n} \end{smallmatrix}$ or $T_3 = \begin{smallmatrix} \bar{n} \\ n \end{smallmatrix}$. By Lemma 3.3.10, equation (3.3.3.1) follows. \square

The following lemmas are used in the proof of Theorem 3.3.6. The proofs of these

lemmas rely on induction on s , as did the proof of Theorem 3.3.6. The base cases $s = 0, 1, 2$ have been checked explicitly.

Lemma 3.3.7. *For all $t \in \tilde{B}^{2,s}$ we have $\langle c, \varepsilon(t) \rangle \geq s$ and $\langle c, \varphi(t) \rangle \geq s$.*

Proof. By the induction hypothesis, $\tilde{B}_{\min}^{2,s-1} = \mathcal{M}_{\min}(s-1)$.

Observe that by Corollaries 3.3.3 and 3.3.4 ι_i^j is level preserving, and by Lemma 3.3.5, the map Υ_{s-1}^s increases the level of a tableau by one. Our induction hypothesis therefore allows us to assume that $t \in B(s\varpi_2) \setminus \iota_{s-1}^s(B((s-1)\varpi_2))$. Combinatorially, we may characterize such tableaux as being those which are legal in the classical sense and for which removing all 1's, $\bar{1}$'s, and null configurations produces a tableau which is Lecouvey D -equivalent to a tableau whose first row has width s . This characterization follows from the combinatorial description of ι_{s-1}^s in Algorithm 3.2.17.

We may further restrict our attention by the observation that if T is minimal, then so is T^* . We may therefore assume that the stratum of the branching component vertex of T is non-negative. In particular, this means that T has no more $\bar{1}$'s than 1's.

Our approach is to consider the tableau T' that results from removing the leftmost column from T . We will show that if T' is minimal, the level of T exceeds the level of T' by at least 2, and if T' is not minimal, the level of T is at least as great as the level of T' .

First consider the case when T' is minimal. Since T is assumed to be such that removing all 1's and $\bar{1}$'s produces a tableau which is Lecouvey D -equivalent to a tableau whose first row has width s , it is the case that removing all 1's and $\bar{1}$'s from T' produces a tableau which is Lecouvey D -equivalent to a tableau whose first row has width $s-1$. The minimal tableaux of $\tilde{B}^{2,s-1}$ with this property are precisely

$\mathcal{M}(s-1)$. By properties of $\mathcal{M}(s-1)$, we know that $\varphi_0(T') = 0$, so $\varphi_0(T) \geq \varphi_0(T')$. Since our base case is $s = 2$, we know that the first column of T is $\frac{a}{b}$, where a and b are both unbarred. Observe that $\varphi(T) = \varphi(T') + 2\Lambda_b + \text{non-negative weight}$ if $b \neq n-1$ or $\varphi(T) = \varphi(T') + \Lambda_{n-1} + \Lambda_n + \text{non-negative weight}$ if $b = n-1$. Hence, the level is increased by at least 2.

Now suppose T' is not minimal. The level of the i -signatures (that is to say, the level of the sum of the weights $\varphi_i(T')$ which depend on i -signatures) cannot have a net decrease for $i = 1, \dots, n$, but there is now a possibility that $\varphi_0(T) < \varphi_0(T')$. We will show that when $\varphi_0(T) < \varphi_0(T')$, the level of the i -signatures goes up by at least $\varphi_0(T') - \varphi_0(T)$.

First, suppose T has no 1's. Then by one of our hypotheses, it also has no $\bar{1}$'s, and is therefore fixed by σ : it follows that $\varphi_0(T) = \varphi_1(T)$, so we may assume the upper-left entry of T to be 1.

We know that $\varphi_0(T)$ is equal to the number of $-$'s in the reduced 1-signature of $\sigma(T)$. Consider the following tableaux:

$$\begin{aligned}
T' &= \begin{array}{cccccccc} 1 & \dots & 1 & a_{m_1+1} & \dots & a_{s-m_2} & a_{s-m_2+1} & \dots & a_s \\ b_1 & & b_{m_1} & b_{m_1+1} & & b_{s-m_2} & \underbrace{\bar{1} \dots \bar{1}}_{m_2} & & \end{array} \\
T &= \begin{array}{cccccccc} 1 & 1 & \dots & 1 & a_{m_1+1} & \dots & a_{s-m_2} & a_{s-m_2+1} & \dots & a_s \\ b & b_1 & & b_{m_1} & b_{m_1+1} & & b_{s-m_2} & \underbrace{\bar{1} \dots \bar{1}}_{m_2} & & \end{array} \\
\sigma(T') &= \begin{array}{cccccccc} 1 & \dots & 1 & 1 & a'_{m_2+1} & \dots & a'_{s-m_1} & a'_{s-m_1+1} & \dots & a'_s \\ b_1 & & b_{m_2-1} & b'_{m_2} & b'_{m_2+1} & & b'_{s-m_1} & \underbrace{\bar{1} \dots \bar{1}}_{m_1} & & \end{array} \\
\sigma(T) &= \begin{array}{cccccccc} 1 & 1 & \dots & 1 & a''_{m_2} & \dots & a''_{s-m_1-1} & a''_{s-m_1} & \dots & a''_s \\ b & b_1 & & b_{m_2-1} & b''_{m_2} & & b''_{s-m_1-1} & \underbrace{\bar{1} \dots \bar{1}}_{m_1+1} & & \end{array}
\end{aligned}$$

Note that our assumption that $m_2 \leq m_1 + 1$ ensures that the absence of primes on b, b_1, \dots, b_{m_2-1} is accurate.

Let us consider all possible ways for the number of $-$'s in the 1-signature to be smaller for $\sigma(T)$ than for $\sigma(T')$. The number of 1's is the same, so the only way this contribution could be decreased is by having more 2's in the first m_2 letters of the bottom row of $\sigma(T)$. This can only come about by having $b = 2$, and only one $-$ may be removed in this way.

The other possibility is for the number of $-$'s contributed by $\bar{2}$'s to be decreased. The only Lecouvey relation which removes a $\bar{2}$ assumes the presence of a column $\frac{2}{2}$, which we disallow, as it is necessarily part of a null-configuration. To decrease this contribution therefore requires an additional $+$ in the 1-signature of $\sigma(T)$ compared to that of $\sigma(T')$, which will bracket one of the $-$'s from a $\bar{2}$. The additional $+$ may come from one of the additional $\bar{1}$'s, or from a 2 that is "pushed out" from under the 1's at the beginning in the case $b = 2$. Note that this second possibility is mutually exclusive with having more 2's bracketing 1's at the beginning.

In any case, we see that $\varphi_0(T) - \varphi_0(T') \leq 2$, and that when this value is 2, the first column of T is $\frac{1}{2}$. This column adds no $+$'s to the i -signatures, but does provide a new $-$ in the 2-signature. Since Λ_2 is a level 2 weight, the level stays the same in this case.

If $\varphi_0(T) - \varphi_0(T') = 1$ and the first column of T is $\frac{1}{2}$, we in fact have a net increase in level. If $b \neq 2$, the i -signature levels go up by at least 1, so still the total level cannot decrease.

□

Lemma 3.3.8. *If $T \in (\tilde{B}^{2,s} \cap B(s\varpi_2))_{\min}$, we have $w_1 + w_2 = w_4 + w_5 = \lfloor s/2 \rfloor$ with*

w_1, w_2, w_4 and w_5 as defined in the beginning of this subsection.

Proof. We first establish that $\langle c, \varphi(T) \rangle \geq 2w_1 + 2w_2 + w_3$, and thus by *-duality, $\langle c, \varepsilon(T) \rangle \geq w_3 + 2w_4 + 2w_5$ as well. Recall that $0 \leq w_3 \leq 1$.

First, observe that every letter in the bottom row of T_1 contributes:

- a $-$ to the reduced a -signature if $2 \leq a \leq n - 2$ is in the bottom row;
- a $-$ to both the $(n - 1)$ -signature and the n -signature if $n - 1$ is in the bottom row;
- a $-$ to the n -signature (resp. $(n - 1)$ -signature) if n (resp. \bar{n}) is the bottom row.

Suppose T_1 has a column of the form $\begin{smallmatrix} a \\ b \end{smallmatrix}$ with $b \neq a + 1$, or $b = \bar{n}$ and $a \neq n - 1$. For the $-$ in the a -signature of T contributed by this a to be bracketed, we must have a column of the form $\begin{smallmatrix} a' \\ a+1 \end{smallmatrix}$ to the left of this column in T_1 , with $a' < a$. Applying this observation recursively, we see that to bracket as many $-$'s as possible we must eventually have a column of the form $\begin{smallmatrix} 1 \\ c \end{smallmatrix}$ for some $c \neq 2$. Note that in the case of columns of the form $\begin{smallmatrix} n-1 \\ n \end{smallmatrix}$ (resp. $\begin{smallmatrix} n-1 \\ \bar{n} \end{smallmatrix}$) the $-$ in the n -signature (resp. $(n - 1)$ -signature) from $n - 1$ that is not bracketed by the $+$ from the n (resp. \bar{n}) below it cannot be bracketed, since n and \bar{n} may not appear in the same row.

Now, consider a column $\begin{smallmatrix} a \\ b \end{smallmatrix}$ in T_2 , so we have $a < b$, and thus also $\bar{a} > \bar{b}$. Recall that T_2 has no n 's or \bar{n} 's, so $b \leq n - 1$. This column contributes $-$'s to the a -signature and the $(b - 1)$ -signature of T . In this case, these $-$'s may be bracketed. Due to the conditions that the rows and columns of T are increasing, the $-$ from the a can only be bracketed by an $a + 1$ in the bottom row of T_1 and the $-$ from the \bar{b} can only be bracketed by a b in the bottom row of T_1 . Furthermore, the letter above these

must be strictly less than a and $b - 1$, respectively. By the reasoning in the previous paragraph, we see that to bracket every $-$ engendered by the column $\frac{a}{b}$ we must have two columns of the form $\frac{1}{a'}$, with each $a' \neq 2$.

If $w_3 = 1$, T has a column of the form $\frac{a}{a}$. We have two cases; $2 \leq a \leq n - 1$, and $a = n$ (resp. $a = \bar{n}$). In the first case, we have a $-$ in the $(a - 1)$ -signature from the \bar{a} in this column. Because of the prohibition against configurations of the form $\frac{a}{a}$, this $-$ can only be bracketed by a $+$ from an a in the bottom row of T_1 . Therefore, this column engenders another column of the form $\frac{1}{a'}$. In the case of $a = n$ (resp. $a = \bar{n}$), we have a $-$ in the $(n - 1)$ -signature (resp. n -signature) which cannot be bracketed.

To bracket the maximal number of $-$'s (i.e., to minimize $\langle c, \varphi(T) \rangle$) we see that unless $T_3 = \frac{n}{\bar{n}}$ or $T_3 = \frac{\bar{n}}{n}$, we must have

$$T_1 T_2 T_3 = \underbrace{\begin{matrix} 1 & \cdots & 1 \\ b_1 & & b_{2w_2+w_3} \end{matrix}}_{2w_2+w_3} \underbrace{\begin{matrix} a_{2w_2+w_3+1} & \cdots & a_{w_1} \\ b_{2w_2+w_3+1} & & b_{w_1} \end{matrix}}_{w_1-(2w_2+w_3)} \underbrace{\begin{matrix} a_{w_1+1} & \cdots & a_{w_1+w_2+w_3} \\ \bar{b}_{w_1+1} & & \bar{b}_{w_1+w_2+w_3} \end{matrix}}_{w_2+w_3}, \quad (3.3.3.2)$$

where each column in the first block contributes 3 to $\langle c, \varphi(T) \rangle$, each column in the second block contributes 2 to $\langle c, \varphi(T) \rangle$, and the third block contributes nothing. In the case $T_3 = \frac{n}{\bar{n}}$ or $T_3 = \frac{\bar{n}}{n}$, we have $w_2 = 0$, so we simply have $T_1 T_2 T_3 = T_1 T_3$, where each column in T_1 increases $\langle c, \varphi(T) \rangle$ by at least 2 and T_3 increases $\langle c, \varphi(T) \rangle$ by 1. We therefore have in the first case $\langle c, \varphi(T) \rangle \geq 3(2w_2 + w_3) + 2(w_1 - 2w_2 - w_3) = 2w_1 + 2w_2 + w_3$, and in the second case $\langle c, \varphi(T) \rangle \geq 2w_1 + w_3 = 2w_1 + 2w_2 + w_3$, as we wished to show.

Since by Lemma 3.3.7 elements in $\tilde{B}^{2,s}$ have level at least s , it follows that when $T \in (\tilde{B}^{2,s} \cap B(s\varpi_2))_{\min}$, we have $w_1 + w_2 \leq \lfloor s/2 \rfloor$, and by $*$ -duality that $w_4 + w_5 \leq \lfloor s/2 \rfloor$. Furthermore, since $s = w_1 + w_2 + w_3 + w_4 + w_5$, it follows that $w_1 + w_2 =$

$w_4 + w_5 = \lfloor \frac{s}{2} \rfloor$ and $w_3 = 0$ if s is even and $w_3 = 1$ if s is odd. \square

Lemma 3.3.9. *Suppose $T \in (\tilde{B}^{2,s} \cap B(s\varpi_2))_{\min}$ has both an unbarred letter and a barred letter in a single column $\frac{a}{\bar{b}}$ other than $\frac{n}{\bar{n}}, \frac{\bar{n}}{n}, \frac{n-1}{\bar{n}}$, or $\frac{n}{n-1}$. Then $T \in \iota_{s-1}^s(B((s-1)\varpi_2))$.*

Proof. By using the reverse of Algorithm 3.2.17, it suffices to show the following:

1. T has a 1;
2. T has a $\bar{1}$;
3. after removing all 1's and $\bar{1}$'s, applying the Lecouvey D relations will reduce the width of T .

The proof of Lemma 3.3.8 shows that if $w_2 \neq 0$, or $w_3 = 1$ and $T_3 \neq \frac{n}{\bar{n}}, \frac{\bar{n}}{n}$, then T has a 1. By $*$ -duality, if $w_4 \neq 0$, or the same condition is placed on w_3 and T_3 , then T has a $\bar{1}$. We will show that if $w_2 + w_3 \neq 0$, then $w_3 + w_4 \neq 0$, which will prove statements (1) and (2) above.

If $w_3 = 1$ this statement is trivial, so we assume $w_3 = 0$. We show that the assumptions $w_2 \neq 0$ and $w_4 = 0$ lead to a contradiction. From the proof of Lemma 3.3.8, we know that for T to be minimal, every $-$ from T_5 must be bracketed. Because of the increasing conditions on the rows and columns of T , the $-$'s from the bottom row of T_5 cannot be bracketed by $+$'s from T_5 , so there must be at least w_5 $+$'s from T_1T_2 . Inspection of (3.3.3.2) shows us that the first block contributes no $+$'s, the second block contributes $w_1 - 2w_2$ many $+$'s, and the third block contributes $2w_2$ many $+$'s. We thus have $w_1 \geq w_5$; but Lemma 3.3.8 tells us that $w_1 + w_2 = w_4 + w_5$, contradicting our assumption that $w_2 \neq 0$ and $w_4 = 0$.

For the proof of statement (3), we must show that every configuration ${}_a^c$ in T avoids the following patterns (recall the Lecouvey D sliding algorithm from section 2.2.3): ${}_x^n$ and ${}_x^{\bar{n}}$ with $x \leq n - 1$; ${}_{n-1}^{\bar{n}}$; ${}_{n-1}^n$; and $c \geq a$, unless $c = a = \bar{b}$. If T has any of these patterns, the top row will not slide over.

First, simply observe that the first four specified configurations exclude the possibility of having a column of the form $\frac{a}{b}$ other than $\frac{n}{\bar{n}}$ or $\frac{\bar{n}}{n}$. It therefore suffices to show that the presence of a column $\frac{d}{e}$, $2 \leq d, e \leq n - 1$ implies that T avoids $c \geq a$, unless $c = a = \bar{b}$. We break our analysis of this criterion into several special cases:

Case 1: a and b are barred, c is unbarred: trivial.

Case 2: a is unbarred, b and c are barred: This excludes the possibility of having $\frac{d}{e} \in T$.

Case 3: a and c are unbarred, b is barred: We know the $-$ in the c -signature from c must be bracketed; if it is by b , we have $b = \bar{c}$. As we saw in the proof of Lemma 3.3.8, we must have the $-$ in the $(c - 1)$ -signature from \bar{c} bracketed by a c in the bottom row. This forces $a \geq c$. If the $-$ in the c -signature from c is bracketed by a $c + 1$, it also must be in the bottom row, forcing $a > c$.

Case 4: a, b, c all unbarred: Suppose $c \geq a$. Let d be the leftmost unbarred letter weakly to the right of c which does not have its $-$ bracketed by the letter immediately below it. (Such a letter exists, since we assume the occurrence of $\frac{d}{e} \in T$, except when $d = e$; this case will be treated below.) This letter d must be bracketed by a $d + 1$ in the bottom row, and it must be weakly to the left of a . But we have $d + 1 > d \geq c \geq a \geq d + 1$; contradiction.

If instead we have a $\frac{d}{d}$ column, we must have the $-$ from the \bar{d} bracketed by a d in the bottom row weakly to the left of a . In this case $d \geq c \geq a \geq d$ so $c = d$, and we have a $\frac{d}{d}$ configuration, contradicting our assumption that $T \in B(s\varpi_2)$.

Case 5: a, b, c all barred: Similarly to case 4, suppose $c \geq a$ and let d be the rightmost barred letter weakly to the left of a which does not have its $+$ bracketed by the letter immediately above it. (If none exists, we have a \bar{d} case, see below.) It must be bracketed by a $\overline{\bar{d}+1}$ in the top row to the right of c . We then have $d \leq a \leq c \leq \overline{\bar{d}+1}$; contradiction.

If we have a \bar{d} column (note that d is barred), the $+$ from the \bar{d} must be bracketed by a d in the top row to the right of c . This implies that $d \geq c \geq a \geq d$, so $a = d$ and we have a \bar{d} configuration, again contradicting our assumption that $T \in B(s\varpi_2)$.

□

Lemma 3.3.10. *Let $T \in (\tilde{B}^{2,s} \cap B(s\varpi_2))_{\min}$ such that T does not contain any column $\frac{a}{b}$ for $1 \leq a, b \leq n$ except possibly $\frac{n-1}{\bar{n}}$, $\frac{n}{\bar{n}}$, or $\frac{n}{n-1}$. Then $T \in \mathcal{M}(s)$.*

Proof. In the notation of section 3.3.5, we have $w_2 = w_4 = 0$, and if $w_3 = 1$, $T_3 = \frac{n}{\bar{n}}$ or $T_3 = \frac{\bar{n}}{n}$. Lemma 3.3.8 thus tells us that $w_1 = w_5$.

Next we show that a column $\frac{j}{i}$ must be of the form $\frac{i-1}{i}$ for T to be in $\tilde{B}_{\min}^{2,s}$. For $i = 2$ we have $j = 1$ by column-strictness. Now suppose that $\frac{j}{i}$ is the leftmost column such that $j < i - 1$. Then j contributes a Λ_j to $\varphi(T)$ and hence $\langle c, \varphi(T) \rangle \geq 2w_1 + w_3 + 1 = s + 1$, so that T is not minimal. By a similar argument $\langle c, \varepsilon(T) \rangle > s$ unless all columns of the form $\frac{\bar{j}}{j}$ must obey $j = i - 1$.

A column $\frac{\bar{i}}{i-1}$ for $i > 2$ (resp. $\frac{n}{n-1}$) contributes a $-$ to the $(i - 2)$ -signature (resp. $(n - 2)$ -signature) of T . This $-$ can only be compensated by a $+$ in the $(i - 2)$ -signature (resp. $(n - 2)$ -signature) from a column $\frac{i-1}{i}$ (resp. $\frac{n-1}{\bar{n}}$). Hence for T to be minimal the number of columns of the form $\frac{i-1}{i}$ (resp. $\frac{n-1}{\bar{n}}$) needs to be the same as the number of columns of the form $\frac{\bar{i}}{i-1}$ (resp. $\frac{n}{n-1}$). This proves that $T \in \mathcal{M}(s)$. □

3.3.6 Uniqueness

Theorem 1.2.2 follows as a corollary from the next Proposition.

Proposition 3.3.11. *$\tilde{B}^{2,s}$ is the only affine finite-dimensional crystal satisfying the properties of Conjecture 2.2.5.*

For the proof of Proposition 3.3.11 we must show that our definition of σ is the only crystal automorphism satisfying the properties of Conjecture 2.2.5. Recall from the beginning of section 2.4 the relationship between σ and $\check{\sigma}$. Let $T \in \tilde{B}^{2,s}$. We know that

$$\text{wt}(T) = \sum_{i=0}^n k_i \Lambda_i \Leftrightarrow \text{wt}(\sigma(T)) = k_1 \Lambda_0 + k_0 \Lambda_1 + \sum_{i=2}^n k_i \Lambda_i. \quad (3.3.3.3)$$

Please note that in this section we often use the phrase “the tableau b is in the branching component vertex v ” to mean $b \in B(v)$.

Lemma 3.3.12. *Let $v \in \mathcal{BC}(k\varpi_2)$ be a branching component vertex in stratum 0 associated with a rectangular partition, and let ℓ be minimal such that $v \in \check{i}_\ell^k(\mathcal{BC}(\ell\varpi_2))$. Then the hypothesis that $\tilde{B}^{2,s}$ is perfect of level s can only be satisfied if $\check{\sigma}(v)$ is the vertex associated with the same shape as v in stratum 0 in $\mathcal{BC}((s + \ell - k)\varpi_2)$.*

Proof. We have already shown that $\check{\sigma}(v)$ has the same shape as v and is in stratum 0, so it only remains to show that $\check{\sigma}(v) \in \mathcal{BC}((s + \ell - k)\varpi_2)$.

First, observe that v must contain a minimal tableau as constructed in section 3.3.4, according to the following table.

shape associated with v	weight of tableau in v
$(2m)$	$m\Lambda_2 + (k - 2m)\Lambda_1 + (s - k)\Lambda_0$
(m, m)	$m\Lambda_3 + (k - 2m)\Lambda_1 + (s - k)\Lambda_0$

Recall from 2.4 that $\text{cw}(b) = \text{wt}(b) - (\varphi_0(b) - \varepsilon_0(b))\Lambda_0$. Let T be the tableau constructed by this prescription, so that $\langle c, \text{cw}(T) \rangle = k$. The criterion that $\langle c, \varphi(T) \rangle \geq s$ forces us to have $\varphi_0(T) = \varphi_1(\sigma(T)) \geq s - k$. We denote $T^{(i)} = i_k^i(T)$, and thus have $\varphi_1(T^{(i)}) = i - \ell$.

We show inductively that $\sigma(T^{(i)}) = T^{(s+\ell-i)}$ for $\ell \leq i \leq s$. As a base case, we see that $\langle c, \text{cw}(T^{(\ell)}) \rangle = \ell$, so we must have $\varphi_1(\sigma(T^{(\ell)})) \geq s - \ell$. The only $T^{(i)}$ for which this inequality holds is $T^{(s)}$, where we have $\varphi_1(T^{(s)}) = s - \ell$.

For the induction step, assume that σ sends $T^{(\ell)}, T^{(\ell+1)}, \dots, T^{(k-1)}$ to $T^{(s)}, \dots, T^{(s+\ell-k+1)}$, respectively. By the above inequality this implies $\varphi_1(\sigma(T^{(k)})) \geq s - k$, which specifies that $\sigma(T^{(k)}) = T^{(s+\ell-k)}$. \square

Definition 3.3.13. Recall the map $\Upsilon_{s'}^s$ from Definition 3.2.13. We define $\check{\Upsilon}_{s'}^s : \mathcal{BC}(\tilde{B}^{2,s'}) \hookrightarrow \mathcal{BC}(\tilde{B}^{2,s})$ by $\check{\Upsilon}_{s'}^s(v) = v'$ if for some $T \in B(v)$, we have $\Upsilon_{s'}^s(T) \in B(v')$.

Lemma 3.3.14. *Let $v \in \mathcal{BC}(k\varpi_2)$ be a branching component vertex in stratum p with $1 \leq p \leq s - 1$ associated to the shape (λ_1, λ_2) . Suppose that for the branching component vertex $w \in \mathcal{BC}(k\varpi_2)$ in stratum $p - 1$ with shape $(\lambda_1 - 1, \lambda_2)$, $\tilde{B}^{2,s}$ has the correct energy function and is perfect only if $\check{\sigma}(w)$ is as described in section 3.1.5. Then $\tilde{B}^{2,s}$ has the correct energy function only if $\check{\sigma}(v)$ is as described in section 3.1.5.*

Proof. First, recall that the partitions associated to vertices in stratum p in $\mathcal{BC}(\tilde{B}^{2,s})$ are produced by adding or removing one box from the partitions associated to vertices

of stratum $p+1$. Since the vertex in stratum s is associated with a rectangle of shape (s) , the only stratum for which we can have a two-row rectangle is stratum 0. It follows that removing a box from the first row of v results in a partition appearing in stratum $p-1$, so there is in fact a vertex w as described in the statement of the lemma.

Let ℓ be minimal such that $v \in \check{i}_\ell^k(\mathcal{BC}(\ell\varpi_2))$. We may assume $v \notin \mathcal{BC}(\ell\varpi_2)$, and let $\check{\sigma}(v)$ be determined by the involutive property of $\check{\sigma}$ in the case $v \in \mathcal{BC}(\ell\varpi_2)$. Specifically, we will show that the vertex $v' \in \mathcal{BC}(s\varpi_2)$ with the same shape and stratum as v has the property that $\check{\sigma}(v')$ is the complementary vertex of v , and therefore $\check{\sigma}(v)$ is the complementary vertex of v' . (Recall the notion of complementary vertex from page 38.)

The top row of w is one box shorter than the top row of v , so that $w \in \check{i}_{\ell-1}^k(\mathcal{BC}((\ell-1)\varpi_2))$, and $\ell-1$ is minimal with this property. By our hypothesis, $\check{\sigma}(w)$ is the vertex with shape (λ_1-1, λ_2) of stratum $-p+1$ in $\mathcal{BC}((s+(\ell-1)-k)\varpi_2)$.

We now use induction on s . Suppose that the only choice of $\check{\sigma}$ for which $\tilde{B}^{2,s-1}$ is perfect and has an energy function is that of section 3.1.5. Part 3 of Conjecture 2.2.5 states that in $\tilde{B}^{2,s}$, the energy on the component $B((s-k)\varpi_2)$ is $-k$, and so the difference in energy between $B((s-k)\varpi_2)$ and $B((s-j)\varpi_2)$ is $j-k$. In order for this to be true for all $1 \leq k, j \leq s-1$, the action of f_0 and e_0 on $\tilde{B}^{2,s}$ must agree with the action on $\tilde{B}^{2,s-1}$. More precisely, if v and w are in different classical components of $\tilde{B}^{2,s-1}$ and $f_0(v) = w$ in $\tilde{B}^{2,s-1}$, then $f_0(\Upsilon_{s-1}^s(v)) = \Upsilon_{s-1}^s(w)$; this statement extends naturally to $\mathcal{BC}(\tilde{B}^{2,s-1})$ and $\mathcal{BC}(\tilde{B}^{2,s})$.

Let v^\dagger denote the vertex with shape (λ_1, λ_2) in stratum $-p$ in $\mathcal{BC}((s+\ell-k)\varpi_2)$. Since we assumed $k \neq \ell$, we know that $v^\dagger \notin \mathcal{BC}(s\varpi_2)$, and therefore v^\dagger has a preimage under $\check{\Upsilon}_{s-1}^s$. From our construction of $\check{\sigma}$ we know that in $\mathcal{BC}(\tilde{B}^{2,s-1})$, $(\check{\Upsilon}_{s-1}^s)^{-1}(v^\dagger)$

has a 0 arrow to $(\check{Y}_{s-1}^s)^{-1}(\check{\sigma}(w))$. Our induction argument tells us that in $\mathcal{BC}(\tilde{B}^{2,s})$, v^\dagger has a 0 arrow to $\check{\sigma}(w)$. Since v has a 1 arrow to w and we must have $f_0 = \sigma f_1 \sigma$, we conclude that in fact $\check{\sigma}(v) = v^\dagger$. \square

Lemma 3.3.15. *Let $v \in \mathcal{BC}(k\varpi_2)$ be a branching component vertex in stratum 0 associated to the non-rectangular shape (λ_1, λ_2) , and suppose that for the branching component vertex $w \in \mathcal{BC}(k\varpi_2)$ in stratum 1 with shape $(\lambda_1, \lambda_2 + 1)$, $\tilde{B}^{2,s}$ has the correct energy function and is perfect only if $\check{\sigma}(w)$ is as described in section 3.1.5. Then $\tilde{B}^{2,s}$ has the correct energy function only if $\check{\sigma}(v)$ is as described in section 3.1.5.*

Proof. (This proof is very similar to the proof of Lemma 3.3.14.)

Let ℓ be minimal such that $v \in \check{i}_\ell^k(\mathcal{BC}(\ell\varpi_2))$, assuming $k \neq \ell$. Note that ℓ is also minimal for $w \in \check{i}_\ell^k(\mathcal{BC}(\ell\varpi_2))$, since the shapes for v and w have the same number of boxes in the first row. By our hypothesis, $\check{\sigma}(w)$ is the vertex with shape $(\lambda_1, \lambda_2 + 1)$ in stratum 1 in $\mathcal{BC}((s + \ell - k)\varpi_2)$. Let v^\dagger be the vertex with shape (λ_1, λ_2) in stratum 0 in $\mathcal{BC}((s + \ell - k)\varpi_2)$. From our construction of $\check{\sigma}$, we know that in $\mathcal{BC}(\tilde{B}^{2,s-1})$, $(\check{Y}_{s-1}^s)^{-1}(w)$ has a 0 arrow to $(\check{Y}_{s-1}^s)^{-1}(\check{\sigma}(v^\dagger))$. It follows from our induction argument that in $\mathcal{BC}(\tilde{B}^{2,s})$, w has a 0 arrow to $\check{\sigma}(v^\dagger)$. Since w has a 1 arrow to v and we must have $f_0 = \sigma f_1 \sigma$, we conclude that in fact $\check{\sigma}(v) = v^\dagger$. \square

Corollary 3.3.16. *Corollary 2.4.1 and Lemmas 3.3.12, 3.3.14 and 3.3.15 determine $\check{\sigma}$ on $\mathcal{BC}(\tilde{B}^{2,s})$ uniquely.*

Proof. For any vertex v associated with shape (λ_1, λ_2) in stratum $p \geq 0$, $\check{\sigma}(v)$ is fixed by the image under $\check{\sigma}$ of a vertex with shape $(\lambda_1 - s + p, \lambda_2)$ and in stratum 0 by Lemma 3.3.14. If $\lambda_1 - s + p \neq \lambda_2$, Lemmas 3.3.14 and 3.3.15 may be used together

to reduce determining $\check{\sigma}(v)$ to determining the action of $\check{\sigma}$ on a rectangular vertex in stratum 0, which is given by Lemma 3.3.12. \square

Chapter 4

Local Properties of Crystals for Modules over Doubly Laced Algebras

4.1 Local Characterization of Simply Laced Crystals

In [46], a local characterization of crystals for highest weight integrable representations of simply-laced algebras is given. Furthermore, Proposition 2.4.4 of [17] states that a crystal with a unique maximal vertex comes from a representation if and only if it decomposes as a disjoint union of crystals of representations relative to the rank 2 subalgebras corresponding to each pair of edge colors. It therefore suffices to address the problem of locally characterizing crystal graphs for rank 2 algebras. The results of [46] apply to the algebras $A_1 \times A_1$ and A_2 ; the obvious next case to consider is

$C_2 \simeq B_2$. In the sequel, a “doubly laced algebra” is a Kac-Moody algebra all of whose regular rank 2 subalgebras are $A_1 \times A_1$, A_2 , or C_2 .

We now recall the results of [46] on the local structure of crystal graphs. While the main theorem of [46] pertains only to simply laced algebras, several statements that apply to crystals for an arbitrary Kac-Moody algebra are also proved there.

We begin by choosing an index set I and a Cartan matrix $A = [a_{ij}]_{i,j \in I}$ for a Kac-Moody algebra, and consider a directed graph X whose edges are colored by the elements of I . We assume that

(P1) All monochromatic directed paths in X have finite length

(P2) For any vertex v of X and every $i \in I$, there is at most one i edge into v and one i edge out of v .

These assumptions (the first two axioms of [46]) allow us to define the i -string through v to be the maximal path in X of the form

$$f_i^{-d}v \rightarrow \cdots \rightarrow f_i^{-1}v \rightarrow v \rightarrow f_i v \rightarrow \cdots \rightarrow f_i^r v.$$

These familiar statistics $d = \varepsilon_i(v)$ and $r = \varphi_i(v)$ are here called the i -depth and i -rise of v , respectively.

Remark 4.1.1. Our conventions differ from those of [46] by the sign of the i -depth and the greek letters denoting these quantities. This is more consistent with the existing literature on crystals.

Stembridge introduces the following local statistics for a crystal vertex v such that

$\varepsilon_i(v) > 0$ and $\varepsilon_j(v) > 0$:

$$\Delta_i \varepsilon_j(v) = \varepsilon_j(v) - \varepsilon_j(e_i v) \quad \text{and} \quad \Delta_i \varphi_j(v) = \varphi_j(v) - \varphi_j(e_i v),$$

and complementarily,

$$\nabla_i \varepsilon_j(v) = \varepsilon_j(v) - \varepsilon_j(f_i v) \quad \text{and} \quad \nabla_i \varphi_j(v) = \varphi_j(v) - \varphi_j(f_i v).$$

He shows that for a crystal of a module over any Kac-Moody algebra, we have the following

$$(P3) \quad \Delta_i \varepsilon_j(v) + \Delta_i \varphi_j(v) = a_{ij}$$

$$(P4) \quad \Delta_i \varphi_j(v) \leq 0 \text{ and } \Delta_i \varepsilon_j(v) \leq 0$$

$$(P5) \quad \text{If } \Delta_i \varepsilon_j(v) = 0, \text{ then } e_i e_j v = e_j e_i v \text{ and } \nabla_j \varphi_i(e_i e_j v) = 0$$

$$(P6) \quad \text{If } \Delta_i \varepsilon_j(v) = \Delta_j \varepsilon_i(v) = -1, \text{ then } e_i e_j^2 e_i v = e_j e_i^2 e_j v, \text{ and } \nabla_i \varphi_j(e_i e_j^2 e_i v) = \nabla_i \varphi_j(e_i e_j^2 e_i v) = -1.$$

$$(P5') \quad \text{If } \nabla_i \varepsilon_j(v) = 0, \text{ then } e_i e_j v = e_j e_i v \text{ and } \Delta_j \varphi_i(e_i e_j v) = 0$$

$$(P6') \quad \text{If } \nabla_i \varepsilon_j(v) = \nabla_j \varepsilon_i(v) = -1, \text{ then } e_i e_j^2 e_i v = e_j e_i^2 e_j v, \text{ and } \Delta_i \varphi_j(e_i e_j^2 e_i v) = \Delta_i \varphi_j(e_i e_j^2 e_i v) = -1.$$

Stembridge proved that these axioms hold for all crystals of highest weight modules of Kac-Moody algebras, and that they precisely characterize those over simply laced algebras. In the work that follows, we show that when generalizing to doubly laced

algebras, there are only two other possible local behaviors,

$$e_i e_j e_i e_j e_i v = e_j e_i^3 e_j v \quad \text{and} \quad e_i e_j^2 e_i^3 e_j v = e_j e_i^3 e_j^2 e_i v.$$

Note that Theorem 1.2.4 does not provide a local characterization of crystals coming from representations of doubly laced algebras. In order to have such a characterization, it would be necessary to provide additional axioms to those stated above and to show that any graph satisfying those axioms is in fact a crystal. Here, we only show the other half of the characterization; we are assured that any graph with a relation not explicitly described in the above theorem is in fact not a crystal over one of these algebras.

Another application of the results of [46] appears in [6], which gives a novel construction of A_2 -crystals based on half-grids. Results such as those in [46] and [6], as well as those discussed below, impart an increased understanding of the graph/poset theoretic aspects of crystal graphs, revealing a new perspective on the representation theory of Lie algebras.

4.2 Realization of Crystals for Modules over Type C_2 Algebras

Recall that a crystal is a colored directed graph in which we interpret an i -colored edge from the vertex x to the vertex y to mean that $f_i x = y$ and $e_i y = x$, where e_i and f_i are Kashiwara crystal operators. The vector representation of C_2 has the following crystal:

$$\boxed{1} \xrightarrow{1} \boxed{2} \xrightarrow{2} \boxed{\bar{2}} \xrightarrow{1} \boxed{\bar{1}}$$

We realize crystals using tableaux filled with the letters $\{1, 2, \bar{2}, \bar{1}\}$ with the total ordering $1 < 2 < \bar{2} < \bar{1}$. The following definition is adapted from that in [24].

Definition 4.2.1. A C_2 Young diagram is a partition with no more than two parts; we draw it as a left-justified two-row arrangement of boxes such that the second row is no longer than the first.

A C_2 tableau is a filling of a C_2 Young diagram by the letters of the above alphabet with the following properties:

1. each row is weakly increasing by the ordering in the vector representation;
2. each column is strictly increasing by the ordering in the vector representation;
3. no column may contain 1 and $\bar{1}$ simultaneously;

4. the configuration

2	*
*	$\bar{2}$

 does not appear in T .

Example 4.2.2. The following is an example of a B_2 tableau.

1	1	2	2	$\bar{2}$	$\bar{2}$	$\bar{1}$
2	2	$\bar{2}$	$\bar{1}$			

Definition 4.2.3. Let T be a type C_2 tableau. The column word W of T is the word on the alphabet $\{1, 2, \bar{2}, \bar{1}\}$ consisting of cd for each column

d
c

 in T , reading left to right, then followed by each entry appearing in a one-row column in T , again reading left to right.

(Compare to Definition 2.2.2)

Example 4.2.4. The column word of the tableau in Example 4.2.2 is $2121\bar{2}\bar{2}\bar{1}\bar{2}\bar{2}\bar{2}\bar{1}$.

We now present a definition of the 1-signature and 2-signature of the column word of a type C_2 tableau, which is easily seen to be equivalent to the conventional definitions (e.g. [11]). Our definition differs by using the extra symbol $*$ to keep track of vacant spaces in the signatures.

Definition 4.2.5. Let a be in the alphabet $\{1, 2, \bar{2}, \bar{1}\}$. Then the 1-signature of a is

- $-$, if a is $\bar{2}$ or 1 ;
- $+$, if a is $\bar{1}$ or 2 ;

The 2-signature of a is

- $-$, if a is 2 ;
- $+$, if a is $\bar{2}$;
- $*$, if a is 1 or $\bar{1}$.

Let W be the column word of a type C_2 tableau T . Then for $i \in \{1, 2\}$ the i -signature of T is the word on the alphabet $\{+, -, *\}$ that results from concatenating the i -signatures of the entries of W .

Example 4.2.6. The 1- and 2-signatures of the tableau in example 4.2.2 are

$+ - + - - + + + - - +$

and

$$- * - * + - * - + + *,$$

respectively.

Definition 4.2.7. Let $S = s_1 s_2 \cdots s_\ell$ be a signature in the sense of Definition 4.2.5. The reduced form of S is the word on the alphabet $\{+, -, *\}$ that results from iteratively replacing every occurrence of $+\underbrace{* \cdots *}_k-$ in S with $\underbrace{* \cdots *}_{k+2}$ until there are no occurrences of $+\underbrace{* \cdots *}_k-$ in S .

Example 4.2.8. The reduced forms of the signatures in Example 4.2.6 are

$$* * * * - + * * * * +$$

and

$$- * - * * * * - + + *,$$

respectively.

The result of applying the Kashiwara operator e_i to a tableau T breaks into several cases. If there are no $+$'s in the reduced form of the i -signature of T , we say that $e_i T = 0$, where 0 is a formal symbol. Otherwise, let a be the entry corresponding to the leftmost $+$ in the reduced form of the i -signature of T . Then $e_i T$ is the tableau that results from changing a to $e_i a$ in T , as defined by the vector representation.

Similarly for f_i , if there are no $-$'s in the reduced form of the i -signature of T , we say that $f_i T = 0$. Otherwise, let a be the entry corresponding to the rightmost $-$ in the reduced form of the i -signature of T . Then $f_i T$ is the tableau that results from changing a to $f_i a$ in T .

Example 4.2.9. Let

$$T = \begin{array}{|c|c|c|c|c|c|c|} \hline 1 & 1 & 2 & 2 & \bar{2} & \bar{2} & \bar{1} \\ \hline 2 & 2 & \bar{2} & \bar{1} & & & \\ \hline \end{array}$$

be the tableau of Example 4.2.2. We then have

$$f_1 T = \begin{array}{|c|c|c|c|c|c|c|} \hline 1 & 1 & 2 & 2 & \bar{2} & \bar{2} & \bar{1} \\ \hline 2 & 2 & \bar{1} & \bar{1} & & & \\ \hline \end{array} ,$$

$$f_2 T = \begin{array}{|c|c|c|c|c|c|c|} \hline 1 & 1 & 2 & \bar{2} & \bar{2} & \bar{2} & \bar{1} \\ \hline 2 & 2 & \bar{2} & \bar{1} & & & \\ \hline \end{array} ,$$

$$e_1 T = \begin{array}{|c|c|c|c|c|c|c|} \hline 1 & 1 & 1 & 2 & \bar{2} & \bar{2} & \bar{2} \\ \hline 2 & 2 & \bar{2} & \bar{1} & & & \\ \hline \end{array} ,$$

and

$$e_2 T = \begin{array}{|c|c|c|c|c|c|c|} \hline 1 & 1 & 2 & 2 & 2 & \bar{2} & \bar{1} \\ \hline 2 & 2 & \bar{2} & \bar{1} & & & \\ \hline \end{array} .$$

4.3 Analysis of Generic C_2 tableaux

A generic C_2 tableau is of the form

$$\begin{array}{|c|c|c|c|c|c|c|c|c|c|c|c|c|c|c|} \hline 1 & \cdots & 1 & 1 & \cdots & 1 & 2 & 2 & \cdots & 2 & \bar{2} & \cdots & \bar{2} & \bar{1} & \cdots & \bar{1} \\ \hline 2 & \cdots & 2 & \bar{2} & \cdots & \bar{2} & \bar{2} & \bar{1} & \cdots & \bar{1} & \bar{1} & \cdots & \bar{1} & & & \\ \hline \end{array} \tag{4.3.4.1}$$

where

- any column may be omitted;

- any of the columns other than $\begin{array}{|c|} \hline 2 \\ \hline \bar{2} \\ \hline \end{array}$ may be repeated an arbitrary number of times;
- the bottom row may be truncated at any point.

We are interested in how the Kashiwara operators e_1 and e_2 act on this tableaux, so we must determine where the left-most $+$ appears in the reduced form of the signatures of the tableau. The relevant $+$'s in the signatures of a generic tableau naturally fall into two groups as described by definition 4.3.1.

Definition 4.3.1. Let T be a C_2 tableau.

- We define the left block of $+$'s in the 1-signature of T to be those $+$'s from 2 's in the top row and $\bar{1}$'s in the bottom row. If no such entries appear in T , we say that the left block of $+$'s in the 1-signature of T has size 0 and its left edge is located on the immediate left of symbol coming from the leftmost $\bar{2}$ or $\bar{1}$ in the top row of T . If there is furthermore no such entry, its left edge is located at the right end of the 1-signature of T .
- We define the right block of $+$'s in the 1-signature of T to be those $+$'s from $\bar{1}$ in the top row of T . If no such entry appears in T , we say that the right block of $+$'s in the 1-signature of T has size 0 and its left edge is located at the right end of the 1-signature of T .
- We define the left block of $+$'s in the 2-signature of T to be those $+$'s from $\bar{2}$ in the bottom row. If such an entry does not appear in T , we say that the left block of $+$'s in the 2-signature of T has size 0 and its left edge is located on the immediate left of the $*$ in the 2-signature coming from the leftmost $\bar{1}$ in the

bottom row of T . If T has no $\bar{1}$'s in the bottom row, we say that its left edge is located at the right end of the 2-signature of T .

- We define the right block of $+$'s in the 2-signature of T to be those $+$'s from $\bar{2}$ in the top row of T . If such an entry does not appear in T , we say that the right block of $+$'s in the 2-signature of T has size 0 and its left edge is located on the immediate left of the $*$ in the 2-signature coming from the leftmost $\bar{1}$ in the top row of T . If there are furthermore no $\bar{1}$'s in the top row of T , we say that its left edge is located at the right end of the 2-signature of T .

In the above cases when a block of $+$'s has positive size we say that its left edge is on the immediate left of its leftmost $+$.

Motivated by this definition, we define the following statistics on a C_2 tableaux T .

- $A(T)$ is the number of $\bar{2}$'s in the top row of T ,
- $B(T)$ is the number of 2 's in the top row of T plus the number of $\bar{1}$'s in the bottom row of T ,
- $C(T)$ is the number of 2 's in the top row of T ,
- $D(T)$ is the number of $\bar{2}$'s in the bottom row of T .

Example 4.3.2. Let

$$T = \begin{array}{|c|c|c|c|c|c|} \hline 1 & 1 & 2 & \bar{2} & \bar{2} & \bar{1} \\ \hline 2 & \bar{2} & \bar{2} & \bar{1} & & \\ \hline \end{array} .$$

Then $A(T) = 2$, $B(T) = 2$, $C(T) = 1$, and $D(T) = 2$.

Claim 4.3.3.

- If e_1 acts on a tableau T with $A(T) < B(T)$, the entry on which e_1 acts corresponds to a symbol in the left block of $+$'s in the 1-signature of T ;
- If e_1 acts on a tableau T with $A(T) \geq B(T)$, the entry on which e_1 acts corresponds to a symbol in the right block of $+$'s in the 1-signature of T ;
- If e_2 acts on a tableau T with $C(T) < D(T)$, the entry on which e_2 acts corresponds to a symbol in the left block of $+$'s in the 2-signature of T ;
- If e_2 acts on a tableau T with $C(T) \geq D(T)$, the entry on which e_2 acts corresponds to a symbol in the right block of $+$'s in the 2-signature of T .

Example 4.3.4. Let

$$T_1 = \begin{array}{|c|c|c|c|c|c|} \hline 1 & 2 & 2 & \bar{2} & \bar{2} & \bar{1} \\ \hline 2 & \bar{2} & \bar{1} & & & \\ \hline \end{array}$$

and

$$T_2 = \begin{array}{|c|c|c|c|c|c|} \hline 1 & 1 & 2 & \bar{2} & \bar{2} & \bar{1} \\ \hline 2 & 2 & \bar{1} & & & \\ \hline \end{array} .$$

In the case of T_1 , we have $A = 2 < 3 = B$, so e_1 will act on the left block of $+$'s in the 1-signature; in this case, it will act on the leftmost 2 in the top row of T_1 . By contrast, in T_2 we have $A = 2 = B$, so e_1 will act on the right block of $+$'s in the 1-signature; this corresponds to the $\bar{1}$ in the top row.

Let

$$T_3 = \begin{array}{|c|c|c|c|c|c|} \hline 1 & 1 & 2 & \bar{2} & \bar{2} & \bar{1} \\ \hline \bar{2} & \bar{2} & \bar{1} & & & \\ \hline \end{array}$$

and

$$T_4 = \begin{array}{|c|c|c|c|c|c|} \hline 1 & 2 & 2 & \bar{2} & \bar{2} & \bar{1} \\ \hline \bar{2} & \bar{2} & \bar{1} & & & \\ \hline \end{array} .$$

In the case of T_3 , we have $C = 1 < 2 = D$, so e_2 will act on the left block of $+$'s in the 2-signature; in this case, it will act on the leftmost $\bar{2}$ in the bottom row of T_3 . By contrast, in T_4 we have $C = 2 = D$, so e_2 will act on the right block of $+$'s in the 2-signature; this will be the leftmost $\bar{2}$ in the top row.

We now show that the entries in T on which a sequence $e_{i_1} \cdots e_{i_\ell}$ acts are determined by which blocks of $+$'s correspond to those entries. To achieve this, we verify that the left edge of a block of $+$'s can be changed only by acting on that block of $+$'s. This goal motivates the following notation.

We write e_1^ℓ to indicate the Kashiwara operator e_1 when applied to a tableau T such that $A(T) < B(T)$ and e_1^r to indicate the Kashiwara operator e_1 when applied to a tableau T such that $A(T) \geq B(T)$. Similarly, we write e_2^ℓ to indicate the Kashiwara operator e_2 when applied to a tableau T such that $C(T) < D(T)$ and e_2^r to indicate the Kashiwara operator e_2 when applied to a tableau T such that $C(T) \geq D(T)$. Note that these are not new operators: we simply use the superscript notation to record additional information about how the operators act on specific tableaux.

Claim 4.3.5. *Let T be a tableau such that $e_1^r T \neq 0$. Then the left edges of both the left and right blocks of $+$'s in the 2-signature of $e_1 T$ and the left edge of the left block of $+$'s in the 1-signature of $e_1 T$ are in the same place as they are in the signatures of T , and the left edge of the right block of $+$'s in the 1-signature of $e_1 T$ is one position to the right of that in T .*

Symmetrically, if $e_1^\ell T \neq 0$, the left edges of the blocks in the 2-signature and the

right block in the 1-signature are unchanged and the left edge of the left block in the 1-signature moves one position to the right; if $e_2^x T \neq 0$, the left edges of the blocks in the 1-signature and the left block in the 2-signature are unchanged and the left edge of the right block in the 2-signature moves one position to the right; and if $e_2^\ell T \neq 0$, the left edges of the blocks in the 1-signature and the right block in the 2-signature are unchanged and the left edge of the left block in the 2-signature moves one position to the right.

Proof. Let $i = 1$ and $j = 2$ or vice versa, and let $\mathbf{x} = \ell$ and $\mathbf{y} = \mathbf{r}$ or vice versa. It is clear from the combinatorially defined action of e_i on C_2 tableaux that if $e_i^{\mathbf{x}} T \neq 0$, the left edge of the \mathbf{y} block of $+$'s in the i -signature of $e_i T$ is in the same place as in the i -signature of T , and that the left edge of the \mathbf{x} block of $+$'s in the i -signature of $e_i T$ is one space to the right of its position in the i -signature of T . We may therefore devote our attention to the j -signature in each of the four cases of concern.

First, consider the case of $e_1^\ell T \neq 0$. By Claim 4.3.3, we know that this operator changes a 2 in the top row to a 1 or a $\bar{1}$ in the bottom row to a $\bar{2}$. In the first case, no $+$'s are added to the 2-signature, and no change is made to those entries of interest to the location of a block of $+$'s of size 0 in the 2-signature. In the other case, one $+$ is added to the left block of $+$'s in the 2-signature; this addition is to the right of the left edge of this block. Finally, the right block of $+$'s in the 2-signature of $e_1 T$ is the same as in the 2-signature of T in any case.

Next, consider the case of $e_1^r T \neq 0$. By Claim 4.3.3, we know that this operator changes a $\bar{1}$ in the top row of T into a $\bar{2}$. This adds one $+$ to the right block of $+$'s in the 2-signature to the right of its left edge and makes no change to the left block of $+$'s.

Now, consider the case of $e_2^\ell T \neq 0$. By Claim 4.3.3, we know that this operator changes a $\bar{2}$ in the bottom row to a 2. This does not contribute a + to either the left or right blocks of the 1-signature of $e_2 T$, nor does it pertain to the location of a block of +'s of size 0 in the 1-signature, so the left edges in this signature are the same as in the 1-signature of T .

Finally, we consider the case of $e_2^r T \neq 0$. By Claim 4.3.3, we know that this operator changes a $\bar{2}$ in the top row to a 2. This has the effect of adding a + to the left block of +'s in the 1-signature to the right of the left edge of this block. Finally, the right block of +'s in the 1-signature of $e_2 T$ is the same as in the 1-signature of T .

□

Corollary 4.3.6. *Let T be a tableau such that $e_1^\ell T \neq 0$, and let E be a sequence of operators from the set $\{e_1^r, e_2^\ell, e_2^r\}$ such that $ET \neq 0$. Then e_1^ℓ acts on the same entry in T as it does in ET . The symmetric statements corresponding to the cases of Claim 4.3.5 hold as well.*

Example 4.3.7. Let

$$T = \begin{array}{|c|c|} \hline \bar{2} & \bar{1} \\ \hline \bar{1} & \\ \hline \end{array},$$

so

$$e_1^r T = \begin{array}{|c|c|} \hline \bar{2} & \bar{2} \\ \hline \bar{1} & \\ \hline \end{array}$$

is the result of acting on the third tensor factor in the column word of T . We find that

$$e_2^\ell e_1^\ell e_2^r T = \begin{array}{|c|c|} \hline 1 & \bar{1} \\ \hline \bar{2} & \\ \hline \end{array},$$

so that indeed we have

$$e_1^r e_2^\ell e_1^\ell e_2^r T = \begin{array}{|c|c|} \hline 1 & \bar{2} \\ \hline \bar{2} & \\ \hline \end{array},$$

which differs from $e_2^\ell e_1^\ell e_2^r T$ in the third tensor factor.

The following four Sublemmas state that the relative values of $A(T)$, $B(T)$, $C(T)$, and $D(T)$ not only determine where e_i acts within a tableau, but also what the values of $A(e_i T)$, $B(e_i T)$, $C(e_i T)$, and $D(e_i T)$ are. This will be an invaluable tool for our analysis in section 4.4.

Sublemma 4.3.8. *Suppose T is a tableau such that e_1 acts on the left block of $+$'s in the 1-signature of T (i.e., such that $A(T) < B(T)$). Then $A(e_1 T) = A(T)$, $B(e_1 T) = B(T) - 1$, and $C(e_1 T) - D(e_1 T) = C(T) - D(T) - 1$.*

Proof. We have two cases to consider; e_1 may act by changing a 2 to a 1 in the top row or a $\bar{1}$ to a $\bar{2}$ in the bottom row. In both of these cases, it is easy to see that the number of $\bar{2}$'s in the top row is unchanged and the number of 2's in the top row plus the number of $\bar{1}$'s in the bottom row is diminished by one; hence $A(e_1 T) = A(T)$ and $B(e_1 T) = B(T) - 1$.

Observe that in the case of a $\bar{1}$ changing into a $\bar{2}$ in the bottom row, the content of the top row is unchanged, but the number of $\bar{2}$'s in the bottom row is increased by 1. In the case of a 2 changing into a 1 in the top row, the bottom row is unchanged, but the number of 2's in the top row is decreased by 1. In both of these cases, we find that $C(e_1 T) - D(e_1 T) = C(T) - D(T) - 1$.

□

Sublemma 4.3.9. *Suppose T is a tableau such that e_1 acts on the right block of $+$'s in the 1-signature of T (i.e., such that $A(T) \geq B(T)$). Then $A(e_1T) = A(T) + 1$, $B(e_1T) = B(T)$, $C(e_1T) = C(T)$, and $D(e_1T) = D(T)$.*

Proof. Since the right block of $+$'s in the 1-signature comes entirely from $\bar{1}$'s in the top row of T , it follows that acting by e_1 changes one of these $\bar{1}$'s into a $\bar{2}$. We immediately see that the number of $\bar{2}$'s in the top row increases by 1, and that the number of 2 's in the top row and $\bar{2}$'s and $\bar{1}$'s in the bottom row are all unchanged. □

Sublemma 4.3.10. *Suppose T is a tableau such that e_2 acts on the left block of $+$'s in the 1-signature of T (i.e., such that $C(T) < D(T)$). Then $A(e_2T) = A(T)$, $B(e_2T) = B(T)$, $C(e_2T) = C(T)$, and $D(e_2T) = D(T) - 1$.*

Proof. The entry on which e_2 acts is a $\bar{2}$ in the bottom row, which will be changed into a 2 . We immediately see that the number of $\bar{2}$'s in the bottom row decreases by 1, and that the number of 2 's and $\bar{2}$'s in the top row and $\bar{1}$'s in the bottom row are all unchanged. □

Sublemma 4.3.11. *Suppose T is a tableau such that e_2 acts on the right block of $+$'s in the 1-signature of T (i.e., such that $C(T) \geq D(T)$). Then $A(e_2T) = A(T) - 1$, $B(e_2T) = B(T) + 1$, $C(e_2T) = C(T) + 1$, and $D(e_2T) = D(T)$.*

Proof. In this case e_2 will change a $\bar{2}$ to a 2 in the top row. It is easy to see that the number of 2 's in the top row increases by 1 and the number of $\bar{2}$'s in the bottom row is unchanged; hence $C(e_2T) = C(T) + 1$ and $D(e_2T) = D(T)$.

	$A < B$	$A = B$	$A = B + 1$	$A > B + 1$
$C < D$	2	2	2	2
$C = D$	4	7	4	2
$C > D$	2	5	4	2

Table 4.1: Degree of relation over T , given its $ABCD$ statistics

Likewise, since the number of $\bar{2}$'s in the top row is decreased by 1 and the number of 2 's in the top row is increased by 1, we find that $A(e_2T) = A(T) - 1$ and $B(e_2T) = B(T) + 1$.

□

4.4 Proof of Theorem 1.2.4

We are now equipped to address Theorem 1.2.4. It is proved as a consequence of Lemmas 4.4.1 through 4.4.14, each of which deals with a certain case of the relative values of $A(T)$, $B(T)$, $C(T)$, and $D(T)$. To see that these cases are exhaustive, refer to Table 4.1.

Lemma 4.4.1. *Suppose T is a tableau such that $C(T) < D(T)$, $e_1T \neq 0$, and $e_2T \neq 0$. Then T has a degree 2 relation above it.*

Proof. From Claim 4.3.3, we know that e_2 acts on the left block of $+$'s, and by Sublemma 4.3.10, we know that $A(e_2T) = A(T)$ and $B(e_2T) = B(T)$; it follows that $e_1e_2T \neq 0$, and that e_1 acts on the same entry in e_2T as it does in T . Furthermore, by Sublemmas 4.3.8 and 4.3.9, we know that either $C(e_1T) - D(e_1T) = C(T) - D(T) - 1$ or $C(e_1T) = C(T)$ and $D(e_1T) = D(T)$; in either case, we still find that $C(e_1T) < D(e_1T)$. Since $C(e_1T) \geq 0$, we are assured that $D(e_1T) \geq 1$, and thus $e_2e_1T \neq 0$. We conclude that e_2 acts on the same entry in e_1T as it does in T .

□

Example 4.4.2. In Figure 4.4.4.1, we have an interval of a crystal in which the bottom tableau T has the statistics $C(T) = 1 < 2 = D(T)$, illustrating Lemma 4.4.1.

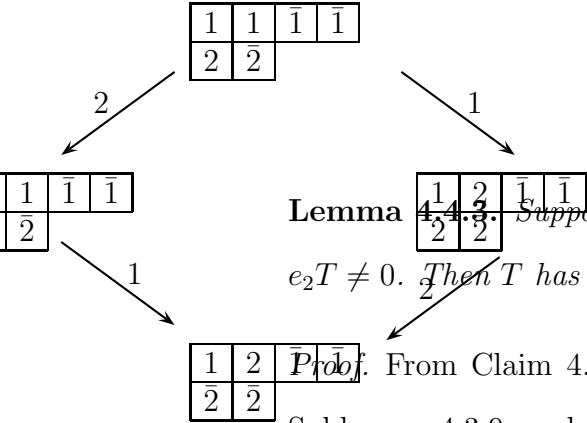


Figure 4.4.4.1:

Lemma 4.4.3. Suppose T is a tableau such that $A(T) > B(T) + 1$, $e_1T \neq 0$, and $e_2T \neq 0$. Then T has a degree 2 relation above it.

Proof. From Claim 4.3.3, we know that e_1 acts on the right block of +’s, and by Sublemma 4.3.9, we know that $C(e_1T) = C(T)$ and $D(e_1T) = D(T)$; thus $e_2e_1T \neq 0$, and e_2 acts on the same entry in e_1T as it does in T . Furthermore, by Sublemmas 4.3.10 and 4.3.11, we know that either $A(e_2T) = A(T)$ and $B(e_2T) = B(T)$ or $A(e_2T) = A(T) - 1$ and $B(e_2T) = B(T) + 1$; in either case, we find that $A(e_2T) > B(e_2T)$ and the size of the right block of +’s in the 1-signature is not diminished. We therefore conclude that $e_1e_2T \neq 0$ and that e_1 acts on the same entry in e_2T as it does in T .

□

Example 4.4.4. In Figure 4.4.4.2, we have an interval of a crystal in which the bottom tableau T has the statistics $A(T) = 2 > 1 = B(T) + 1$ illustrating Lemma 4.4.3.

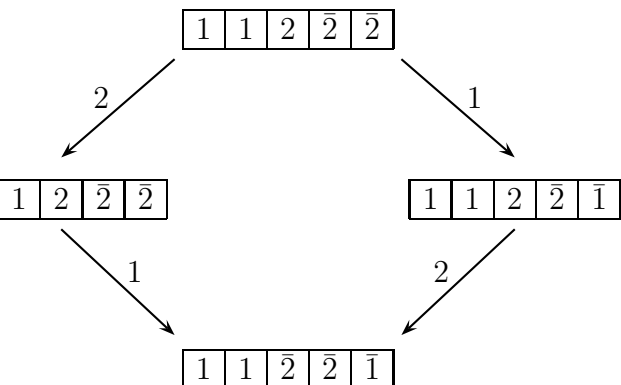


Figure 4.4.4.2:

Lemma 4.4.5. *Suppose T is a tableau such that $A(T) < B(T)$, $C(T) > D(T)$, $e_1T \neq 0$, and $e_2T \neq 0$. Then T has a degree 2 relation above it.*

Proof. By Claim 4.3.3, we know that e_1 acts on the left block of +’s in T and e_2 acts on the right block of +’s in T . By Sublemma 4.3.11, we know that $A(e_2T) = A(T) - 1$ and $B(e_2T) = B(T) + 1$. It follows that $A(e_2T) < B(e_2T)$, and since $A(e_2T) \geq 0$, this ensures that $B(e_2T) \geq 1$, and thus $e_1e_2T \neq 0$. We conclude that e_1 acts on the same entry in e_2T as it does in T . Furthermore, by Sublemma 4.3.8, we know that $C(e_1T) - D(e_1T) = C(T) - D(T) - 1$; it follows that $C(e_1T) \geq D(e_1T)$. Since we also know that the size of the right block of +’s in the 2-signature of e_1T is at least as large as that of T , it is the case that $e_2e_1T \neq 0$, and so e_2 acts on the same entry in e_1T as it does in T .

□

Example 4.4.6. In Figure 4.4.4.3, we have an interval of a crystal in which the bottom tableau T has the statistics $A(T) = 1 < 2 = B(T)$ and $C(T) = 1 > 0 = D(T)$, illustrating Lemma 4.4.5.

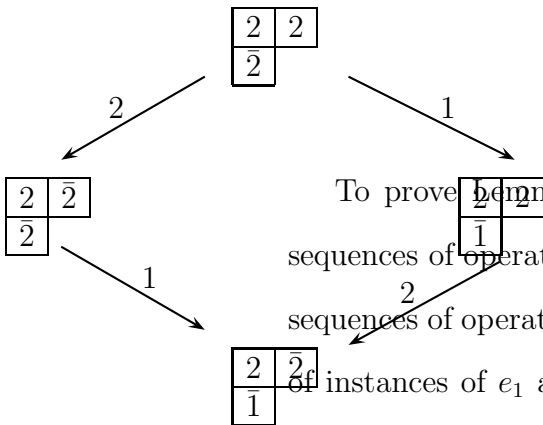


Figure 4.4.4.3:

To prove Lemmas 4.4.8 through 4.4.14, we must not only show that the given sequences of operators act on the same entries, but also that no pair of homogeneous sequences of operators (i.e., a pair (P_1, P_2) such that P_1 and P_2 have the same number of instances of e_1 and e_2) with shorter or equal length act on the same entries. To assist in our illustration of this fact, we will refer to figures that encode the generic behavior of all sequences of operators on a tableau with content as specified by the

edge pointing to the right	acting by e_1
edge pointing to the left	acting by e_2
solid edge	acting on the right block of + 's
dashed edge	acting on the left block of + 's
vertex labeled by (d_1, d_2)	tableau T with statistics such that $A(T) = B(T) + d_1$ and $C(T) = D(T) + d_2$

Table 4.2: Legend for Figures 4.4.4.4 through 4.4.4.12

hypothesis of each lemma. Table 4.2 is a legend for the figures used to prove Lemmas 4.4.8 through 4.4.12. In the picture used to prove Lemma 4.4.14, we instead use an edge pointing down to indicate acting by e_1 and an edge pointing up to indicate acting by e_2 ; otherwise the legend is the same.

To assist in proving that the sequences in question do not kill our tableaux, we have the following Sublemma.

Sublemma 4.4.7. *Let E be a dashed edge from v up to w ; i.e., an operator e_i^ℓ acts on v to produce w . Then $e_i v \neq 0$.*

Proof. The Kashiwara operator e_i acts on the left block of + 's of a tableau T precisely when $A(T) < B(T)$ or $C(T) < D(T)$ in the cases of $i = 1$ or $i = 2$, respectively. Since these numbers are all non-negative integers, we conclude that $B(T) > 0$ or $D(T) > 0$. Since these statistics indicate the number of + 's in the left block of their respective signatures, we are assured that there is an entry on which e_i can act.

□

Thus it suffices to prove that the solid edges in the paths of concern do not produce 0.

Lemma 4.4.8. *Suppose T is a tableau such that $A(T) = B(T) + 1$, $C(T) \geq D(T)$, $e_1 T \neq 0$, and $e_2 T \neq 0$. Then T has a degree 4 relation above it.*

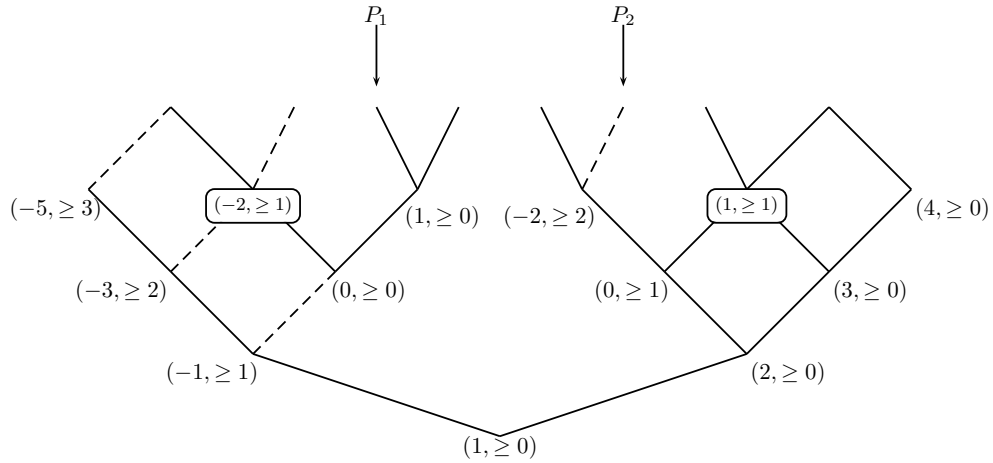


Figure 4.4.4.4: Picture for Lemma 4.4.8

Proof. We must first confirm that the sequences $e_1e_2^2e_1$ and $e_2e_1^2e_2$ do not produce 0 when applied to T . First, observe that since e_1 acts on the right block of $+$'s in T , it changes a $\bar{1}$ to a $\bar{2}$ in the top row. This adds a $+$ to the reduced 2-signature of the tableaux, so we know that $e_2^2e_1T \neq 0$. By Sublemma 4.4.7, we know that $e_1e_2^2e_1T \neq 0$. On the other hand, we know that e_2 acts on T by changing a $\bar{2}$ to a 2 in the top row; this means that the reduced 1-signature of e_2T has a single $+$ in the left block and its right block has at least one $+$, as did the 1-signature of T . We conclude that $e_1^2e_2T \neq 0$. We know that in e_1e_2T , e_1 changes a $\bar{1}$ to a $\bar{2}$ in the top row; since the $+$'s in the 2-signature from this entry cannot be paired with any $-$'s, we conclude that $e_2e_1^2e_2T \neq 0$.

Now that we know that neither of these sequences produces 0 when applied to T , it is clear that we have $e_1e_2^2e_1T = e_2e_1^2e_2T$, as the paths P_1 and P_2 leading from the base of the graph in Figure 4.4.4.4 to the indicated leaves both have one solid right edge, one dashed right edge, and two solid left edges. We must now confirm that among all pairs (Q_1, Q_2) of increasing paths from the base in these graphs such

that Q_1 begins by following the left edge and Q_2 begins by following the right edge, (P_1, P_2) is the only pair with the same number of each type of edge.

Since the right edge from the base of the graph is solid, our candidate for Q_1 must have a solid right edge. Inspecting the graph tells us that this path must begin with the path corresponding to $e_1^2 e_2$. This path has a dashed left edge, and the only candidate for Q_2 with this feature is in fact P_2 , which has two solid right edges. The only way to extend $e_1^2 e_2$ to have the same edge content as P_2 is by extending it to P_1 .

□

Example 4.4.9. In Figure 4.4.4.5, we have an interval of a crystal in which the bottom tableau T has the statistics $A(T) = 2 = B(T) + 1$ and $C(T) = 1 > 0 = D(T)$, illustrating Lemma 4.4.8.

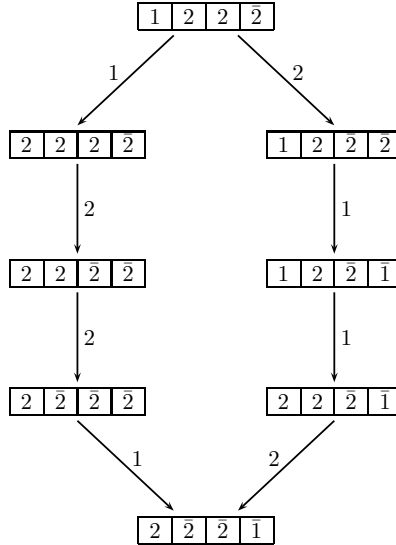


Figure 4.4.4.5:

Lemma 4.4.10. *Suppose T is a tableau such that $A(T) < B(T)$, $C(T) = D(T)$, $e_1 T \neq 0$, and $e_2 T \neq 0$. Then T has a degree 4 relation above it.*

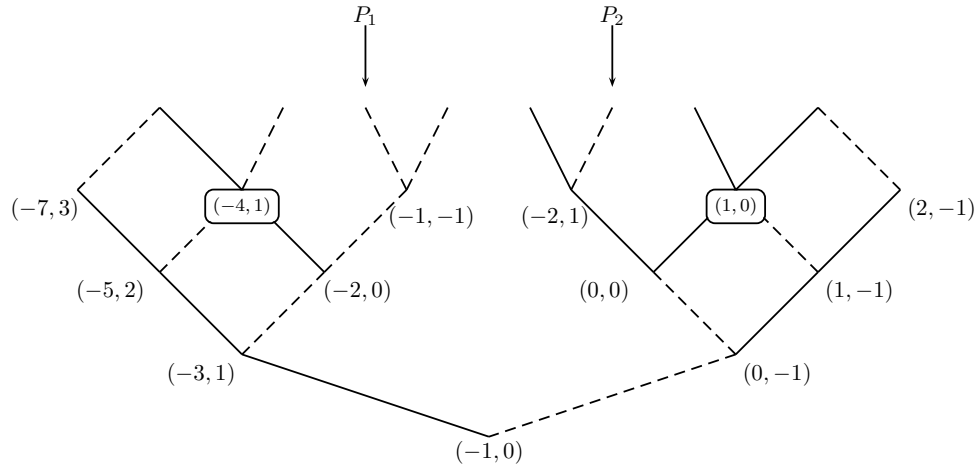


Figure 4.4.4.6: Picture 1 for Lemma 4.4.10

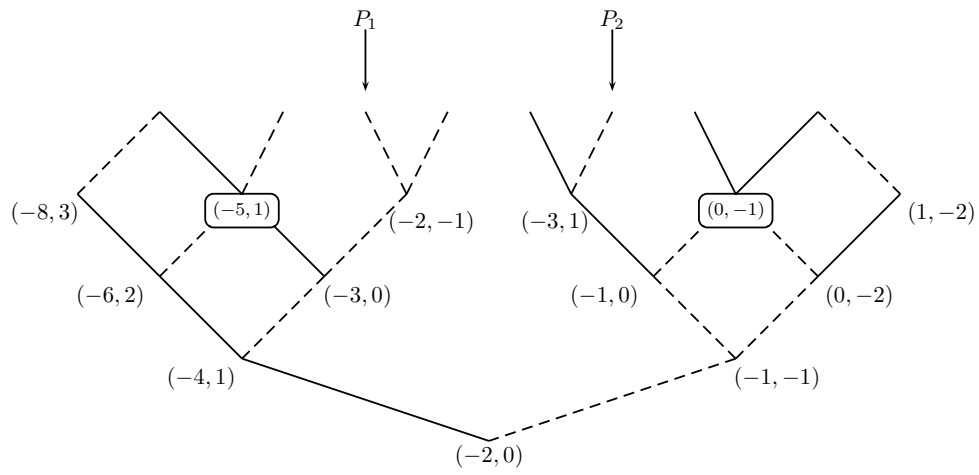


Figure 4.4.4.7: Picture 2 for Lemma 4.4.10

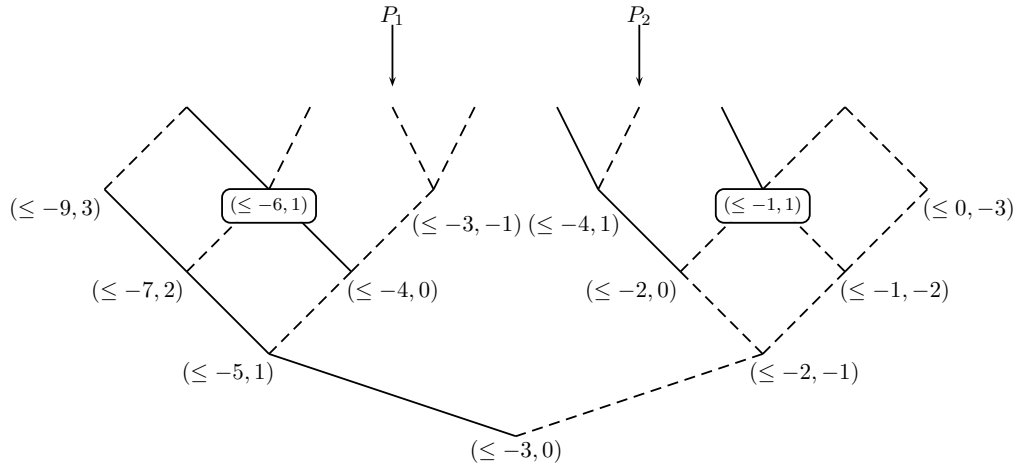


Figure 4.4.4.8: Picture 3 for Lemma 4.4.10

Proof. We must first confirm that the sequences $e_1e_2^2e_1$ and $e_2e_1^2e_2$ do not produce 0 when applied to T . By Sublemma 4.4.7 it suffices to show that $e_2^2e_1T \neq 0$, since $e_2T \neq 0$ by assumption and all other edges in P_1 and P_2 are dashed. To see this, simply observe that there is at least one + in the right block of the reduced 2-signature of T ; the sequence e_2e_1 acts on the left blocks of +’s, so the corresponding entry remains available for e_2 to act on.

Now that we know that neither of these sequences produces 0 when applied to T , it is clear that we have $e_1e_2^2e_1T = e_2e_1^2e_2T$, as the paths P_1 and P_2 leading from the base of the graph in Figures 4.4.4.6 through 4.4.4.8 to the indicated leaves have two dashed right edges, one solid left edge, and one dashed left edge. We must now confirm that among all pairs (Q_1, Q_2) of increasing paths from the base in these graphs such that Q_1 begins by following the left edge and Q_2 begins by following the right edge, (P_1, P_2) is the only pair with the same number of each type of edge.

This is easy to see by the following argument. Every candidate for Q_2 (i.e., every path in the right half of the graphs in Figures 4.4.4.6 through 4.4.4.8) has at least

one dashed left edge. The only candidate for Q_1 (i.e., the only path in the left half of the graphs in Figures 4.4.4.6 through 4.4.4.8) with a dashed left edge is P_1 . By inspecting Figures 4.4.4.6 through 4.4.4.8, P_2 is the only candidate for Q_2 with two dashed right edges and one solid left edge.

□

Example 4.4.11. In Figure 4.4.4.9, we have an interval of a crystal in which the bottom tableau T has the statistics $A(T) = 1 < 2 = B(T)$ and $C(T) = 1 = D(T)$, illustrating Lemma 4.4.10.

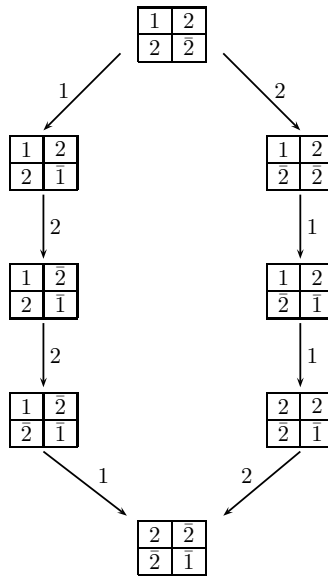


Figure 4.4.4.9:

Lemma 4.4.12. *Suppose T is a tableau such that $A(T) = B(T)$, $C(T) \geq D(T) + 1$, $e_1T \neq 0$, and $e_2T \neq 0$. Then T has a degree 5 relation above it.*

Proof. We must first confirm that the sequences $e_2e_1^3e_2$ and $e_1e_2e_1e_2e_1$ do not produce 0 when applied to T . First, note that there is at least one + in the right block of the

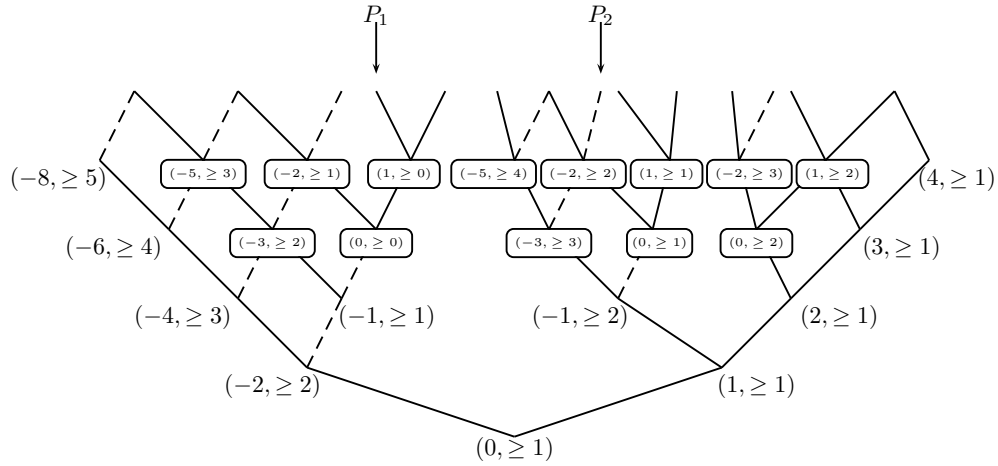


Figure 4.4.4.10: Picture for Lemma 4.4.12

reduced 1-signature of T . Since e_2 acts on the right block of $+$'s in the 2-signature of T , there are as many $+$'s in the right block of the 1-signature of e_2T as in that of e_1T . Observe that $A(e_2T) = B(e_2T) - 2$, so we know that there are additionally two $+$'s in the left block of the reduced 1-signature of e_2T . This implies that $e_1^3e_2T \neq 0$. The third of these applications of e_1 changes a $\bar{1}$ to a $\bar{2}$ in the top row; the $+$ in the 2-signature of $e_1^3e_2T$ entry cannot be bracketed, so we know that $e_2e_1^3e_2T \neq 0$. On the other hand, we know that the right block of the reduced 2-signature of T has at least one $+$. Since e_1 changes a $\bar{1}$ to a $\bar{2}$ in the top row of T , we know that e_2 will change this entry to a 2 so that the right block of the reduced signature of e_1T has at least two $+$'s that cannot be bracketed by $-$'s. The leftmost of these entries will be acted upon by e_2 , so $e_2e_1T \neq 0$. Furthermore, since $A(e_2e_1T) = B(e_2e_1T) - 1$, we know that $e_1e_2e_1T \neq 0$. At least one $+$ remains in the right block of the reduced 2-signature of $e_1e_2e_1T$, so $e_2e_1e_2e_1T \neq 0$. Finally, since $A(e_2e_1e_2e_1T) = B(e_2e_1e_2e_1T) - 2$, we know that $e_1e_2e_1e_2e_1T \neq 0$.

Now that we know that neither of these sequences produces 0 when applied to

T , it is clear that we have $e_2e_1^3e_2T = e_1e_2e_1e_2e_1T$, since the paths P_1 and P_2 leading from the base of the graph in Figure 4.4.4.10 to the indicated leaves have no solid left edges, two dashed left edges, one solid right edge, and two dashed right edges. Note that these paths are equivalent to $e_1^2e_2^2e_1T$, due to the degree 2 relation above e_2e_1T ; we may denote this alternative path by P'_2 . We must now confirm that among all pairs (Q_1, Q_2) of increasing paths from the base in these graphs such that Q_1 begins by following the left edge and Q_2 begins by following the right edge, (P_1, P_2) and (P_1, P'_2) are the only pairs with the same number of each of the above types of edges.

Since the right edge from the base of the graph is solid, our candidate for Q_1 must have a solid right edge. Observe that all paths in the left half of this graph with at least one solid right edge have two dashed right edges. The only candidates for Q_2 with two dashed edges are P_2 and P'_2 , both of which have two dashed left edges. The only remaining candidate for Q_1 with two dashed left edges is in fact P_1 .

□

Example 4.4.13. In Figure 4.4.4.11, we have an interval of a crystal in which the bottom tableau T has the statistics $A(T) = 2 = B(T)$ and $C(T) = 1 \geq 1 = D(T) + 1$, illustrating Lemma 4.4.12.

Lemma 4.4.14. *Suppose T is a tableau such that $A(T) = B(T)$, $C(T) = D(T)$, $e_1T \neq 0$, and $e_2T \neq 0$. Then T has a degree 7 relation above it.*

Proof. Note that in order to increase the readability of the graph in Figure 4.4.4.12, it has been oriented to grow to the right rather than up. We therefore take a down edge to indicate acting by e_1 and an up edge to indicate acting by e_2 . Otherwise, the legend from Table 4.2 applies.

We must first confirm that the sequences $e_2e_1^2e_2^3e_1$ and $e_1e_2^3e_1^2e_2$ do not produce 0 when applied to T . By Sublemma 4.4.7, we need only show that $e_1^3e_2T$, $e_2^2e_1^3e_2T$, and $e_2^2e_1T$ are not 0. First note that there is at least one $\bar{1}$ in the top row of T , and the application of e_1^2 to e_2T acts on entries corresponding to the left block of $+$'s. It follows that the $\bar{1}$'s in the top row of T are also present in $e_1^2e_2T$, so $e_1^3e_2T \neq 0$. This final application of e_1 changes a $\bar{1}$ to a $\bar{2}$. Since e_2 acts on the left block of $+$'s in $e_1^3e_2T$, it leaves this $\bar{2}$ alone, and it can be acted on by the next application of e_2 , so $e_2^2e_1^3e_2T \neq 0$. Finally, note that there is a $\bar{2}$ in the top row of T and e_1 changes a $\bar{1}$ to a $\bar{2}$ in the top row of T . Thus, there are at least two $\bar{2}$'s in the top row of e_1T , and $e_2^2e_1T \neq 0$.

Now that we know that neither of these sequences produces 0 when applied to T , it is clear that we have $e_2e_1^2e_2^3e_1T = e_1e_2^3e_1^2e_2T$, since the paths corresponding to these

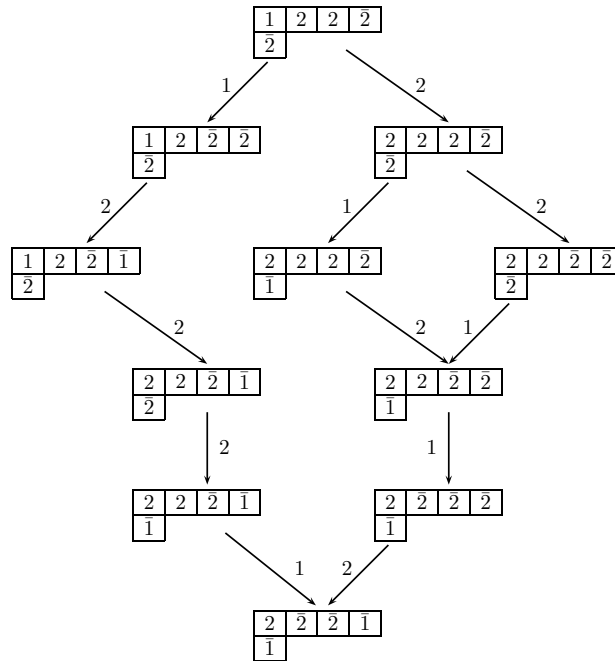


Figure 4.4.4.11:

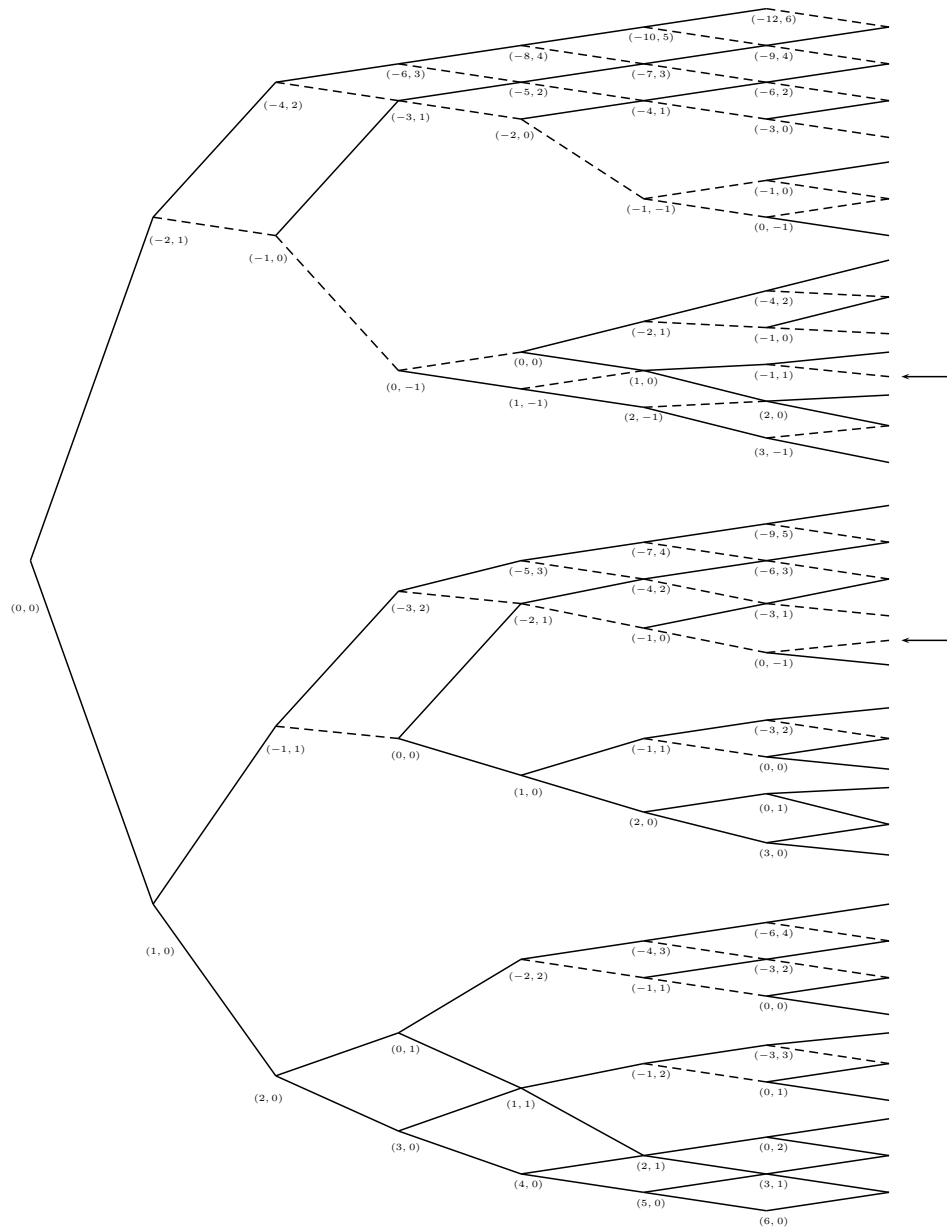


Figure 4.4.4.12: Picture for Lemma 4.4.14

sequences leading from the base of the graph in Figure 4.4.4.12 to the leaves marked by arrows have one solid down edge, three dashed down edges, two solid up edges, and one dashed up edge. Note that these paths are equivalent to $e_2e_1e_2e_1e_2^2e_1T = e_1e_2^2e_1e_2e_1e_2T$, due to the degree 2 relations above $e_2^2e_1T$ and e_1e_2T ; we denote these alternative paths by P'_1 and P'_2 respectively. We must now confirm that among all pairs (Q_1, Q_2) of increasing paths from the base in these graphs such that Q_1 begins by following the up edge and Q_2 begins by following the down edge, (P_1, P_2) , (P_1, P'_2) , (P'_1, P_2) and (P'_1, P'_2) , are the only pairs with the same number of each of the above types of edges.

We first address pairs of paths of length no greater than 5. For a path to be a candidate for Q_1 , it must have at least one solid down edge. The only such paths are those beginning with $e_1^2e_2T$. As these paths have two dashed down edges, their only possible Q_2 mate is $e_1^2e_2^2e_1T$, but none of our Q_1 candidates have the same edge content as this path.

We now consider paths of length 6. As in the preceding paragraph, our only candidates for Q_1 are those paths that contain a solid down edge and begin with $e_1^2e_2T$; all such paths have exactly two dashed down edges. Up to degree 2 relations, there are three candidates for Q_2 : $e_1^2e_2^3e_1T$, $e_1e_2e_1^2e_2e_1T$, and $e_1^2e_2^2e_1^2T$. None of these paths contain a dashed up edge, which leaves only $e_1^5e_2T$ as our only candidate for Q_1 ; this cannot be paired with any of our three potential Q_2 paths.

Finally, we restrict our attention to paths of length 7. There are six paths (again, up to degree 2 relations) in the top half of the graph with solid down edges: $e_1^5e_2^2T$ and those paths beginning with $e_1^3e_2T$. The former has four dashed down edges, a feature lacking from all paths in the bottom half of the graph. We may also exclude from our consideration $e_1^6e_2T$, as all candidates for Q_2 with only one up edge have at

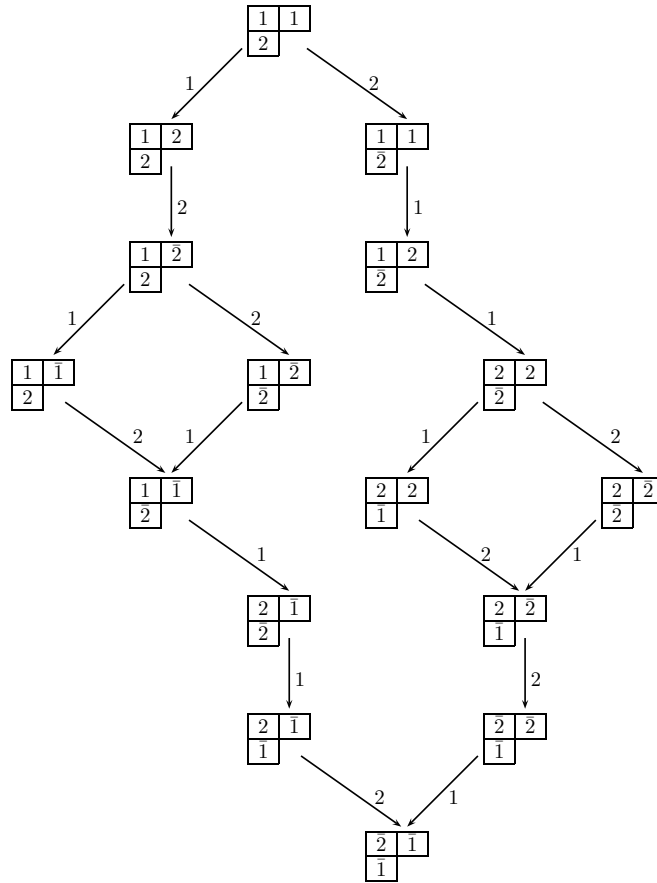


Figure 4.4.4.13:

most one dashed down edge.

The remaining three paths that might be Q_1 all have a dashed up edge; the only Q_2 candidates with this feature are P_2 and P'_2 . The only paths in the top half of the graph with the same edge content as these are P_1 and P'_1 .

□

Example 4.4.15. In Figure 4.4.4.13, we have a crystal in which the bottom tableau T has the statistics $A(T) = B(T) = 1$ and $C(T) = D(T) = 0$, illustrating Lemma 4.4.14.

Chapter 5

A User's Manual for CrystalView

5.1 Overview

CrystalView is a software package for visualizing crystals for irreducible highest weight modules of classical Lie algebras. Based on user input, the program will produce an image file with the requested crystal graph. The program will automatically produce an .epsf file, which can be included directly in a L^AT_EX file. Using the web interface, the user can see the tableau associated to a vertex of the crystal by moving the mouse pointer over it.

When running this program locally (as opposed to via the web), the program produces a list of all tableaux in the specified crystal. This can be used to carry out calculations on crystals, including searches for tableaux with specified properties. Additionally, Kashiwara operators may be applied to the tableaux.

All calculations on tableaux are carried out using python. Image files are automatically generated PostScript. The web interface uses html, javascript, and css.

5.2 Requirements

CrystalView may be run using a web interface or from source code. The web interface can, in principle, be used from any browser that supports form input (any “modern” browser). However, some aspects of the interface will only work with a browser that complies with standard html, javascript, and css. In particular, Internet Explorer is known to have issues with some dynamic aspects of the web interface. Firefox is a recommended alternative.

To run the software from source code, the user must have Python 2.4 installed on their local machine. Other versions of Python (both older and newer) may not run CrystalView properly. See <http://www.python.org> for further information regarding python. Python is available free of charge for all major operating systems, and is included pre-installed on many modern computers, including almost all distributions of Unix/Linux.

If used to generate image files locally, the user is advised that for large crystals, these images can get quite large. See section 5.8.

5.3 User input

The user may specify the following Lie theoretic data:

- symmetry type of the algebra being represented;
- rank of the algebra being represented;
- highest weight of the representation.

Additionally, the user may specify how the edges of the crystal graph will be drawn. There are two default settings, color and grayscale, as well as an option for custom settings. If the custom option is selected, the user may specify the following:

- red/green/blue values for each edge color on a scale from 0 to 1 (Default = 1),
- line width on a scale from 1 to 5 (Default = 5),
- dash pattern; none, short, long (Default = none).

There are numerous resources on the web and preinstalled on many computers to assist the user in finding red/green/blue values for their desired colors.

The user may also choose to have the output converted to .pdf, .jpg, .gif, and/or .tiff formats. These conversions are carried out by ImageMagick.

5.4 Limitations

Currently, only types A and B (i.e., \mathfrak{sl}_n and \mathfrak{so}_{2n+1}) are supported. Furthermore, in the case of type B , only even multiples of the highest fundamental weight (corresponding to the short root) may be specified. These limitations are due to the current stage of the development cycle; future versions of the software will add support for types C and D and all dominant weights.

The rank of the algebra is currently restricted by the web interface to be no larger than 5. This is an artificial limitation; any rank of algebra may be specified when running CrystalView from source.

The web interface only allows crystals with as many as 4,000 vertices to be calculated to prevent excessive strain on the server. Considering the resolution at which

these images can be viewed/printed, it is unlikely that producing crystals larger than this would be useful to most users. However, this limitation is artificial; when running the program on a local machine, the user is limited only by their own patience and hard disk space.

5.5 How it works

The web interface for CrystalView is written in dhtml; i.e., html enhanced by javascript and css. The Weyl dimension formula is used to calculate the number of vertices in the currently specified crystal.

The tableaux are produced by generating the list of all column tableaux for the column lengths appearing in the shape specified by the dominant weight. To determine what constitutes a legal tableaux, the criteria of [11] are used. The columns are then compared pairwise in order of decreasing length to build the set of all legal tableaux. In the case of type B crystals, the “split form” criterion of [29] is used to determine which columns can be adjacent in a legal tableau.

The graph is ensured to have a reasonable number of edge crossings by ordering the vertices of the graph as follows, starting from the top and going down the rows, and proceeding through each row from left to right. First, the tableaux are collected into rows according to content. There is only one tableau in the first row (the highest weight tableau), so the first row is in order. Now, given that row n is in order, row $n + 1$ is put in the following order. The leftmost vertices in row $n + 1$ will be the non-zero images of the Kashiwara operators f_i on the leftmost vertex in row n , taken in order from f_1 up through f_r , where r is the rank of the algebra. The next leftmost vertices in row $n + 1$ are those tableaux that result from applying f_i to the next vertex

from row n , excluding those that have been placed to the left already. This process continues until all vertices have been placed in their final position.

5.6 How to get the software

This software can be accessed at the following url:

<http://www.math.ucdavis.edu/~sternberg/crystalview/>

The source code is available upon request from the author.

5.7 Examples of output

Figures 5.7.5.1 and 5.7.5.2 feature examples of the graphical output of CrystalView.

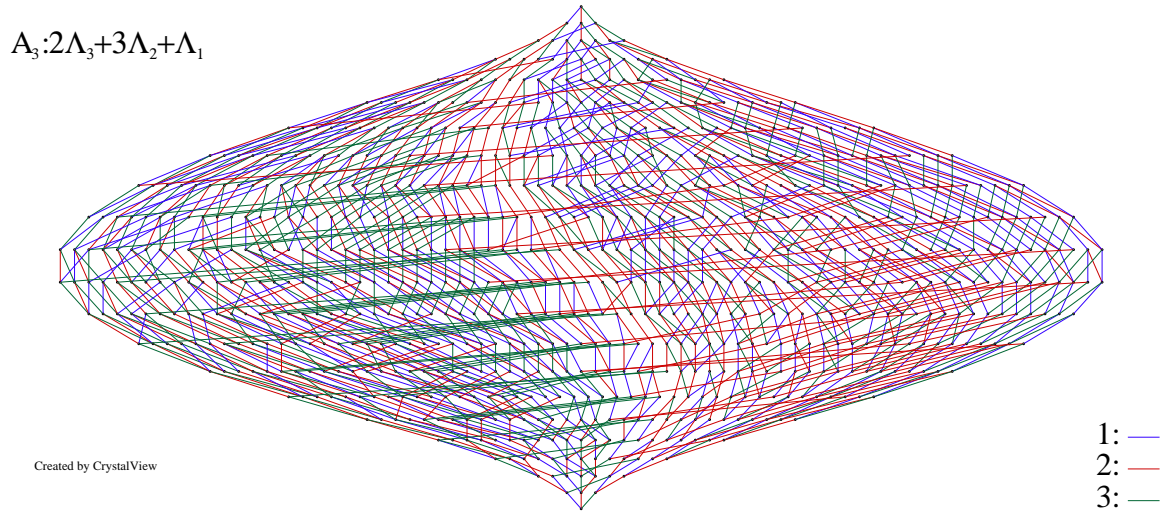


Figure 5.7.5.1:

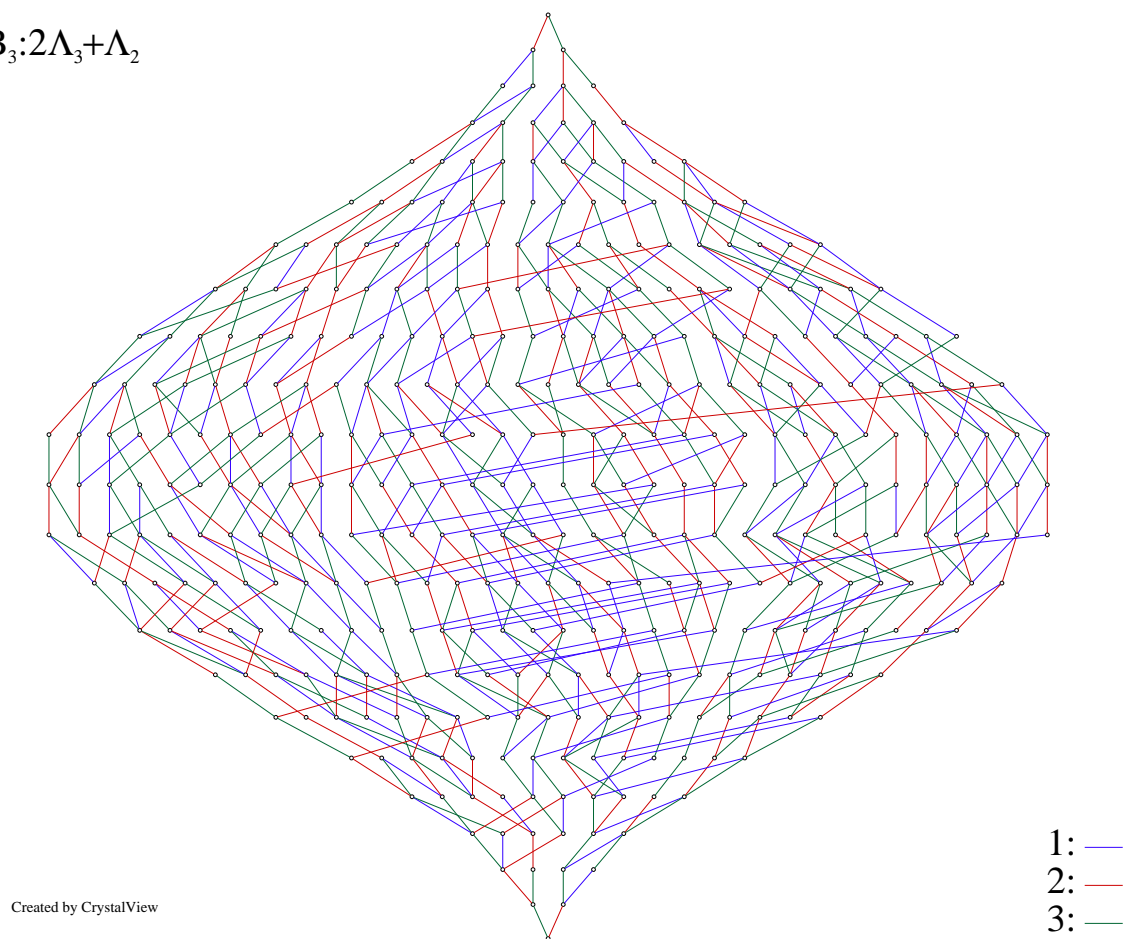
$B_3:2\Lambda_3+\Lambda_2$ 

Figure 5.7.5.2:

5.8 Legal disclaimer

This software is provided without warranty; use is at the user's sole risk. Under no circumstances will any user hold the author of this software liable for any damages that may result from the use of this software. Use of the software implies that the user agrees to these terms.

References

- [1] G. Benkart, I. Frenkel, S-J. Kang, H. Lee, *Level 1 Perfect Crystals and Path Realizations of Basic Representations at $q=0$* , arXiv:math.RT/0507114.
- [2] V. Chari, *On the fermionic formula and the Kirillov-Reshetikhin conjecture*, Internat. Math. Res. Notices 2001, no. 12, 629–65.
- [3] V. Chari and A. Pressley, *Quantum affine algebras and their representations*, Representations of groups (Banff, AB, 1994), 59–78, CMS Conf. Proc., **16**, Amer. Math. Soc., Providence, RI, 1995.
- [4] V. Chari and A. Pressley, *Twisted quantum affine algebras*, Comm. Math. Phys. **196** (1998) 461–476.
- [5] V. G. Drinfeld, *Hopf algebra and the Yang–Baxter equation*, Soviet. Math. Dokl. **32** (1985) 254–258.
- [6] V. I. Danilov, A. V. Karzanov and G. A. Koshevoy, *Combinatorics of A_2 -crystals*, arXiv:math.RT/0604333.
- [7] G. Fourier, A. Schilling and M. Shimozono, *Demazure structure inside Kirillov-Reshetikhin crystals*, to appear in J. Algebra.

- [8] W. Fulton and J. Harris, *Representation Theory: A First Course*, Graduate Texts in Mathematics 129, Springer-Verlag, New York, NY, 1991.
- [9] G. Hatayama, A. Kuniba, M. Okado, T. Takagi and Z. Tsuboi, *Paths, crystals and fermionic formulae*, MathPhys odyssey, 2001, 205–272, Prog. Math. Phys., 23, Birkhäuser Boston, Boston, MA, 2002.
- [10] G. Hatayama, A. Kuniba, M. Okado, T. Takagi and Y. Yamada, *Remarks on fermionic formula*, Recent developments in quantum affine algebras and related topics (Raleigh, NC, 1998), 243–291, Contemp. Math., **248**, Amer. Math. Soc., Providence, RI, 1999.
- [11] J. Hong and S.-J. Kang, *Introduction to quantum groups and crystal bases*, Graduate Studies in Mathematics, 42. American Mathematical Society, Providence, RI, 2002.
- [12] M. Jimbo, *A q -difference analogue of $U(\mathcal{G})$ and the Yang–Baxter equation*, Lett. Math. Phys. **10** (1985) 63–69.
- [13] N. Jing, K. Misra, and M. Okado, *q -wedge modules for quantized enveloping algebras of classical type*, J. of Alg. bf 230 (2000), 518–593.
- [14] V.G. Kac, *Infinite-dimensional Lie algebras*. Third edition. Cambridge University Press, Cambridge, 1990. xxii+400 pp. ISBN: 0-521-37215-1.
- [15] S-J. Kang, M. Kashiwara and K. Misra, *Crystal bases of Verma modules for quantum affine algebras*, Compositio Math **92** (1994), 299-325.

- [16] S.-J. Kang, M. Kashiwara, K.C. Misra, T. Miwa, T. Nakashima and A. Nakayashiki, *Perfect crystals of quantum affine Lie algebras*, Duke Math. J. **68** (1992), no. 3, 499–607.
- [17] S.-J. Kang, M. Kashiwara, K.C. Misra, T. Miwa, T. Nakashima and A. Nakayashiki, *Affine crystals and vertex models*, Infinite analysis, Part A, B (Kyoto, 1991), 449–484, Adv. Ser. Math. Phys., **16**, World Sci. Publishing, River Edge, NJ, 1992.
- [18] M. Kashiwara, *Crystalizing the q -analogue of universal enveloping algebras*, Comm. Math. Phys. **133** (1990), no. 2, 249–260.
- [19] M. Kashiwara, *On crystal bases of the q -analogue of universal enveloping algebras*, Duke Math. J. **63** (1991), no. 2, 465–516.
- [20] M. Kashiwara, *Crystal base and Littelmann’s refined Demazure character formula*, Duke Math. J., **71** (1993), 839–858.
- [21] M. Kashiwara, *On crystal bases*, in: Representations of groups (Banff, AB, 1994), 155–197, CMS Conf. Proc., 16, Amer. Math. Soc., Providence, RI, 1995.
- [22] M. Kashiwara, *On level-zero representation of quantized affine algebras*, Duke Math. J. **112** (2002) no. 1, 117–195.
- [23] M. Kashiwara, *Level zero fundamental representations over quantized affine algebras and Demazure modules*, Publ. Res. Inst. Math. Sci. **41** (2005), no. 1, 223–250.
- [24] M. Kashiwara and T. Nakashima, *Crystal graphs for representations of the q -analogue of classical Lie algebras*, J. Algebra **165** (1994), no. 2, 295–345.

- [25] S. V. Kerov, A. N. Kirillov and N. Y. Reshetikhin, *Combinatorics, the Bethe ansatz and representations of the symmetric group*, J. Soviet Math. **41** (1988), no. 2, 916–924.
- [26] A. N. Kirillov and N. Y. Reshetikhin, *The Bethe ansatz and the combinatorics of Young tableaux*, J. Soviet Math. **41** (1988), no. 2, 925–955.
- [27] A. N. Kirillov, A. Schilling and M. Shimozono, *A bijection between Littlewood-Richardson tableaux and rigged configurations*, Selecta Mathematica (N.S.) **8** (2002) 67–135.
- [28] Y. Koga, *Level one perfect crystals for $B_n^{(1)}$, $C_n^{(1)}$, and $D_n^{(1)}$* , J. Algebra **217** (1999), no. 1, 312–334.
- [29] C. Lecouvey, *Schensted-type correspondences and plactic monoid for types B_n and D_n* , J. Algebraic Combin. **18** (2003), no. 2, 99–133.
- [30] P. Littelmann, *A Littlewood-Richardson rule for symmetrizable Kac-Moody algebras*, Invent. Math. **116** (1994), 329–246.
- [31] P. Littelmann, *Paths and root operators in representation theory*, Ann. of Math. **142** (1995), 499–525.
- [32] G. Lusztig, *Quantum deformation of certain simple modules over enveloping algebras*, Adv. Math. **70** (1988), no. 2, 237–249.
- [33] H. Nakajima, *t -analogue of the q -characters of finite dimensional representations of quantum affine algebras*, Physics and combinatorics, 2000 (Nagoya), 196–219, World Sci. Publishing, River Edge, NJ, 2001.

- [34] S. Naito and D. Sagaki, *Path model for a level zero extremal weight module over a quantum affine algebra*, Int. Math. Res. Notices **48** (2003), 1731–1754.
- [35] S. Naito and D. Sagaki, *Construction of perfect crystals conjecturally corresponding to Kirillov-Reshetikhin modules over twisted quantum affine algebras*, Comm. Math. Phys. **263** (2006) 749–787.
- [36] M. Okado, personal communication, 2005.
- [37] M. Okado, A. Schilling and M. Shimozono, *A crystal to rigged configuration bijection for nonexceptional affine algebras*, ”Algebraic Combinatorics and Quantum Groups”, Edited by N. Jing, World Scientific (2003), 85–124.
- [38] M. Okado, A. Schilling and M. Shimozono, *Virtual crystals and fermionic formulas of type $D_{n+1}^{(2)}$, $A_{2n}^{(2)}$, and $C_n^{(1)}$* , Represent. Theory **7** (2003) 101–163.
- [39] M. Okado, A. Schilling and M. Shimozono, *Virtual crystals and Kleber’s algorithm* Comm. Math. Phys. **238** (2003) 187–209.
- [40] A. Schilling, *A bijection between type $D_n^{(1)}$ crystals and rigged configurations*, J. Algebra **285** (2005), no. 1, 292–334.
- [41] A. Schilling, *$X = M$ Theorem: Fermionic formulas and rigged configurations under review*, to appear in MSJ Memoirs (published by the Mathematical Society of Japan).
- [42] A. Schilling and M. Shimozono, *$X = M$ for symmetric powers*, J. Algebra **295** (2006), no. 2, 562–610.
- [43] A. Schilling and M. Shimozono, personal communication, 2006.

- [44] A. Schilling and P. Sternberg, *Finite-Dimensional Crystals $B^{2,s}$ for Quantum Affine Algebras of type $D_n^{(1)}$* J. Alg. Comb. **23** (2006), 317–354.
- [45] M. Shimozono, *Affine type A crystal structure on tensor products of rectangles, Demazure characters, and nilpotent varieties*, J. Algebraic Combin. **15** (2002), no. 2, 151–187.
- [46] J. Stembridge, *A local characterization of simply-laced crystals*, Trans. Amer. Math. Soc. **355** (2003), 4807–4823.
- [47] P. Sternberg, *On the local structure of doubly laced crystals*, to appear in J. Comb. Theory, Ser. A.
- [48] S. Yamane, *Perfect crystals of $U_q(G_2^{(1)})$* , J. of Alg. **210** (1998), 440–486.